Cape Peninsula
University of Technology

The use of fluorescent flow cytometry to evaluate the inactivation of Saccharomyces cerevisiae by sequential application of ultrasound (20 kHz) and heat

by

Brett Arthur Wordon

Thesis submitted in fulfilment of the requirements for the degree

Master of Technology: Food Technology

in the Faculty of Applied Sciences

at the Cape Peninsula University of Technology

Supervisor: Dr Lynn Mc Master

Cape Town

October 2009

DECLARATION

I, Brett Arthur Wordon, declare that the contents of this dissertation/thesis represent my own unaided work, and that the dissertation/thesis has not previously been submitted for academic examination towards any qualification. Furthermore, it represents my own opinions and not necessarily those of the Cape Peninsula University of Technology.

Signed **Date**

ABSTRACT

The primary aim of this study was to establish the effects of both cavitation, (20 KHz), and heat (55°C or 60°C) on *Saccharomyces cerevisiae* GC210 (*MATα lys2*) suspended in physiological saline. Fluorescent flow cytometry was used to determine the effects of moist heat and acoustic cavitation on *S. cerevisiae* cells. Results from this study could be used as a guide for use by the food industry for the combined use of heat and sonication to disinfect various solutions contaminated with *S. cerevisiae.*

Initially, conditions required to generate constant and optimum inertial cavitation using a Vibracell VCX750 ultrasonic processor (20 KHz) were determined. To do this, sonochemical studies on sonicated aqueous solutions were performed using two techniques viz., luminol chemiluminescence and oxidation of iodine to form tri-iodide. In a comparison of three ultrasonic horns (tapered, stepped and standard), luminol chemiluminescence showed that most inertial cavitation was generated by the standard horn (13 mm tip diameter). Using this horn at maximum displacement amplitude (124 µm), cavitation was intense and reproducible. Spatially, cavitation occurred as a localised zone at the base of the three horns tested. Iodide formation supported the observation that the standard horn generated most cavitation. As a result, the standard horn was selected for further evaluation. Over a 10 min period of continuous sonication, cavitation was generated in an iodine solution at a constant rate. The influence on inertial cavitation of hydrostatic pressure (100, 200, 300, 400 and 500 kPa), dissolved gases (argon, nitrogen and oxygen) and pulsed soundwaves (20, 40, 60, 80% duty cycle) was investigated. Hydrostatic pressure increased inertial cavitation but was impractical due to the high wear and tear on the equipment. Tri-iodide formation was increased by 283.03% and 69.88% when the treatment solution was saturated with argon and oxygen respectively, when compared to a degassed solution. However saturation with nitrogen decreased the tri-iodide by 32.86%. Pulsed sound waves increased tri-iodide formation when the ultrasonic duty cycle was set to 40 - 60%. The effect of test solution volume on cavitation was investigated. It was found that the amount of tri-iodide generated was doubled when the test solution was reduced from 100 ml to 50 ml. The amount of cavitation generated.min^{-1} was constant, despite the test volume. However, the tri-iodide generated was more concentrated due to the decreased volume. When the volume was below 50 ml, vortexing occurred in the solutions. This was undesirable as vortexing introduced additional air bubbles into the solution thus influencing the consistency of the cavitation generated. The position of the standard horn tip above the base of the treatment vessel influenced the amount of inertial cavitation. Optimum position was 20 mm above the base of the treatment vessel. As a result of these studies, the treatment solution volume used throughout all applications to *S. cerevisiae* was 60 ml, and the standard horn was positioned 20 mm above the base of the vessel. Amplitude selected was 124 µm. All solutions used were degassed. Due to

practicality considerations, pulsed sound waves, increased hydrostatic pressure, and argon or oxygen were not used during sonication of samples.

Fluorescent flow cytometry was used for the evaluation of *S. cerevisiae*. As the instrument is primarily used for mammalian cells, it was first calibrated for *S. cerevisiae*. The instrument settings needed to be set to detect non-fluorescent *S. cerevisiae*. These settings were then further optimised such that fluorescence by thiazole orange (TO) and propidium iodide (PI) labelled *S. cerevisiae* cells were detected. Various reagents added to *S. cerevisiae* suspensions during preparation for cytometric acquisition, were screened. The extent and location of associated noise signals was determined and removed from acquired data. The reproducibility of the flow cytometer was checked to ensure satisfactory acquisition of *S. cerevisiae* suspensions. The counting of *S. cerevisiae* was reproducible regardless of sample flow rate, or selected endpoint of the acquisition.

The fluorophores thiazole orange (TO) and propidium iodide (PI) were used to rapidly determine numbers of viable, dead and boundary-injured *S. cerevisiae* cells subjected to heat or cavitation. When subjected to 55°C, the age of the culture, determined using spectrophotometry (OD_{600}), influenced viable cell response. The D_{ht55} ranged between 9.85 min (OD_{600} 0.152) to >20 min (OD_{600} 1.058). Therefore cultures of a similar age (OD_{600} ~1) were used in all subsequent studies. When exposed to 60°C, the D_{ht60} as determined by measuring the decrease in viable cells, was 2.96 min. Uptake of PI showed that the decline in living cells by 92.2% after 5 min exposure was primarily due to the formation of a population of membrane-injured cells which comprised 70.2% of the population. Dead cells formed 25.0% of the population. The exposure of cells to sonication for 20 min caused rapid death. After 1 min sonication, only 59.2% of the cells remained viable and 42.3% were dead. A D_{us} 3.06 min was calculated. Although scanning electron micrographs (SEM) clearly showed severe cell boundary damage during the first minute of sonication, the formation of a "stable" injured PI-fluorescent population as seen in the heat treatments was not observed for sonicated cells. It is likely that severe membrane injury caused by ultrasound was immediately lethal. The total population of intact cells declined by 41.8% during 5 min sonication. This was due to fragmentation of cells. However, cell disintegration was not the principal cause of death.

Synergy was noted between sonication and heat when combined as microbicidal treatments. Preliminary "hurdle" technology studies showed that the application of 1 min sonication to *S. cerevisiae* markedly enhanced death of the cells when subsequently exposed to 55 or 60°C over 5 min. The D_{hd55} and D_{hd60} were measured as 1.93 and 1.03 min respectively. Fluorescence evaluation of these cells showed that the time period of membrane injury at

both temperatures was markedly reduced. Hence pre-sonication of *S. cerevisiae* resulted in unidentified nonlethal intracellular injuries, not detected by PI.

The use of fluorescent flow cytometry enabled rapid testing of *S. cerevisiae* exposed to heat and/or ultrasound. In particular, cell fluorescence showed that the major response of heated cells was microbistatic, manifested by the appearance of a membrane injured population. Over a time period of 5 min, ultrasound was microbicidal. Fluorescent techniques were sensitive enough to show that 1 min sonication caused intracellular injuries which markedly increased the sensibility of cells to heat. By reducing the time of sonication undesirable effects of cavitation on foods and beverages, such as alterations in flavour, disintegration of equipment, and costs, would be minimised. The combination of a short burst of high power ultrasound followed by heat applied at either 55 or 60°C offers the food industry a promising hurdle treatment for the killing of *S. cerevisiae* contaminating liquid suspensions and should be investigated further.

ACKNOWLEDGEMENTS

I wish to thank:

- Dr. Lynn McMaster, from who I've learnt much and was well guided and assisted by in all aspects of this research
- Dr. Bruce Mortimer, for always being willing to help and for adding valuable insight and advice
- Prof. E Carr Everbacht, Swarthmore College, Pennsylvania USA, for kindly sharing his extensive knowledge of ultrasound and cavitation with me
- Prof. Amy Vollmer, Swarthmore College, Pennsylvania USA, for kindly sharing her extensive knowledge of the biological applications of cavitation with me
- Financial assistance from the University Research Fund of the Cape Peninsula University of Technology
- Rhodes Food Group, for financial assistance
- Nampak, Research and Development, for financial assistance
- My Family, for their encouragement and moral support.
- The friends of 'spangees', thanks for doing what you do best, and for having the patience to listen to me go on about my research.

The financial assistance of the National Research Foundation towards this research is acknowledged. Opinions expressed in this thesis and the conclusions arrived at, are those of the author, and are not necessarily to be attributed to the National Research Foundation.

TABLE OF CONTENTS

CHAPTER THREE: PREPARATION OF FLUORESCENCE FLOW CYTOMETER TO DETECT *SACCHAROMYCES CEREVISIAE*

LIST OF FIGURES

LIST OF TABLES

APPENDICES

GLOSSARY

Terms/Acronyms/ Abbreviations	Definition/Explanation
nm	Nano meter
ms	Millisecond
µl	Micro liter
rpm	Revolutions per minute
V	Volt
$W.cm^{-1}$	Intensity
Hz	Hertz
Ln	Natural logarithm
Pa	Pascals
P	Pressure
$Ø_{int}$	Internal diameter
R_0	Initial bubble radius
R_{max}	Maximum bubble radius
R_B	Blakes radius
P_B	Blakes pressure
CW	Continuous wave
τp	Length of time that the pulse persists
τs	'Off time', a period in which no sound waves are generated
τv	Represents the carrier period
CFU	Colony forming unit
YPDB	Yeast peptone dextrose broth
MEA	Malt extract agar
Tv	Time value
Av	Aperture value
EDTA	Ethylenediaminetetraacetic (acid)
TO	Thiazole orange
PI	Propidium iodide
FITC	Fluorescein isothiocyanate
PE	Phytoerythrin
PerCP	Peridinin chlorophyll protein
SSC-H	Side scatter signals
FSC-H	Forward scatter signal
FL1-H	Fluorescent signal in channel 1
FL2-H	Fluorescent signal in channel 2
FL3-H	Fluorescent signal in channel 3

OD	Optical density
N_V	Viable fraction of total population
N_I	Injured fraction of total population
N_D	Dead fraction of total population
D	Decimal reduction time / D value
D_{ht55}	D value when heated at 55°C
D_{ht60}	D value when heated at 60°C
D_{us}	D value when sonicated
D_{hd55}	D value when heated at 55°C, after pre-sonication (hurdle)
D_{hd60}	D value when heated at 60°C, after pre-sonication (hurdle)
SEM	Scanning electron microscope
TEM	Transmission electron microscope
EDS	Electron dispersion spectrophotometry
n	Sample size/number
GRAS	Generally Recognised As Safe
<	'Less than'
>	'Greater than'

CHAPTER ONE
LITERATURE REVIEW

1.1 Principles of ultrasonics and its application in food systems

1.1.1 Introduction

Ultrasound refers to sound waves that are produced at frequencies above the audible limit of the human ear i.e. frequencies above 18 kHz. Ultrasound generally has two applications in the food industry: for non invasive analytical purposes and assisting with processing (Povey & Mason, 1998). These two different applications make use of a different range of frequencies. The frequencies used to induce changes in a food system are typically 20 kHz – 100 kHz (Povey & Mason, 1998).

When sound waves with a large enough pressure amplitude traverse a liquid, a phenomenon known as cavitation occurs (Scherba, Weigel & O'Brien, 1991). Cavitation, described as the 'activation' of a gas inclusion in a liquid by an acoustic field, is the process whereby many small bubbles expand and contract at a frequency corresponding to the frequency of the sound wave (Scherba *et al.*, 1991). Physical and chemical changes induced in systems when exposed to ultrasound are thought to be a result of cavitation.

Cavitation is a complex phenomenon. In order for the process to be successfully applied in industry a thorough knowledge of the fundamentals is required. These fundamentals, including both equipment and the phenomenon of cavitation, are reviewed below

1.1.2 Equipment used to generate ultrasound

There are various methods of generating ultrasound and the manner in which acoustic energy can be introduced into a liquid medium. The equipment needed for this process is composed of three main parts: a power source (generator), a transducer, and a horn (a delivery system that conveys the vibration into a liquid medium) (Povey & Mason, 1998) (Fig. 1.1).

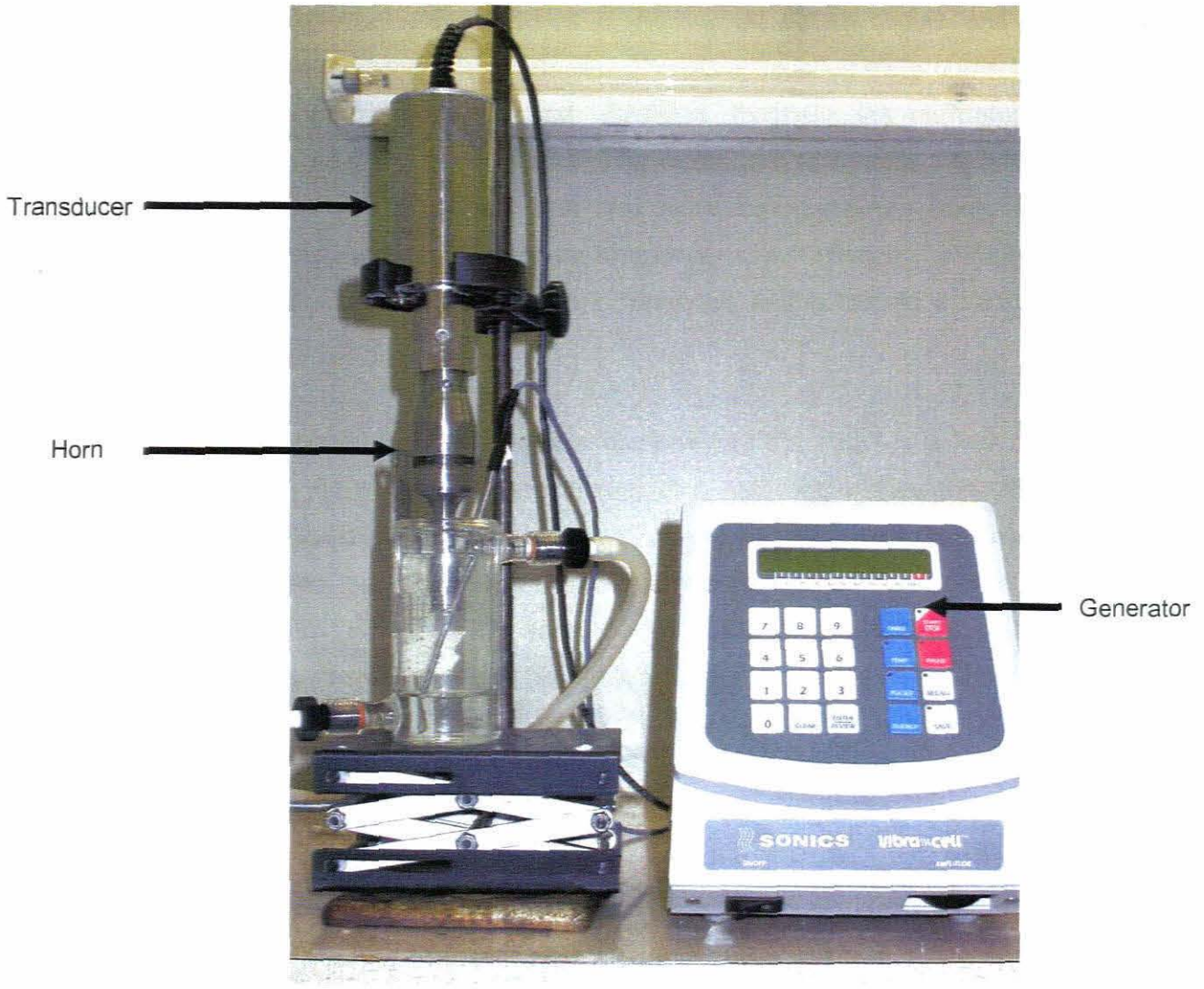

Figure 1.1: A typical ultrasound generation and delivery system. Note the three essential components: the generator, the transducer and the horn

The generator converts mains voltage into the required voltage and frequency necessary to drive the transducer.

The acoustic energy is derived from electrical energy, supplied by the generator. An ultrasonic transducer converts the electrical energy into acoustic energy. The length of the transducer should typically be a multiple of half the wavelength to optimize the efficient conversion of electrical energy to acoustic energy. For ultrasound applications requiring high power, lower frequencies (20 - 100 kHz) are preferred as the power output is inversely proportional to the square of the frequency (Povey & Mason, 1998). The two most common ultrasonic transducers are: magnetostrictive and piezoelectric (Perkins, 1990).

A common commercially available piezoelectric transducer system was utilized in this study (Sonics and Materials, 2002). These transducer devices usually consist of piezoelectric ceramic materials such as barium titanate or lead zirconate titanate. When a current is

passed through piezoelectric ceramics a mechanical stress occurs and the ceramic is displaced. The displacement is reversible. Therefore an alternating current applied across the face of the ceramic will produce vibrations. Normally the piezoelectric element is sandwiched between two metal blocks. The metal blocks protect the brittle piezoelectric element and also act as a heat sink and more importantly as linked impedances (or waveguides) in the mechanical resonant transducer circuit (Perkins, 1990; Povey & Mason, 1998). This configuration is well known in acoustics and is termed a Langevin transducer configuration.

The means by which the vibrations are conveyed to the liquid is a key component. The transducers may be attached to the bottom of a bath and deliver the vibrational energy directly into the liquid medium, such as with ultrasonic baths (used for cleaning). For high-power applications the vibration is usually carried from the transducer to the conducting medium via a horn (Fig. 1.1). The horn has the ability to transform the sound wave as the amplitude of the sound wave can be altered by the geometry of the horn. The horn is a transformer relating force and velocity components, and is analogous to an electrical transformer that relates voltage and current components. As with the transducer, the horn should generally be half the wavelength of the sound wave allowing optimal transfer of sound waves (Povey & Mason, 1998).

In this particular study a piezoelectric transducer was used to produce sound waves at a frequency of 20 kHz. The maximum displacement amplitude occurs at 124, 211 or 228 μm, depending on the horn used. The Vibracell VCX 750 is capable of maintaining a constant displacement amplitude by monitoring the current through the piezoelectric and adjusting the power on entry to the transducer (Sonics and Materials, 2002). The power reading displayed on the Vibracell unit is the electrical power supplied to the transducer and does not take into account the efficiency of the transducer.

1.1.3 Principles of acoustics

Sound is defined as a series of alternating high and low pressures travelling through a medium originating from any vibrating source (Halliday, Resnick &Walker, 2001).

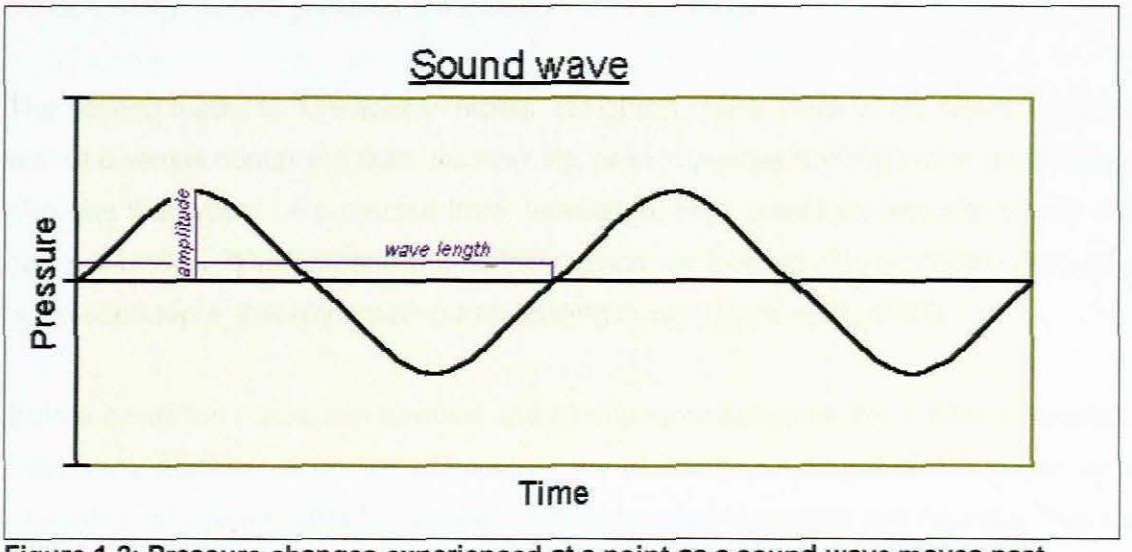

Figure 1.2: Pressure changes experienced at a point as a sound wave moves past

Figure 1.2 shows the pressure changes experienced by any point traversed by a sound wave. The distance from the base to a peak or trough of the sound wave is known as the amplitude. The greater the amplitude, the greater the change in pressure in the conducting medium and therefore the greater the power of the sound wave. The distance to complete one cycle (a peak and trough) is known as the wavelength. The frequency is the number of wavelengths passing through a point in one second, expressed as cycles/second or Hertz (Hz) (Halliday *et al.*, 2001).

Under certain conditions, sound waves are capable of inducing an effect known as 'acoustic cavitation'. Acoustic cavitation can be defined as the formation, expansion and collapse of gas bubbles due to the presence of an acoustic field. The bubbles are formed from pre-existing impurities and/or pockets of air, collectively known as 'cavitation nuclei'. Once formed, the bubbles react to the oscillating pressure (i.e. sound wave) by expanding and contracting. The expansion and contraction of the bubble can manifest in various ways, each resulting in various cavitation phenomenon (Povey & Mason, 1998).

1.1.4 Cavitation inception

Cavitation inception occurs when an acoustic field is applied to a liquid. A liquid such as pure water has a tensile strength of $1x10^8$ Pa, and therefore requires an unattainable acoustic pressure of more than $1x10^8$ Pa. However most liquids contain cavitation nuclei which act as seeds of cavitation. Cavitation nuclei are stabilised gas bubbles (Leighton 2007).

Gas bubbles are naturally removed from solution by buoyancy or dissolution but can be stabilized by two mechanisms. The first mechanism is the "Variably Permeable Skin Model" (Leighton, 1994; Duck, Baker & Starritt, 1997) where a layer of hydrophobic impurities on the surface of the bubble prevents dissolution from occurring.

The second model is "Crevices In Motes" (Leighton, 1994; Duck *et al.*, 1997). Crevices in the wall of a vessel containing fluid, the horn tip, or in impurities floating in the liquid, can be filled with gas that would be protected from dissolution. High amplitude acoustic waves cause the gas pockets to either expand out of the crevice, or to shed micro-bubbles through surface wave oscillations thereby creating free floating nuclei (Duck *et al.*, 1997).

Before cavitation nuclei can cavitate, the tensile force acting on the bubble to prevent it from expanding must be exceeded. Therefore the pressure amplitude of the sound wave must exceed a minimum threshold to allow cavitation nuclei to expand and cavitate. This threshold is a function of the equilibrium bubble radius, pressure amplitude and frequency (Apfel, 1981). Parameters such as hydrostatic pressure, temperature, dissolved gas as well as other characteristics of the liquid have an effect on these parameters (Leighton, 2007).

Once cavitation inception has occurred two possible types of cavitation can occur: inertial and non-inertial. Inertial cavitation is associated with immense bubble growth and violent collapses while non inertial cavitation is associated with bubbles lasting for many cycles (up to hours), oscillating around an equilibrium bubble radius. The type of cavitation that is induced is mainly determined by equilibrium bubble radius, pressure amplitude and frequency. There is no distinct boundary between the two types and both may occur simultaneously. This can complicate research that requires one type of cavitation or examines the influence of one type of cavitation on a test particle(s). Studying the effects of cavitation on microorganisms and optimizing the conditions of a microbicidal ultrasonic treatment will be influenced by the ratio of inertial to non-inertial cavitation components (Leighton, 2007).

1.1.5 Inertial cavitation

Inertial cavitation is characterized by an explosive growth followed by a violent collapse of the bubble, lasting for only one or two cycles. The explosive growth occurs when a cavitation nucleus is transversed by the negative pressure cycle of the sound wave. Therefore the pressure amplitude must exceed the hydrostatic pressure in order for a negative pressure to occur during rarefaction. (Rarefaction refers to the localised decrease in pressure and density in a medium, as it is transversed by a sound wave (Halliday *et al*, 2001). This can be

achieved in two ways. Either the pressure amplitude can be increased, or the hydrostatic pressure can be decreased. The smaller the cavitation nuclei are, the more negative the pressure needs to be. This is due to the fact that the surface tension is more active in smaller bubbles than larger bubbles. The result is that for every bubble radius there is an associated negative pressure that needs to be exceeded in order for inertial cavitation to occur. Alternatively for every negative pressure there is a minimum radius that the bubble must exceed in order to undergo explosive expansion. The pressure and radius threshold are known as Blake's pressure (P_B) and Blake's radius (R_B) respectively (Leighton, 1994).

The response time of the bubble i.e. the speed at which the bubble reacts to the negative pressure, is also an important property that determines whether a bubble collapse will be inertial or not. If the bubble expansion time is too long, the size of the bubble is insufficient to undergo inertial collapse once the following positive pressure wave moves past. It follows that the higher the sound frequency the less time a bubble has to expand, therefore less likely that inertial cavitation will occur. However if the amplitude is increased, the response time will increase. Therefore a direct relationship occurs between amplitude and frequency with regards to inertial threshold (Leighton, 1994). Viscous and inertial effects as well as the surface tension of the liquid also determine the response time (Leighton, 1994). In this study 20 kHz ultrasound was used. This frequency is selective for inertial cavitation.

There are two phenomena of interest that arise from inertial cavitation. These are production of free radicals due to the hydrolysis of water, and microjet formation. Both phenomena exert an influence on micro organisms (Povey & Mason, 1998)

1.1.5.1 Free radical formation and sonochemistry

Sonochemistry refers to chemical reactions that are catalyzed by acoustic cavitation (Mason, 1999).

Temperatures of 5000°C and pressures 10^5 kPa are postulated to occur during an inertial collapse (Povey & Mason, 1998). Under these conditions water molecules are split into free radicals that recombine to form hydrogen peroxide (Eq 1.1) (Inoue, Okada, Sakura & Sakakibara, 2005)

(1) $H_2O \rightarrow H^{\bullet} + OH^{\bullet}$
(2) $2OH^{\bullet} \rightarrow H_2O_2$
(3) $2OH^{\bullet} \rightarrow O^{\bullet} + H_2O$
(4) $2O^{\bullet} \rightarrow O_2$
(5) $O^{\bullet} + H_2O \rightarrow H_2O_2$

Equation 1.1

The formation of hydrogen peroxide during cavitation is directly proportional to both the amount of cavitation and the force at which the bubbles collapse. Therefore one can measure the cavitational effect by determining the amount of hydrogen peroxide formed during sonication. However measurement of hydrogen peroxide cannot distinguish between the amount of cavitation or the force of bubble collapse. The quantity of hydrogen peroxide produced during the sonication of a liquid is determined using various techniques. One method is the potassium iodide dosimetry. The hydrogen peroxide oxidizes iodide to tri-iodide (Eq 1.2). The amount of tri-iodide released is quantified by spectrophotometric analysis (OD_{352}). (Weissler, 1950)

$$2\ KI + \text{free radical} \rightarrow I_2 + 2\ KOH$$

Where free radical = $HO^{\cdot}$ or $HO_2^{\cdot}$

$$I_2 + I^- \leftrightarrow I_3^-$$

Equation 1.2 (Weissler, 1950)

Free radical formation can also be used to illuminate an area of inertial cavitation. A solution of luminol (3-aminophthalhydrazide) reacts with the free radicals, and light (430 nm) is emitted as a result (Parejo, Codina, Petrakis & Kefalas, 2000) (Ref eq. 1.3). The zone of inertial cavitation appears as a glowing blue area in the liquid being sonicated.

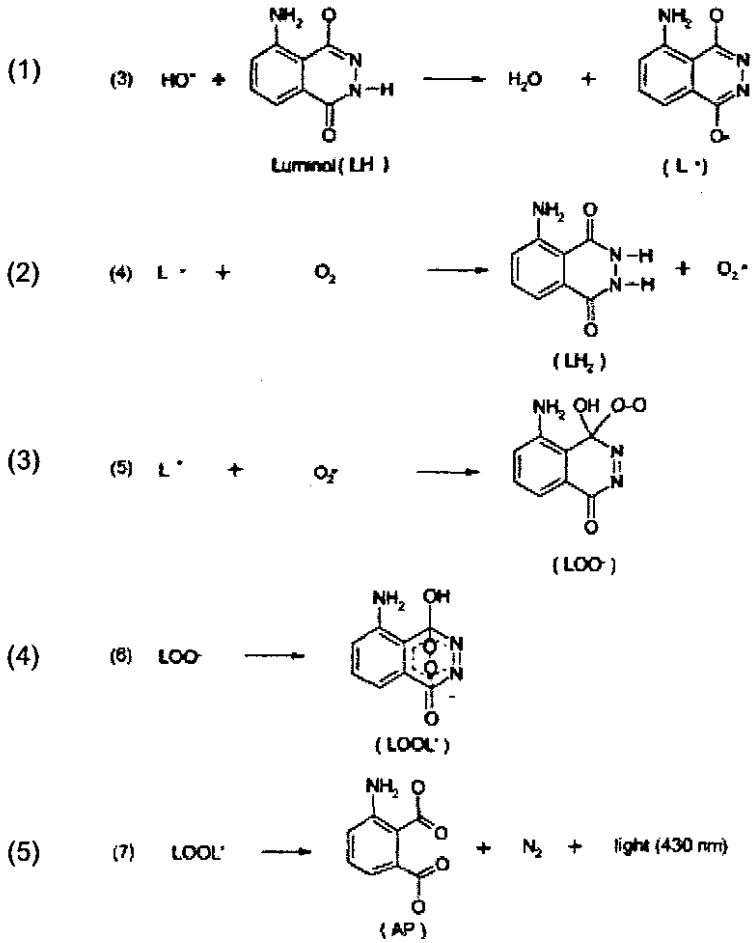

Equation 1.3

(Adopted from Parejo *et al.*, 2000)

1.1.5.2 **Microjets**

Cavitation is known to have an erosive effect. The first evidence of this was noted on submarine propellers, which become pitted after long exposure to deep seas. Studies of collapsing bubbles near the surface of an object have revealed a phenomenon known as microjets. An inertial collapse under normal circumstances is symmetrical. When a bubble collapses near the surface of an object, the surface causes the collapse to be asymmetrical. The asymmetrical collapse is characterized by a jet of water shooting through the bubble as seen in Fig. 1.3. The velocity has been calculated to be 300 $m.s^{-1}$ (Leighton, 1994, Povey & Mason, 1998)

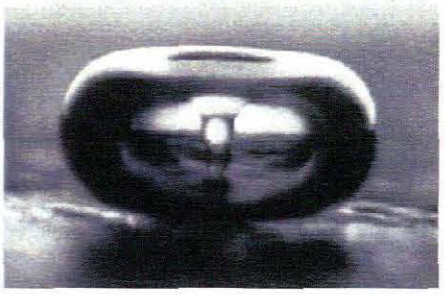

Figure 1.3: A image of a jet of water (microjet) piercing the bubble as a result of an asymmetrical bubble collapse. Bubble diameter approximately 1mm

(Image from University of Washington, Applied Physics Laboratory, Lawrence Crum, Ph.D.)

1.1.6 Non-inertial cavitation

Non-inertial cavitating bubbles are bubbles that oscillate around an equilibrium radius. The alternating pressure of the sound wave drives the oscillations. The bubbles can exist for many cycles and have been reported to last for days, for as long as sonication is continued (Leighton, 2007).

Two interactions occur between the bubble and the surrounding liquid during the bubble oscillations. The first is the phase change of water liquid external to the bubble, to water vapour within the bubble. Phase changes of the vapour in the bubble occur more rapidly than the change in bubble size and are therefore a quasi-static interaction. The second interaction is the flux of gas across the bubble boundary during expansion and contraction of the bubble. The flux of gas in and out of the bubble is unequal and results in rectified diffusion (Leighton, 1994).

1.1.6.1 Rectified diffusion

When the bubble radius is less than the equilibrium radius ($R<R_0$), the gas inside the bubble is compressed and diffuses into the surrounding liquid. The opposite occurs when $R>R_0$. Rectified diffusion is the process where, over time, there is a net migration of dissolved gas from the liquid into the bubble. There are two simultaneous mechanisms which result in this net migration: the area effect and the shell effect (Leighton, 1994).

Area effect: The net flux of gas in and out of the bubble is unequal as its surface area is greater when $R>R_0$ than when $R<R_0$. Therefore more gas diffuses into the bubble than out of the bubble (Leighton, 1994)

Shell effect: this is more complex. It refers to the concentration gradient of the dissolved gas, which is influenced by the bubble compressing the liquid surrounding the bubble (Leighton, 1994).

The area and shell effect work together to increase the size of the bubble over a period of time. If a bubble grows too large it will be removed from the solution by buoyancy, resulting in the liquid being degassed. This has a direct effect on cavitation. Alternatively the bubble may grow to a radius that lies within the inertial threshold. Hence a non inertial cavitating bubble may transform and undergo an inertial collapse. Another factor is the creation of new cavitation nuclei through the fragmentation of existing bubbles. When inertial bubbles collapse, these can fragment into many smaller bubble / cavitation nuclei. Rectified diffusion can cause these fragments to develop into cavitation bubbles (Apfel, 1981; Leighton, 1994).

1.1.6.2 **Micro-streaming**

When sound waves travel through a medium, the acoustic energy is absorbed by the medium. The momentum of the wave is conserved during the transfer of energy. As a result, a stream develops in the liquid that flows in the same direction as the sound. On a microscopic scale, microcurrents are set up due to the oscillating bubbles (Buldakov, Hassan, Zhao, Feril, Kudo, Kondo, Litvyakov, Bolshakov, Rostov, Cherdyntseva & Riesz 2009)

1.1.7 Factors that influence cavitation

Both the acoustic field and the properties of the liquid undergoing sonication influence cavitation. Therefore any change in the acoustic field or the properties of the liquid will influence cavitation. Enhancing, inhibiting, or selecting for a particular types of cavitation or increasing the force of the bubble collapse are some of the common ways in which cavitation can be altered. The manner in which various acoustic properties and liquid properties influence cavitation is discussed below.

1.1.7.1 **Acoustic Field**

- Amplitude

  As previously referred to, the amplitude must exceed a certain threshold before a bubble will undergo cavitation. In addition, the threshold between non inertial and inertial cavitation is influenced by amplitude, as inertial cavitation requires a greater displacement amplitude (Apfel, 1981;Leighton, 1994).

- Frequency

  The frequency of the sound determines the size of the cavitating bubbles. Low frequencies induce large cavitating bubbles, which decrease in size as the frequency increases (Suslick, 1989). As frequency increases, it becomes more difficult to induce cavitation. The reason is that the change in pressure experienced by cavitation nuclei

is so rapid that the nuclei have no time to expand and contract. This can be overcome by using more powerful generators and transducers to increase the amplitude (Povey & Mason, 1998).

- Bubble populations

  Population dynamics of cavitation bubbles are non linear. Most research done on the behaviour of cavitating bubbles has been conducted using a single bubble. Suslick (1989) has shown that a bubble behaves differently when other bubbles are in the vicinity. Bubbles fuse together, fragment into daughter bubbles on collapse and shed daughter bubbles via surface oscillations. In addition, non inertial bubbles can become inertial bubbles. Bubble interactions make it difficult to predict the behaviour of a population of bubbles (Apfel, 1981).

1.1.7.2 Liquid undergoing sonication

- Hydrostatic pressure

  Hydrostatic pressure influences the threshold of cavitation. An increased hydrostatic pressure requires greater pressure amplitude to reach negative pressures during rarefaction. The result is that cavitation is harder to induce. In addition, the bubble radius decreases when the hydrostatic pressure is increased, therefore some of the cavitation nuclei will dissolve away. Despite an increased cavitation threshold and less cavitation nuclei, the collapse of cavitating bubbles is more forceful (Povey & Mason, 1998). Ultrasound may be applied in beverage systems with increased hydrostatic pressure to improve the cavitational effect (Pagan, Manas, Raso and Condon, 1999). Such applications are known as manosonication (Pagan *et al.,* 1999).

- Liquid temperature

  Cavitation is also affected by temperature. Increasing the temperature increases the vapour pressure and simultaneously decreases the tensile strength of the water. Therefore cavitation threshold decreases as the temperature is increased until it reaches zero at boiling point. Higher temperatures mean that cavitation nuclei and bubbles form and grow more quickly. Although there are more bubbles cavitating, the force with which the bubbles collapse is less (Alliger, 1975). The hydrostatic pressure of applications requiring elevated temperatures may be increased (<100 °C). Therefore the force of the bubble collapse is increased, compensating for the increased vapour pressure and decreased tensile strength of water). Such applications are known as manothermosonication (Raso, Pagan, Condon & Sala, 1998).

- Dissolved gases within the liquid

  The role of dissolved gases in cavitation is relatively simple. As referred to above (Section 1.1.6), when a bubble cavitates, dissolved gas from the surrounding liquid will diffuse in and out of the bubble. The rate of diffusion during the collapse of an inertial bubble is not fast enough to allow for a constant partial pressure within the bubble. This leads to the gases being compressed during the collapse of a bubble. This has two consequences (Leighton, 1994).

  Firstly, gases have a cushioning effect on the bubble, as the gas is compressed during the collapse. It follows that a degassed solution has more violent inertial collapse as there is less cushioning gas within the bubble (Povey & Mason, 1998). The type of gas also influences the amount of cushioning that occurs. Different gasses have different solubilities in a liquid. Less soluble gases diffuse more slowly back into solution from the bubble during collapse, and therefore cushions the collapse to a greater extent than a more soluble gas (Leighton, 2007).

  Secondly, the temperature of the gas increases as it is compressed during the collapse. This results in the formation of hot spots in the middle of a collapsing bubble. Gases with a low thermal conductivity prevent the heat generated from dissipating into the surrounding liquid therefore increasing the temperature inside the bubble during collapse. Didenko and Suslick (2000) have demonstrated that associated high temperatures cause the formation of free radicals during an inertial collapse. Hence, saturation with low thermal conductivity gases, such as noble gases, increases cavitation dependant events such as free radical formation (Entezari & Kruus. 1996; Didenko, McMamara & Suslick, 2000). Moshaii, Rezaei-Nasirabad, Imani, Silatani and Sadighi-Bonabi (2008) reported that free radical yields were increased using noble gases in the order of Xe > Kr > Ar > Ne > He.

- Impurities included in the liquid undergoing sonication

  The addition of electrolytes to fluids increases the cavitation threshold similar to the manner in which the boiling point of water is increased. Polyionic electrolytes are more effective than di-ionic electrolytes as the former dissociate into more ions than di-ionic electrolytes (Povey & Mason, 1998).

  Surfactants or surface-active compounds have two effects on cavitation. Firstly it reduces the surface tension at the bubble / liquid interface therefore lowering the cavitation threshold (Leighton, 1994). These also tend to form a layer around a bubble and this hampers processes such as rectified diffusion. It also cushions the collapse of inertial bubbles. The dominating effects will depend on the surfactants used (Povey & Mason, 1998).

- Physical properties of the liquid

  The specific heat and thermal conductivities of the liquids being sonicated affect the cavitation threshold and the temperatures produced by the cavitation (Sala, Burgos, Condon, Lopez & Raso 1995).

  The viscosity of a fluid can dampen the transversing sound wave. Highly viscous media reduce the diffusion of sound waves, as the particles of the fluid are less able to vibrate. This decreases the amount of cavitation that occurs. Better penetration of viscous liquids can be achieved with lower kilohertz frequencies (Sala *et al.*, 1995).

- Geometry of equipment

  The geometry and volume of the vessel in which sonication occurs is related to the efficiency of the treatment. In addition the geometry of the horn influences cavitation. Horns that have smaller surface areas of the emitting face, concentrate the acoustic energy over a smaller area, therefore increasing the intensity of the ultrasound. The intensity is expressed as $W.cm^{-2}$ (Perkins, 1990).

1.1.8 The use of ultrasound in food processing

Ultrasound (with or without cavitation) is used in the food industry for various applications. Examples of these are: crystallization, degassing, homogenizing, extraction and tenderizing (Povey & Mason, 1998). Since the microbistatic / microbicidal effect of ultrasound was observed, much research has investigated the possibility of using ultrasound as an alternate disinfection technique. The study presented here concentrates on the disinfecting properties of cavitation in liquids.

Most ultrasound and cavitation research is conducted in water. The challenge of using ultrasound in the food or beverage industry is that beverages differ from water physically and chemically, therefore sound wave properties and the cavitation effect differ. In addition, the physical and chemical attributes of the beverage may fluctuate between production runs. Section 1.1.7 summarises the manner in which the various physical and chemical properties of a liquid influence cavitation.

In order for sonication to be industrially used as a disinfecting technique, it is important to understand how cavitation is affected by experimental parameters. Once the factors influencing cavitation have been quantified, by using methods such as potassium iodide dosimetry, the technique may be optimised for various applications.

1.2 The use of ultrasound to disinfect beverages

1.2.1 The microbicidal / microbistatic action of ultrasound

It is well known that ultrasound can induce prokaryotic and eukaryotic cell death. However results reported regarding the efficacy of ultrasound as a successful disinfectant vary widely. The precise mechanism(s) causing cell death are unknown because studying the mechanism(s) of cellular inactivation by sonication is complicated by physical and biological variables.

Physical variables include those discussed in Section 1.1.7, such as experimental design, dissolved gases, presence of electrolytes, etc. Biological variables refer to those inherent differences between microbial populations, such as growth phase, concentration, genus / species, cell shape (Piyasena, Mohareb & McKellar, 2003).

A survey of the literature clearly showed that the ultrasound equipment used differs among research groups and that these differences impact on results obtained. Changing the generator, transducer or horn can alter the frequency, amplitude, intensity, or any other sound wave property (Section 1.1.7). In addition minor changes in the liquid conducting the sound influence cavitation. These include variations in dissolved gases, temperature, cavitation nuclei, pressure, volume, all of which alter cavitation (Section 1.1.7). It is obvious that changes in experimental design can potentially alter the acoustic field and therefore the nature of the cavitation that occurs. It is critical that these variables are considered when interpreting and comparing results from different experiments done elsewhere.

As with other disinfection techniques, it can be expected that resistance to killing by cavitation would vary among microorganisms. It has been shown that Gram-positive bacteria are more resistant than Gram negative (Ahmed & Russell, 1975), smaller cells are more resistant than larger cells (Ahmed & Russell, 1975) and cocci are more resistant than rods (Alliger, 1975). Typically bacterial endospores are more resistant than vegetative cells (Sanz, Palacios, Lopez & Ordonez, 1985). Sensitivity to cavitation also seems to vary with microbial CFU.ml^{-1} and growth phase (Povey & Mason, 1998).

It is not yet clarified as to whether the killing mechanism of microbes is a result of inertial and/or non inertial cavitation. Each type of cavitation is associated with inherently different effects. In addition, the two types of cavitation occur under different circumstances. Despite the afore-mentioned problems, three mechanisms of microbial cell death / injury induced by cavitation are commonly reported. These are: damage to microbial cells by free radicals formed during inertial cavitation, shearing or abrasive forces, and cell lysis. Both of the latter mechanisms are associated with the mechanical forces of non-inertial and inertial cavitation.

Non-inertial cavitation is less violent than inertial. However reports suggested that non inertial cavitation is powerful enough to induce cell death (Kinsloe, Ackerman & Reid, 1954). The proposed mechanism is microstreaming. It was demonstrated that microstreaming is powerful enough to disrupt bacterial cell membranes, causing fractures and leaky spots that resulted in cell death (Kinsloe *et al.,* 1954). By 1975 it had been demonstrated that ultrasound causes a thinning of the bacterial cell walls that was attributed to the separation of the cytoplasmic membrane from the cell wall (Alliger, 1975).

1.2.2 Influence of ultrasound on bacteria (prokaryotic cells)

There are numerous studies documenting the effect of ultrasound on bacteria. Some of the more relevant papers are reviewed in this section.

Hao, Wu, Chen, Tang & Wu (2003) sonicated large batch volumes (800 and 1200 ml) of the cyanobacterium *Arthrospira platensis* at 20 kHz, 200 kHz and 1.5 MHz for up to 20 min. It was demonstrated that cavitation had the ability to alter the physical structure of *A. platensis.* Bumps, holes and indistinct cell edges were noted after ultrasound. It was also observed that the efficacy of the sound frequencies were in the order 200 kHz > 1.5 MHz > 20 kHz. The mechanism of cell inactivation was due to the collapse of gaseous vesicles naturally present in *A. platensis* cells as the vesicle reportedly underwent inertial collapse. In the same study it was shown, using iodine dosimetry as the indicator, that more iodide was oxidized at 200 kHz thus explaining why 200 kHz was more effective than 1.5 MHz or 20 kHz (Hao *et al.,* 2003). It was further proposed that 1.5 MHz was more effective than 20 kHz, as 1.5 MHz was calculated to be of a similar frequency to the gas vesicles theoretical natural resonance frequency.

McInnes, Engel & Martin (1990), sonicated 200 µl of a Gram negative *Photobacterium phosphoreum* suspension at 100, 200, 400, 800 Hz for 80 s. Bacterial bioluminescence was used as a quantitative measure of decreased cell activity. It was reported that when ultrasound was administered without cavitation, *Photobacterium phosphoreum* remained unaffected. Therefore cavitation was required to induce cell injury / death. Depending on the frequency, a 50-70% reduction in activity in luminescence was noted after exposure to cavitation. These authors were unable to determine the exact mechanism by which luminescence was reduced. Previous electron microscopic studies conducted by McInnes *et al.,* (1990) discounted the possibility of cell wall rupture. It was suggested that as portions of the luminescence system are bound to the cell membrane, a reduction in luminescence was associated with bacterial cell membrane damage.

Vollmer *et al.,* (1998) showed that cavitation induced four of five stress responses tested when Gram negative *E. coli* in log phase of growth was sonicated with a 1 MHz pulse acoustic field. Killing or damage only took place when cavitation was present. The stress responses activated were: membrane damage, heat shock, oxidative damage and the SOS[1] response. Also tested was the stress response to ammonia starvation. However, this was not activated under the experimental conditions used. Vollmer *et al.,* (1998) proposed that the damage caused by cavitation was due to microjets from asymmetrical bubble collapses, as well as free radical formation, both a result of inertial cavitation.

Scherba *et al.,* (1991) treated 10 ml aqueous suspensions of *Escherichia coli*, *Staphylococcus aureus*, *Bacillus subtilis* and *Pseudomonas aeruginosa* using 26 kHz for 30 min. Improved killing was achieved with increased sonication time or increased amplitude for all the species tested. It was proposed that the target for ultrasonic damage is the cytoplasmic membrane and that inactivation was due to inertial cavitation. No explanation as to the inactivation mechanism of cells was offered.

Qian, Sagers & Pitt (1997), treated the Gram negative bacterium *Pseudomonas aeruginosa* at various frequencies (44 kHz to 10 MHz) and simultaneously exposed the bacteria to antibiotics. The efficacy of ultrasound decreased with an increase in frequency. Pulsed ultrasound did not influence kill rates. However, when *P. aeruginosa* was sonicated in the presence of gentamicin sulphate, which inhibits protein synthesis, an increase in killing due to synergy was observed. It was suggested that the killing mechanism was not due to oscillatory shear forces or free radical production. Instead Qian, *et al.,* (1997), suggested that it was a result of microstreaming induced by non inertial cavitation.

The addition of solid particles to a microbial suspension undergoing sonication can enhance the killing effects of cavitation. Ince and Belen (2001) added ceramic granules, metallic zinc particles and activated carbon. It was noticed that the added particles increased the amount of cavitation. This is expected as the crevices on the particle surface harbour gas bodies, which act as cavitation nuclei. It is also likely that the solid particles punctured and disintegrated cells at the high velocities achieved when the particles were accelerated by microstreaming. The active carbon was the most effective. The authors also developed a predictive model for the inactivation of *E. coli* using this method. However this method of enhanced inactivation and predictive model is limited as food systems are more complicated than the deionised water that was used to derive the model. In addition, contamination of food product with the solid particles would be unfavourable in the food industry.

[1] The SOS repair process is induced by severe DNA damage. The recA protein participates in this repair. (Prescott *et al.,*, 1996)

A study performed by Lee, Kermasha & Baker (1989) found that the medium in which sonication occurred influenced the kill rates of *Salmonella typhimurium*. A 4 $\log_{10}$ reduction was achieved in a peptone solution. For the same ultrasonic exposure (160 kHz, 100 W), cell numbers of *S. typhimurium* decreased by more than 3 $\log_{10}$ when treated in brain heart infusion broth. The same treatment in skim milk resulted in only 2.5 $\log_{10}$ decrease (Wrigley & Llorca, 1992).

Ultrasound has also been used to remove *E. coli* biofilms. Johnson, Peterson & Pitt (1998) used 70 kHz with gentamicin sulfate to reduce *E. coli* biofilms by up to 97% in 2 hours. A 2 $\log_{10}$ reduction of *Pseudomonas aeruginosa* was measured using 70 kHz together with antibiotic erythromycin (Rediske, Rapport & Pitt, 1999). The enhanced killing effect was attributed to the increased permeability of the cell membrane due to the action of ultrasound therefore enhancing the movement of the antibiotic into the cell (Rediske *et al.*, 1999).

The bacterial endospore is typically more resistant to ultrasound than vegetative cells (Povey & Mason, 1998). Although there are many conflicting results reported, it is generally accepted that when treated with ultrasound alone, little or no effect on the endospore viability is detected. Sanz *et al.*, (1985) showed that the heat resistance of *Bacillus stearothermophilus* endospores was decreased after sonication (20 kHz, 120 W, 12°C, 40 ml, 60 min). Palacios, Burgos, Hoz, Sanz and Ordonez (1991) determined some of the effects of cavitation on *B. stearothermophilus* endospores. It was reported that ultrasound induced the release of calcium, dipicolinic acid and a glycopeptide of 7 kDa from the endospore. After sonication fatty acids, acyl glycerols and glycolipids were detected in the sonicated medium, as reported by Sanz *et al.*, (1985). A decrease in heat resistance induced by sonication was noted by Palacios *et al.*, (1991) and was attributed to the release of low molecular weight substances from the spore protoplast with consequent modification of the hydration state.

1.2.3 Influence of ultrasound on yeast (eukaryotic cells)

Research groups have also studied the effect of ultrasound on yeast. Yeasts are eukaryotic cells whereas bacteria are prokaryotic. Ciccolini, Taillandier, Wilhelm, Delmas and Strehaiano (1997), suggested that complex cell types such as eucaryotic (as opposed to organelle-free prokaryotic cells) could harbour cavitation nuclei, thereby causing both internal cavitation and internal streaming. In addition, the cell boundary, suspected by some authors to be involved in cell inactivation by cavitation, differs between yeast and bacteria. Some of the more relevant papers are reviewed in this section.

Guerrero, Lopez-Malo & Alzamora (2001) studied the influence of temperature, pH and sound wave amplitude on the survival of *S. cerevisiae*. The parameters tested were: 20 kHz frequency, 71 – 110 µm displacement amplitude, 35, 45, 55°C heat, pH 3 & 5.6. The resistance of the yeast to cavitation decreased as the amplitude increased. The combination of ultrasound and heat showed a synergistic effect at temperatures of 35 and 45°C but not at 55°C. Structural studies performed on cells after exposure to 45°C and 95.2 µm showed puncturing to the cell wall with leakage of the contents, as well as damage to cells at the subcellular level. No structural damage was observed when ultrasound was applied to cells at 55°C. Sonication at either pH 3 or 5.6 had no effect on death rates except when the amplitude was 71.4 µm and the temperature was 45°C.

Cameron (2007) reported decimal reduction times of 2.8 min when subjecting *S. cerevisiae* to 20 kHz ultrasound with a displacement amplitude of 124 µm. Using transmission electron microscopy, it was reported that intracellular damage as well as cell boundary damage occured. This supports suggestions that cavitation may occur within the cell and therefore injure / kill cells, even while the cells are still intact.

In a study involving the *S. cerevisiae* sonicated at either 1 MHz or 20 kHz for up to 30 min, Thacker (1973) demonstrated that cavitation disrupted the cell walls of the yeast. There was no evidence of intracellular damage to unruptured cells. It was suggested that cavitation caused the yeast to experience velocity gradients which resulted in yeast rotation. Rotating bodies experience periodic tension forces that can result in cell disruption. This theory agrees with experimental evidence that has shown that larger cells as well as irregular cells experience greater tension forces (Thacker, 1973). The rotation of the yeast was suggested to increase as acoustic power increased. This would expose the cell to greater tension forces. Hence treatments using higher powered ultrasonication are more effective. Furthermore Thacker (1973) used the rotating tension forces to explain the 'tail' of living cells occurring in many death curves obtained after microorganisms are subjected to ultrasound. It is commonly reported that killing rates are relatively high at the commencement of sonication, but this rate is reduced towards the completion of sonication, leaving a small population of viable cells that seem 'immune' to sonication. This small population is visible in death curves as a tail. Thacker (1973) suggested that the tail consisted of the smallest cells that experience very little tension forces due to their small size.

Kinsloe *et al.*, (1954) studied the response of *S. cerevisiae* to a 9 kHz sound field. It was found that exponential cultures of four hours were more susceptible to sonic disruption than stationary phase cultures. In the four-hour culture, 50% of the total population was comprised of budding cells, whereas the 24 hour culture only contained about 5% budding cells. With

the younger culture, an increase cell death occurred when sonication was executed at 25°C rather than at 15°C. Variation of pH (4, 5 and 7) had no significant impact on sonication-induced cell death in either culture. Electron microscopy of sonicated yeast cells revealed that many cells were fragmented. It was noted that in some cells there was fracture of the ends of cells whereas in others, the cell remained intact but they exhibited marked irregularity in the density of the protoplasm.

Tsukamoto *et al.*, 2004 used calorimetric analysis as well as plate counts in order to evaluate quantitative and qualitative change to the *S. cerevisiae*. A heat conduction type multiplex calorimeter equipped with 24 calorimetric units was used to measure the metabolic heat evolution from the growth of *S. cerevisiae* cells. Signals from the thermogram indicated microbicidal and microstatic effects. The calorimetric signals increased as the growth of the yeast cells reached maximum growth, forming a peak, and then diminished when the nutrients were exhausted. Results showed that the time required to achieve the maximum growth peak during subsequent incubation was increased after *S. cerevisiae* was sonicated.

Tsukamoto, Yim, Stavarache, Furuta, Hashiba & Maeda (2003) sonicated solutions of *S. cerevisiae* using either a horn type sonicator (27.5 kHz) or a squeeze-film-type sonicator (26.6 kHz). It was found that cell inactivation only occurred at amplitudes that exceeded the cavitation threshold, determined using potassium iodide dosimetry. The yeast cells showed pseudo first order kinetics behaviour, and kill rates increased with amplitude. Tsukamoto *et al.*, (2003) also showed that killing rates depended on the initial cell concentration. Concentrations of 10^2 to 10^5 CFU.ml^{-1} were tested at an amplitude of 4 μm. The samples with higher initial cell concentration had lower killing rates. It was suggested that it might be due to less cavitation events occurring due to the presence of more yeast cells. The squeeze type sonicator reduced the *S. cerevisiae* population by 1 $\log_{10}$ after 60 min at 0.158 W.ml^{-1}. This experiment clearly demonstrated how different kill rates are recorded for the same microorganism using different sonicators.

Ultrasound may work best as a bactericidal agent when used in combination with other processes to induce stress reactions resulting in metabolic exhaustion in the population treated. In the food industry this application is known as Hurdle Technology. Hurdle technology has been developed to keep up with the modern consumer's desire for "near to natural" foods (Gould and Gould, 1995).

Recently, Oyana *et al.*, (2009) studied the effects of sonication executed at 200 kHz on *S. cerevisiae* with the aid of flow cytometry. At that frequency, the damaging physical effects of cavitation viz., membrane damage and cell inactivation, were not noted. Instead, within the cell, DNA and RNA synthesis were inhibited possibly by the hydrogen peroxide

generated during sonication. These results again demonstrate the influence of frequency on microbistatic/cidal effects.

1.2.4 Synergism between ultrasound and other microbicidal techniques, as a hurdle technology application

Microbial stability and safety of foods can depend on the use of a combination of intrinsic, extrinsic or implicit factors. The careful combination of these factors in foods is known as Hurdle Technology, where each factor is referred to as a "hurdle" (Leistner, Rodel & Krispien 1981). By understanding how each hurdle inhibits microorganism growth, combinations of hurdles can be used to bring about microbial stability to a food (Gould and Gould, 1995). Examples of intrinsic and extrinsic hurdles applied include: temperature, water activity, pH, redox potential and high pressure. Hurdles should not adversely influence sensory qualities of the food but must prevent the microbial population present on foods from causing spoilage or food borne illness (Gould and Gould, 1995).

The success of hurdle technology relies on disturbing homeostasis of a microorganism in the presence of combination of hurdles (Gould, 1988). Ideally when Hurdle Technology is utilized, the hurdles do not have an additive effect but act synergistically (Leistner, 1994). In many cases the hurdles simultaneously target different areas of the cell (e.g. DNA, cell membrane, enzymes systems, a_w, Eh) causing cumulative stress reactions, which adversely affect the microorganism. It is suggested that it is more effective to use different preservatives in smaller quantities rather than only one at high intensity (Leistner, 1994).

Ciccolini *et al.,* (1997) demonstrated synergism between ultrasound and heat in *S. cerevisiae*. Using ultrasound at a frequency of 20 kHz and electrical powers of 50, 100 and 180 W, it was reported that $D_{S.\ cerevisiae}$ values decreased when ultrasound was combined with heat of 50 and 55°C. No synergism was recorded at 45°C. Maximum reduction in D values occurred at 100 W. The authors suggested that 50 W was not powerful enough to induce cavitation and that at 180 W acoustic clouding occurred which decreased the efficiency of sound propagation.

Guerrero *et al.,* (2001) performed another study on the combined use of ultrasound, temperature and pH in *S. cerevisiae*. The temperatures tested were 35, 45, 55°C and the pH values applied were 3 and 5.6. Ultrasound was generated at 20 kHz at amplitudes of 71.4, 83.3, 95.2 and 107.1 μm. Initial cell concentrations were $5x10^6$ cells.ml^{-1}. Contrary to Ciccolini *et al.,* (1997), Guerrero *et al.,* (2001) found that synergism occurred at 35 and 45°C but not at 55°C. Reducing pH did not enhance synergism. Transmission electron microscope

(TEM) images of the yeast showed that cell walls were punctured and cellular contents were leaking out. Injury at subcellular level was also evident.

Guerrero, Tognon & Alzamora (2005) studied the possible synergism of chitosan (1000 ppm) and ultrasound (600 W, 20 kHz, 95.2 μm) on *S. cerevisiae*. Two methods were tested – pre-incubation in a chitosan solution or exposure to sonication in the presence of chitosan. In both cases a synergistic effect was recorded. Transmission electron microscope images showed varying results, depending on the treatment. In samples where the cells were sonicated in the presence of chitosan, the cell lumen was intensely vacuolated. Swollen and loose walls were also noted. The cell walls appeared fragmented and in many locations the plasmalemma could not be visualized. When the *S. cerevisiae* cells were pre-incubated with chitosan for 30 min followed by sonication, the cell walls appeared swollen and more densely stained. Disrupted cytoplasm appeared separated from the wall. The plasma membrane was not visible.

Petin , Zhurakovskaya & Komarova (1998) proposed a mathematical model to describe the combined action of ultrasound (20 kHz, 0.053 $W.cm^{-1}$) and heat (20 – 49°C) on *S. cerevisiae*. The model determined a synergistic enhancement ratio that could be implemented to predict the degree of synergism. There was a significant correlation between the theoretical and experimental data. It was concluded that, for this particular experiment, maximum synergism occurred at 46°C.

The effects of a hurdle application using heat and pressure in combination with ultrasound were tested on *Listeria monocytogenes*. Pagan *et al.,* (1999) found that D values decreased by 65% when ambient pressure was increased to 200 kPa at 20 kHz and a 117 μm displacement amplitude was applied. A decrease in D values of 75% was achieved when the pressure was increased to 400 kPa. Increasing the temperature up to 50°C in combination with ultrasound did not have any effect on cell inactivation. Above this temperature a considerable effect was noted. When heat was used in combination with manosonication (ultrasound combined with pressure) an additive rather than synergistic effect was noted.

Pagan *et al.*, (1999) further reported that the growth temperature used to cultivate *L. monocytogenes* affected the heat resistance of the bacteria during thermosonication. Cultures grown at 4°C were half as resistant to heat as those grown at 37°C. It was also reported that lower pH and greater sucrose concentration in the growth medium increased the killing rates.

Ordonez, Sanz, Hernandez & Lopez-Lorenzo (1983) studied the effect of ultrasound in combination with heat to synergistically decrease populations of the Gram positive coccus *Streptococcus faecium* and *S. durans*. Four observations were made: (1) for cells subjected to ultrasound only, the decimal reduction time (D value) decreased as the temperature at which sonication occurred increased, (2) for cells that were sonicated and then subjected to heat, the D_{62} values were substantially less than those recorded from cells that were heat treated only, (3) for these cells, the heat resistance was reduced as the temperature at which sonication took place increased and (4) in cells subjected simultaneously to ultrasound and heat at 62°C, the effect of both agents yielded D values that were 6-11 times more effective than the D_{62} obtained without previous ultrasonic treatment.

Munkacsi and Elhami (1976) found that treatment of milk with ultrasound resulted in the elimination of 93% of coliforms. When the milk was subjected to 20 s of ultraviolet irradiation after sonication (800 kHz for 1 min), 99% of coliforms were inactivated.

The use of ultrasound (47 kHz, 200 W) to inactivate *Salmonella* spp present on broiler chicken skin had little effect. Sams and Feria (1991) found no reduction in aerobic plate counts after 0, 7 or 14 days of incubation. Sonication was more effective when used in combination with chlorine (0.5 ppm) to remove *Salmonella* from broiler skin (Lillard 1993).

A study performed by Joyce, Mason, Phull & Lorimer (2003) used ultrasound (40 kHz, 0.05 $W.cm^{-2}$) and hypochlorite as hurdles on *Klebsiella pneumoniae* populations. Electrolysis was used to create hypochlorite in a saline solution. On its own as a microcide, hypochlorite was limited, as agglomeration of the microorganism prevented the disinfectant from reaching the all *K. pneumonia* cells. It was found that all of the electrolysis treatments on *K. pneumonie* were enhanced by the use ultrasound. The beneficial effect was attributed to three factors: (1) increased mixing of the bacterial suspension, (2) mechanical damage to the bacterial cells rendering them more susceptible to attack by hypochlorite, and, (3) cavitation exerted a cleaning effect on the electrode surface, which prevented the build-up of a fouling layer, resulting in the optimal continual synthesis of hypochlorite.

Garcia, Burgos, Sanz & Ordonez (1989) studied the potential of ultrasound to act as a hurdle for extending the shelf life of food. It was found that there was no synergistic effect when a population of *Bacillus subtilus* was subjected to ultrasonic cavitation (20 kHz and 150 W power) followed by sequential heat (100°C). However when *B. subtilus* endospores were treated with ultrasound (20 kHz and 150 W) and heat (70 – 95°C) simultaneously, a synergistic effect was noticed. Heat resistance of the endospores was reduced by 70% when exposed to 70°C and 99.9% when exposed to 95°C. When using a combination of pressure

(500 kPa), heat (110 – 112°C) and ultrasound (20 kHz and 150 µm) (manothermosonication), the heat resistance of *B. subtilus* endospores underwent a 10 fold reduction compared to the use of heat only (Sala *et al.*, 1995). Raso *et al.*, (1998) also demonstrated that manothermosonication was more effective than thermosonication. By increasing sound wave amplitude, microbicidal properties of the treatment were increased. Increasing the pressure up to 500 kPa increased lethality. However, any further increase in pressure decreased the lethality of the treatment (Raso *et al.*, 1998).

Although results vary, it is evident that ultrasonic cavitation has potential for use as a hurdle in the food industry for disinfection of beverages. In combination with other factors, ultrasonic cavitation is more effective as a microbicide than when used on its own.

1.3 Aims and Objectives

The primary aim of this study was to investigate the effect of high power ultrasound (20 kHz, 124 µm amplitude) and/or moist heat (55°C and 60°C) on *Saccharomyces cerevisiae* strain GC210 (MATα lys2) suspended in physiological saline as a model system. This was to be performed by conducting quantitative and qualitative cell measurements using fluorescent flow cytometry. The fluorophores selected were thiazole orange (TO) and propidium iodide (PI).

Prior to achieving this aim, objectives were firstly to calibrate the ultrasound system used (Vibracell VCX 750, Materials and Sonics, Conn., USA) such that the equipment generated constant and optimum cavitation. Secondly, it was essential to produce a fluorescent flow cytometric assay, commonly used with mammalian cells, that was suitable for use with *S. cerevisiae*.

Finally, from this model system, it was hoped to provide data that could be used by the food industry as a guide for using combined ultrasound and heat as hurdles for inactivating yeasts contaminating various beverages or effluents.

CHAPTER TWO

FUNDAMENTAL INVESTIGATION INTO THE INFLUENCE OF EXPERIMENTAL PARAMETERS ON INERTIAL CAVITATION

2.1 Introduction

Acoustic cavitation is a result of an interaction between sound waves and the liquid through which they transverse (Section 1.1.4). The number and properties of cavitating bubbles are influenced by the properties of the acoustic wave (frequency, amplitude, pulsed wave)(Section 1.1.7).

The sound wave properties are in part determined and controlled by the generator connected to a transducer. The geometric properties of the transducer and horn system conveying the sound wave to the liquid also influence both the sound wave and resultant cavitation (Section 1.1.7).

Sound waves are affected by the intrinsic (dissolved gas content, hydrostatic pressure) and extrinsic parameters (volume, depth of the horn beneath the surface) of the liquid through which they propagate. The influence of these parameters on sound waves is reflected by changes in the properties of the cavitation produced.

Because of these variables, it is important that the effect of experimental setup on cavitation is predetermined before studying microbicidal application of cavitation. Studying the effect of various key parameters of the experimental setup should:

- prevent misinterpretation of results;
- increase the reproducibility of experiments;
- optimize experimental setup to achieve maximum cavitation for microbicidal applications

The influence of these variables on the microbicidal effects of cavitation has been outlined in Section 1.2.1 of the literature review. This chapter investigates the effect of various experimental parameters on cavitation. This was done by the use of two sonochemical techniques viz., potassium iodide oxidation and luminol fluorescence. These sonochemical techniques provide rapid and accurate means of quantitatively and qualitatively determining cavitation. However it must be emphasised that only inertial cavitation can be measured this way.

2.2 Methods and Materials

Two sonochemical techniques were used to gauge the influence of various experimental setup on cavitation. These were the use of luminol (3-aminophthalhydrazide) (Atanassova *et al.*, 2005) and iodine oxidation (Weissler, 1950) techniques. The Vibra-Cell VCX 750 ultrasound apparatus was assembled in a similar manner for all assays.

2.2.1 The influence of horn type on cavitation

Three types of Vibra-Cell horns were tested in order to determine which horn yielded optimum cavitation (Table 2.1, Fig. 2.1 & 2.5). These were the tapered microtip (A), the stepped microtip (B) and the standard horn.

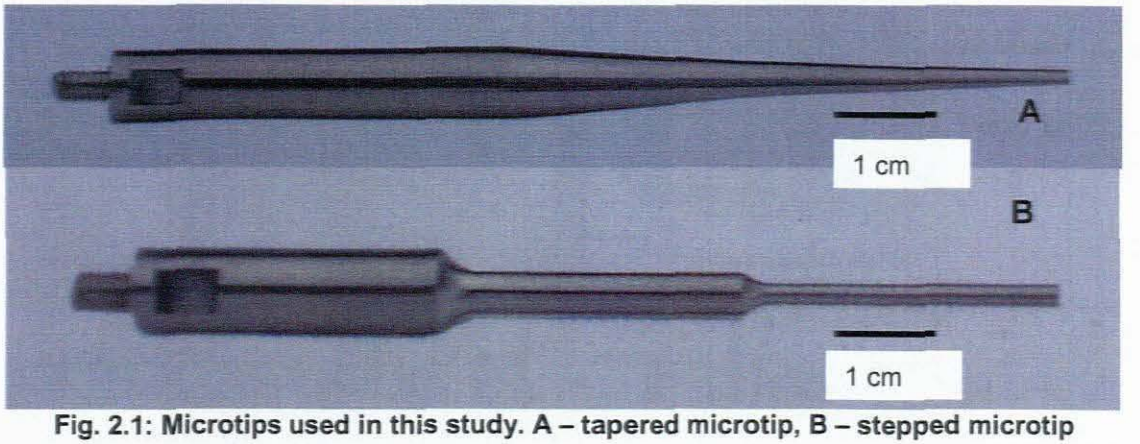

Fig. 2.1: Microtips used in this study. A – tapered microtip, B – stepped microtip

Table 2.1: Specifications of the Vibra-Cell horns used. (Sonics and Materials, 2002)

	Horn type		
	Standard	Tapered microtip	Stepped microtip
Volume range	10 – 250 ml	1 – 10 ml	250 µl – 10 ml
Amplitude*	124 µm	228 µm	211 µm
Tip diameter	13 mm	3 mm	3 mm

* Maximum displacement amplitude

The horns were individually attached to a Vibra-Cell 20 kHz piezoelectric transducer connected to the Vibra-Cell 750 VCX power unit (Fig. 2.2). The horns are constructed from a titanium alloy (titanium aluminium vanadium, TI-AL-4V) (Sonics and Materials, Connecticut, USA, 2002).

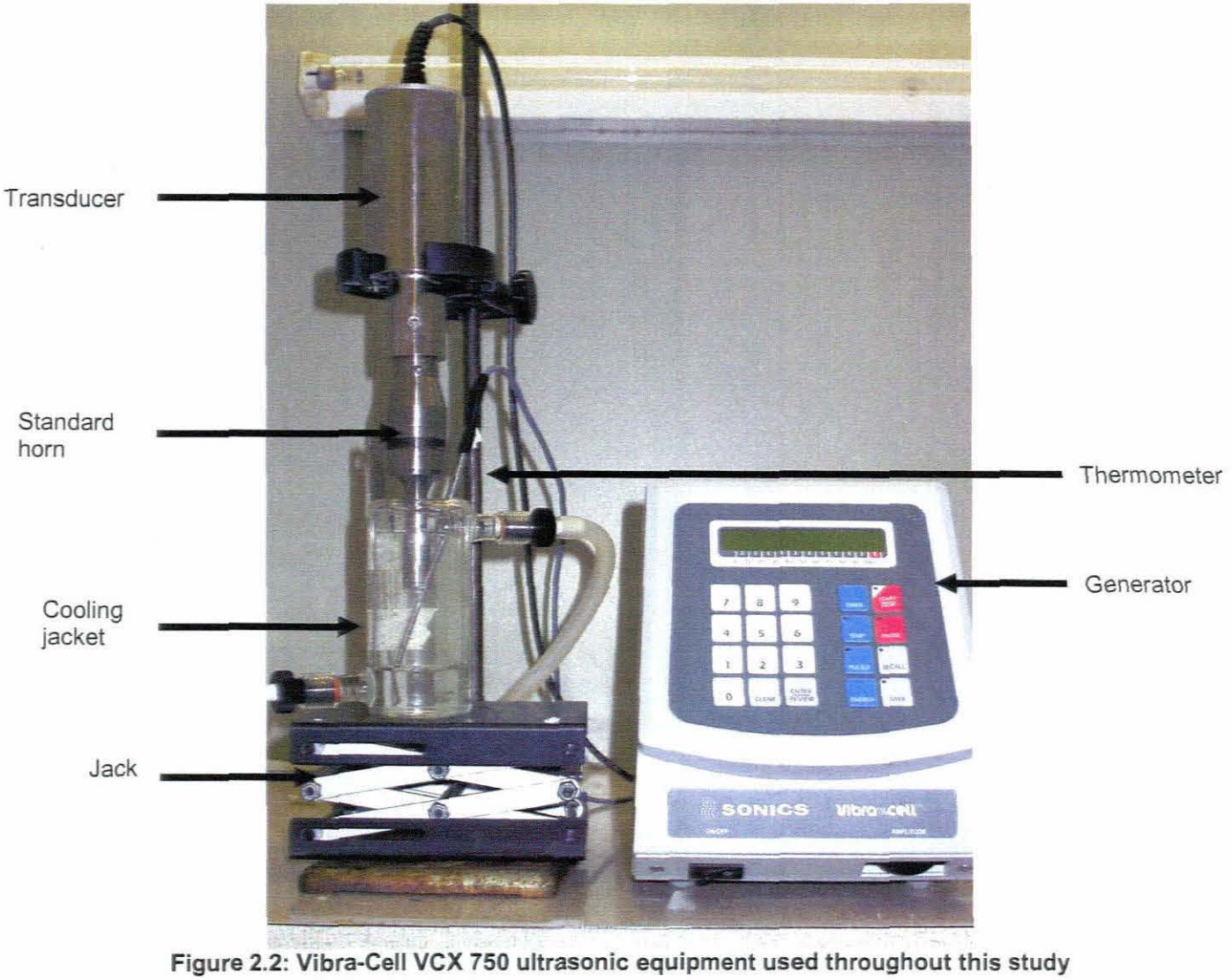

Figure 2.2: Vibra-Cell VCX 750 ultrasonic equipment used throughout this study

The volume of solution to undergo sonication depended on the horn used. Unless stated otherwise a volume of 100 ml was used with the standard horn, and 5 ml were used with either the tapered or stepped microtips. The required volumes of sterile, degassed saline water (0.8% NaCl m/v) were carefully decanted into either a Vibra-Cell 100 ml glass-cooling jacket (100 mm x 40 mm) for the standard horn or into a Vibra-Cell 10 ml glass-cooling jacket (54 mm x 18 mm) for the microtips. To avoid increasing the dissolved gas content, solutions were decanted from a reservoir of degassed water into the cells by siphoning through silicon tubing ($Ø_{int}$ 4 mm). All containers and horns were sterilized in sealed paper packets or aluminium foil using an autoclave (121°C, 10^4 kg.m^{-2}, 15 min) (Model HA-300D, Hirayama Manufacturing Corporation, Japan).

Glass cooling jackets containing known volumes of solution were connected by silicone tubing ($Ø_{int}$ 7 mm) to a circulating cooling water bath, (Thermomix 1440, B, Braun Melsungen AG, Germany) set at 10°C. The water in the bath was circulated through the glass cooling

jacket by a Braun Melsungen AG, Thermo Mix 1440 (Germany) pump (Fig. 2.3). The flow rate of the cooling water was 80 $ml.s^{-1}$.

Fig. 2.3: The Thermomix 1440, Braun Melsungen AG (Germany) pump used for circulating cooling water (10°C) through glass cooling jackets

The glass cooling jackets were accurately positioned on a Vibra-Cell laboratory jack, beneath the horn attached to the Vibra-Cell unit (Fig. 2.2). Unless stated otherwise, the glass cooling jacket containing the cooled degassed solution to undergo sonication was raised using a Vibra-Cell laboratory jack, such that the tip of the standard horn was situated 40 mm above the base of the 100 ml glass cooling jacket, and 10 mm above the base of the 10 ml glass cooling jacket for both the stepped and tapered microtips. It was also ensured that the horns made no contact with the sides of the glass cooling jacket.

The luminol or iodine solutions, constituted as described in Section 2.2.1., were sonicated continuously for 5 min, and cooled by 10°C circulating water. The maximum allowable electrical power for each horn was used i.e. 100% electrical power for the standard horn and 40% electrical power for the tapered and stepped microtips. This corresponded to displacement amplitudes of 124 µm for the standard horn and 228 µm and 211 µm for the tapered and stepped microtips respectively (Table 2.1). The Vibra-Cell 750VCX is designed

such that a constant displacement amplitude is maintained, regardless of varying load conditions (Sonics and Materials, 2002).

2.2.1.1 Location of zones of maximum inertial cavitation, using luminol

Prior to sonication, 500 ml distilled water were measured into a 500 ml Duran Schott bottle (Schott UK Ltd, United Kingdom). Teflon tape was secured around the thread of the bottle and the lid was loosely fitted (Fig. 2.4). The distilled water underwent a standard autoclave cycle (121°C, 10^4 kg.m^{-2}, 15 min). On completion of the cycle, the bottle lid was immediately tightened while the headspace was filled with steam. Thereafter the sterile, degassed water was cooled to ambient temperature (22°C). The luminol solution was comprised of: 100 g.L^{-1} luminol (Biolab Diagnostics, Midrand, South Africa), 0.05 M boric acid (Biolab Diagnostics) and 8.4 x 10^{-4} M $CoCl_2.6H_2O$ (Biolab Diagnostics) (Atanassova *et al.*, 2005). The pH was adjusted to 9 using 1 M NaOH (Biolab Diagnostics) (Atanassova *et al.*, 2005).

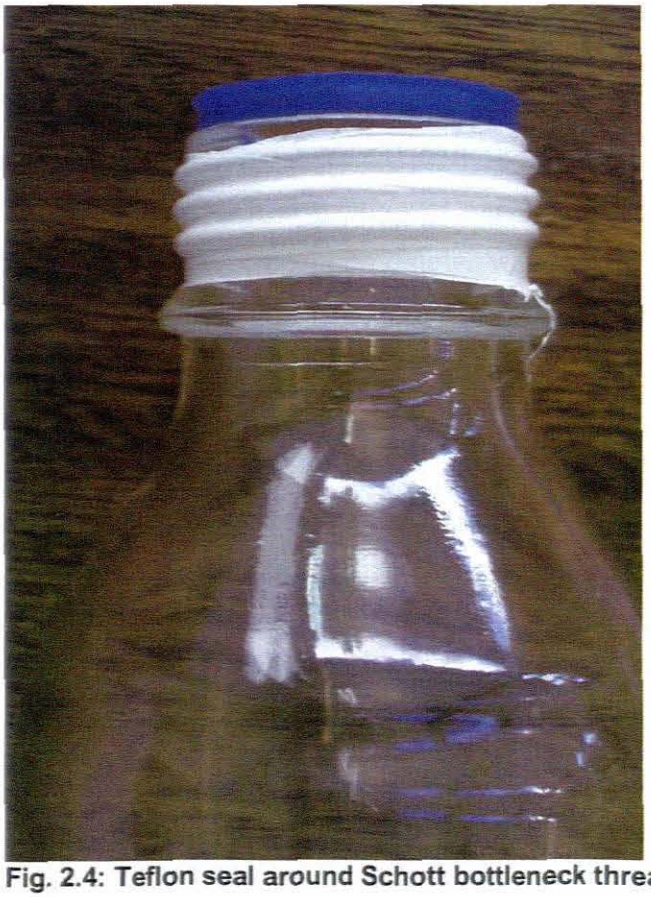

Fig. 2.4: Teflon seal around Schott bottleneck thread.

The experiments were conducted in a dark room where all visible light was excluded. A Nikon E4500 COOLPIX digital camera was placed on a tripod at a horizontal distance of 60 mm from the cooling jacket. The camera settings were:

- Tv = 300 s
- Av = f/2.6
- ISO speed = 100

such that a constant displacement amplitude is maintained, regardless of varying load conditions (Sonics and Materials, 2002).

2.2.1.1 Location of zones of maximum inertial cavitation, using luminol

Prior to sonication, 500 ml distilled water were measured into a 500 ml Duran Schott bottle (Schott UK Ltd, United Kingdom). Teflon tape was secured around the thread of the bottle and the lid was loosely fitted (Fig. 2.4). The distilled water underwent a standard autoclave cycle (121°C, 10^4 kg.m^{-2}, 15 min). On completion of the cycle, the bottle lid was immediately tightened while the headspace was filled with steam. Thereafter the sterile, degassed water was cooled to ambient temperature (22°C). The luminol solution was comprised of: 100 g.L^{-1} luminol (Biolab Diagnostics, Midrand, South Africa), 0.05 M boric acid (Biolab Diagnostics) and 8.4 x 10^{-4} M $CoCl_2.6H_2O$ (Biolab Diagnostics) (Atanassova *et al.*, 2005). The pH was adjusted to 9 using 1 M NaOH (Biolab Diagnostics) (Atanassova *et al.*, 2005).

Fig. 2.4: Teflon seal around Schott bottleneck thread.

The experiments were conducted in a dark room where all visible light was excluded. A Nikon E4500 COOLPIX digital camera was placed on a tripod at a horizontal distance of 60 mm from the cooling jacket. The camera settings were:

- Tv = 300 s
- Av = f/2.6
- ISO speed = 100

Exposures to 5 min sonication in either 100 ml or 5 ml luminol solution for the standard horn and the microtips respectively were recorded. Digital images were edited using Adobe® Photo Deluxe™ 2.0 software. The digital images were enhanced as described in Appendix 2.A.

2.2.1.2 The use of tri-iodide to relate efficiency of horn type to inertial cavitation generation

The sonication apparatus was assembled as described in Section 2.2.1. A potassium iodide solution was made up according to Koda, Kimura, Kondo & Mitome, (2002). In addition, ammonium heptamolybdate (0.01% $m.v^{-1}$) $(NH_4)_6Mo_7O_{24}.4H_2O$ (Biolab Diagnostics) was added to the solution. The distilled water used for the iodine oxidation solution was sterilized and degassed as described in Section 2.2.1.1

After 5 min of sonication, the solution was cooled to room temperature by the circulating 10°C water. Once cooled, 1 ml volumes of the iodine solution were removed from the glass cooling jackets and the optical density was measured at a wavelength of 352 nm (OD_{352}) using a Beckmann Model DU 650 spectrophotometer (Beckmann Coulter Inc, CA, United States of America). The OD_{352} of each 1 ml sample was automatically recorded every 6 s over 3 min. The spectrophotometer was calibrated using 1 ml of potassium iodine solution removed from the glass treatment cell prior to sonication. An increase in OD_{352} indicated an increase in inertial cavitation (Hao *et al.*, 2003).

2.2.2 The effect of the duration of sonication on inertial cavitation

A potassium iodide solution was made up as described in Section 2.2.1.2. Aliquots (100 ml) of potassium iodide solution were sonicated at 124 µm displacement amplitude in the 100 ml glass-cooling jacket, using the Vibra-Cell standard horn (Sonics and Materials, 2002). The solution was sonicated for 10 min, and during that time 1 ml samples were removed every minute for spectrophotometric analysis (OD_{352}), using a Beckmann Model DU 650 spectrophotometer. Determination of tri-iodide formation was done using the method described in Section 2.2.1.2. Horn immersion depth was 40 mm above the base of the container. The solution was cooled throughout by circulating water at 10°C using a Thermomix 1440, B, Braun Melsungen AG pump. Each test was repeated five times.

2.2.3 The effect of volume of treated solution on inertial cavitation

A potassium iodide solution was made up (Section 2.2.1.2). Volumes of 50, 60, 70, 80, 90 and 100 ml sterile saline (0.8% m/w) were sonicated at 124 µm displacement amplitude in the 100 ml glass-cooling jacket, using the standard horn. The solution was sonicated for

5 min, after which 1 ml was removed for spectrophotometry. Determination of tri-iodide formation was done using the method described in Section 2.2.1.2. The horn depth was fixed at 20 mm above the base of the container for all volumes tested. During sonication, circulating water at 10°C cooled the solution as described in Section 2.2.1. Each test was repeated five times. All other parameters were kept constant.

2.2.4 The effect of horn placement on inertial cavitation

A potassium iodide solution was made up as described in Section 2.2.1.2. The Vibra-Cell standard horn was immersed to depths of 20, 30, 40 or 50 mm above the base of the container of 60 ml of the solution in the glass cooling jacket. Sonication was done using maximum electrical power output in the 100 ml glass-cooling jacket. The solutions were sonicated for 5 min, after which 1 ml was removed for spectrophotometry. Determination of tri-iodide formation was done using the method described in Section 2.2.1.2. During sonication, water circulating at 10°C cooled the solution as described in Section 2.2.1. Analyses were determined in triplicate for all depths tested.

2.2.5 Effect of pulsed vs. continuous wave application on inertial cavitation

A potassium iodide solution was made up (Section 2.2.1.2). The Vibra-Cell unit was programmed such that pulses of 20, 40, 60 or 80% duty cycle were achieved. A period of 5 s was used in all experiments (that is a total 'on' and 'off' time for each pulse was 5 s). The Vibra-Cell unit was adjusted such that a total 'on' time of 5 min was achieved for all experiments. Sonication was performed at 124 μm displacement amplitude in the 100 ml glass-cooling jacket using the standard horn. After sonication, 1 ml aliquots were removed for tri-iodide determination using spectrophotometry (Section 2.2.1.2). As a comparison, a 5 min continuous sound wave application was applied under same conditions as was the pulsed sound wave described above. Horn immersion depth was 40 mm above the base of the container. During sonication, circulating water at 10°C cooled the solution as described in Section 2.2.1. Analyses were determined in triplicate for all pulses tested.

2.2.6 The effect of selected dissolved gases (O_2, N_2,or Ar) on inertial cavitation

2.2.6.1 The effect of O_2, N_2 and Ar on inertial cavitation, as indicated by tri-iodide

A potassium iodide solution was prepared (Section 2.2.1.2). The solution was degassed by autoclaving at 121°C for 15 min (Section 2.2.1.1). Oxygen (O_2), nitrogen (N_2) or argon (Ar) were bubbled through the solutions for 20 min (6000 $ml.h^{-1}$). The solutions were kept in an enclosed plastic bag while the gas was bubbled through. This sealed environment had previously been flushed with oxygen, nitrogen or argon. The solution was sonicated for 5 min using displacement amplitude of 124 μm in the 100 ml glass-cooling jacket, using the standard horn. The standard horn was positioned 40 mm above the base of the cooling glass

container. After 5 min, 1 ml was removed for spectrophotometry. Each test was repeated three times. Determination of tri-iodide formation was done as described (Section 2.2.1.2).

2.2.6.2 The effect of O_2, N_2 and Ar on inertial cavitation, as indicated by luminol fluorescence

A luminol solution was made up (Section 2.2.1.2). Oxygen, nitrogen or argon was bubbled through the solutions for 20 min (Section 2.2.6.1). The solutions were kept in an enclosed plastic bag while the gas was bubbled through. The closed environment had previously been flushed with oxygen or nitrogen or argon. The solution was sonicated for 5 min at a displacement amplitude of 124 μm in the 100 ml glass-cooling jacket, using the standard horn. The standard horn was positioned 40 mm above the base of the cooling glass container. The experiments were conducted in a dark room where all visible light was excluded. A Nikon 4500 COOLPIX digital camera was placed on a tripod at a horizontal distance of 60 mm from the cooling jacket. Refer to Section 2.2.1.1 for the camera settings.

The Nikon 4500 COOLPIX digital camera was set to record a 5 min exposure of cavitation occurring in 100 ml luminol solution. Digital images were edited using Adobe® Photo Deluxe™ 2.0 software. The digital images were enhanced as described in Appendix 2.A.

2.2.7 The effect of hydrostatic pressure on inertial cavitation

A potassium iodide solution was made up as described in (Section 2.2.1.2). Aliquots (50 ml) were placed in a Vibra-Cell stainless steel 'Sealed Atmosphere Treatment Chamber'. The chamber was pressurized with nitrogen gas (Afrox, Cape Town, South Africa) at pressures of 100, 200, 300, 400 or 500 kPa. Sonication was conducted at 31, 62 or 124 μm. The solutions were sonicated for 5 min, after which 1 ml was removed for spectrophotometry. Tri-iodide release was determined using spectrophotometry (Section 2.2.1.2). During sonication, water circulating at 10°C cooled the solution (Section 2.2.1). Tests were done in triplicate for all pressures tested.

2.3 Results and Discussion

2.3.1 The influence of horn type on cavitation

Horns in ultrasonics have two functions; firstly, to convey the vibrations from the transducer to the liquid to be sonicated and secondly, the horn geometry influences properties of the sound wave. The shape of the horn as well as the ratio between the area of the receiving and emitting face (D:d) increases or decreases the intensity ($W.cm^{-2}$) of the acoustic wave, and therefore the amplitude (Section 1.1.7). Amplitude is directly proportional to the amount of cavitation (Povey and Mason, 1998).

The smaller diameter of the microtips (3 mm), when compared to that of the standard horn (13 mm), causes the same vibrational energy produced by the transducer to occur over a smaller area. The displacement amplitude of the microtip is therefore greater than the standard horn. The displacement amplitude of the microtips is 211 and 228 µm, whereas the standard horn is 124 µm (Table 2.1). Furthermore the geometry of the two microtips further impacts on the amplitude, even though both have the same D:d ratio. A tapered shape horn increases the sound wave intensity exponentially, unlike the stepped horn which increases the sound wave intensity in a linear manner. Hence, for the same tip diameter of 3 mm, the tapered horn has a greater displacement amplitude than the stepped horn (Materials and Sonics, 2002; Povey and Mason, 1998).

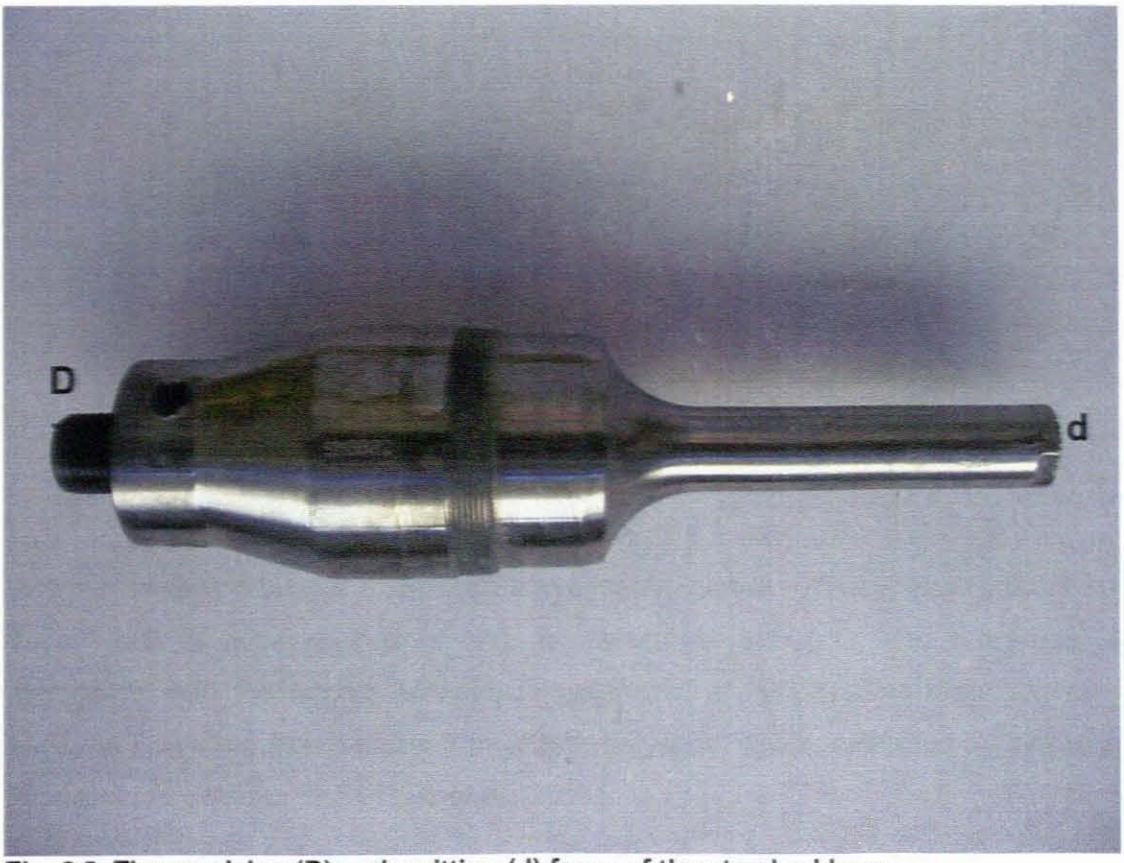

Fig. 2.5: The receiving (D) and emitting (d) faces of the standard horn

2.3.1.1 Location of zones of maximum inertial cavitation, determined by using luminol

Under basic conditions (pH >7) monodissociated luminol reacts with hydroxyl radicals to form a luminol radical (reaction 1, Equation 2.1). In the presence of oxygen, this is oxidized to form an unstable 5-aminohyphenthalazine-1,4dione (reaction 2, Equation 2.1). This compound undergoes internal rearrangement to form an endoperoxide, which decomposes and emits light at 430 nm, known as chemiluminescence (reaction 4 and 5, Equation 2.1) (Parejo *et al.*, 2000)

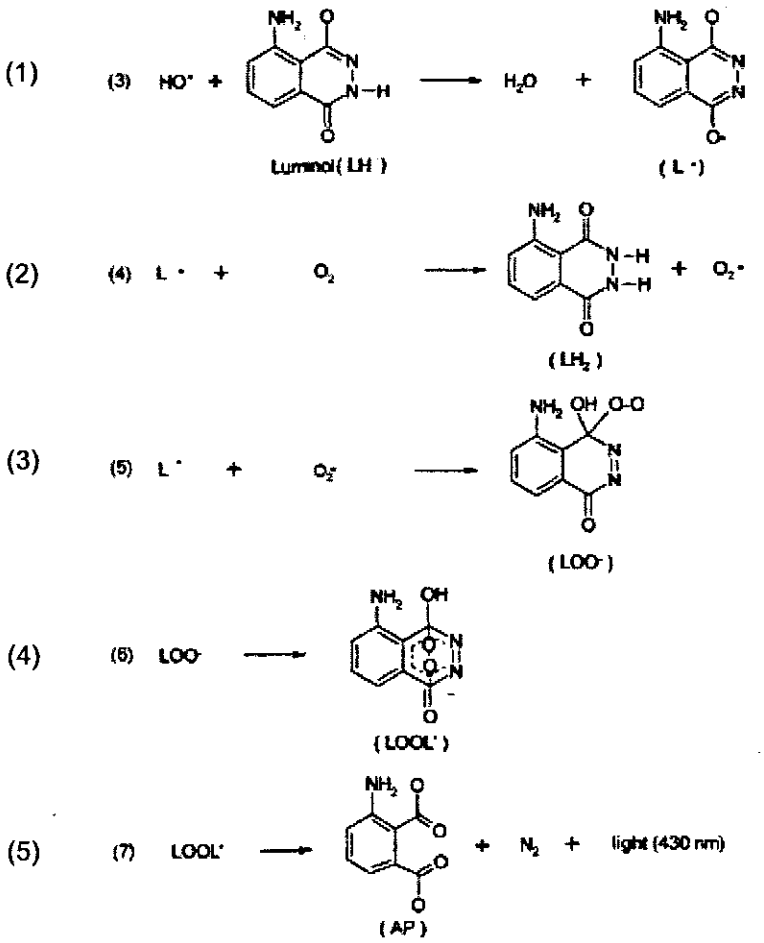

Equation 2.1

(Adopted from Parejo *et al.*, 2000)

When a cavitation bubble undergoes a symmetric inertial collapse, free radicals are formed as a result of micro-regions of high temperatures (5 500°C) and pressures (10^5 kPa) associated with the bubble collapse (Piyasena *et al.*, 2003). The formation of hydrogen peroxide and other free radicals from the hydrolysis of water, catalysed by inertial cavitation is outlined in Equation 2.2 (Inoue *et al.*, 2005).

(1) $H_2O \rightarrow H^{\bullet} + OH^{\bullet}$
(2) $2OH^{\bullet} \rightarrow H_2O_2$
(3) $2OH^{\bullet} \rightarrow O^{\bullet} + H_2O$
(4) $2O^{\bullet} \rightarrow O_2$
(5) $O^{\bullet} + H_2O \rightarrow H_2O_2$

Equation 2.2

The free radicals generated react with luminol, forming a region of blue light. This appeared as a discrete zone in the solution (Fig. 2.6). A Nikon 4500 Cool Pix digital camera was used to record areas of chemiluminescence during sonication. The images clearly indicated localized regions of maximum inertial cavitation. Non-inertial cavitation does not produce free radicals as the temperatures and pressures reached during bubble collapse are not sufficient. Therefore luminol does not detect non-inertial cavitation.

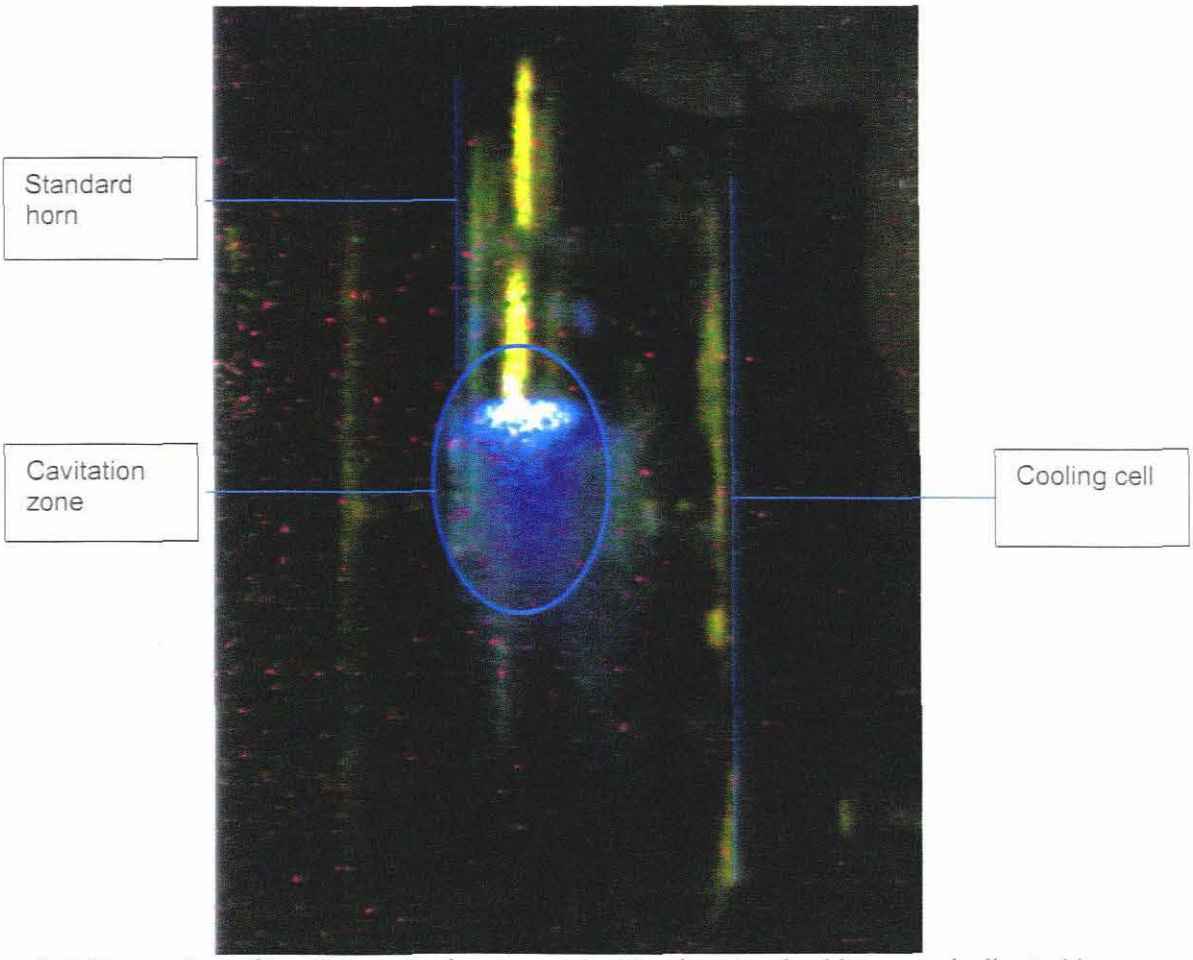

Fig. 2.6: The region of inertial cavitation generated by the standard horn, as indicated by luminol (5 min exposure)

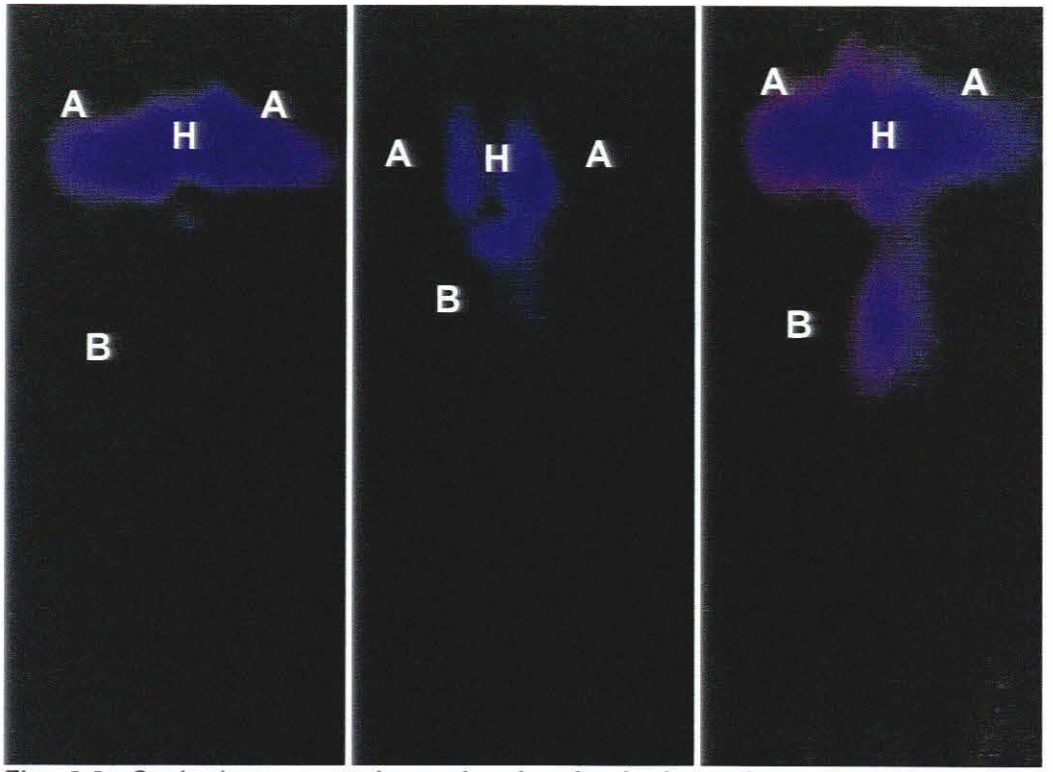

Fig. 2.8. Cavitation zones, located using luminol, produced by the tapered microtip. (A) Indicates cavitation zones adjacent to the sidewalls of the microtip. (B) Indicates cavitation zones created at the end of the microtip. (H) indicates the position of the horn tip

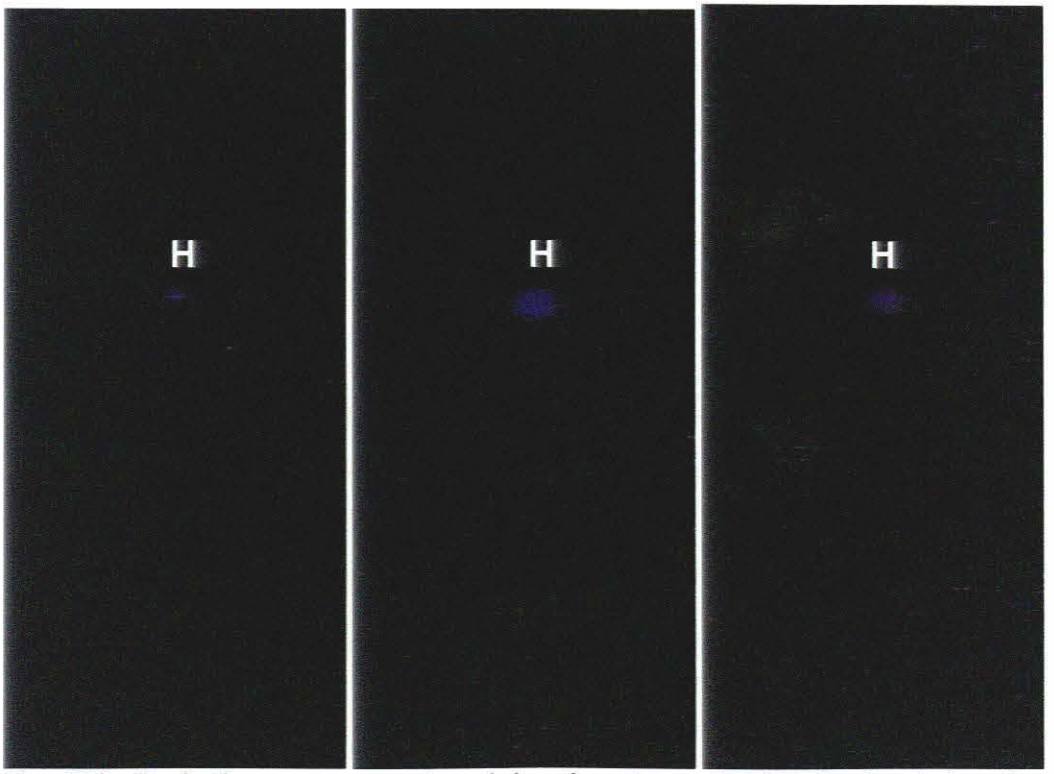

Fig. 2.9: Cavitation zones produced by the stepped microtip located using luminol. (H) indicates the microtip base.

In summary, the luminol studies clearly indicated that the stepped microtip was least effective in producing inertial cavitation and the cavitation 'zone' was inconsistent (Fig. 2.9). The tapered microtip produced a spatially uneven, inconsistent cavitation zone. It was however more intense than that produced by the stepped microtip. Horn specifications as supplied by the manufacturers (Sonics and Materials, 2002) state that the displacement amplitude of the tapered microtip (228 µm) is greater than that of the stepped microtip (211 µm), which in turn is greater than the standard horn (124 µm)(Table 2.1). However from results obtained in this study, it was clearly evident that despite having the lowest displacement amplitude, the standard horn generated a reproducible intense cavitation zone. The reason for this difference noted between the microtips and standard horn is unclear, but may be related to the intensity ($W.cm^{-2}$) of the horns.

2.3.1.2 The use of tri-iodide to determine the influence of horn type on the generation of inertial cavitation

Quantitative measurement of iodine oxidation can be used to assess inertial cavitation. Free radicals, formed from water during sonication (Eq 2.2), oxidize a potassium iodide (KI_{aq}) solution to produce tri-iodide (I_3^-) (Eq 2.3). Tri-iodide absorbs light at a wavelength of 352 nm. Therefore as cavitation commences and forms free radicals, iodide is oxidized to tri-iodide. Hence the optical density of the solution at 352 nm increases.

$$2\ KI + \text{free radical} \rightarrow I_2 + 2\ KOH$$
$$\text{Where free radical} = HO^{\cdot} \text{ or } HO_2^{\cdot}$$

$$I_2 + I^- \leftrightarrow I_3^-$$

Equation 2.3

Tri-iodide is unstable and is reduced back to I_2 and I^- (Eq 2.3) (Weissler, 1950). Decomposition of tri-iodide is suppressed by buffering the potassium iodide solution to a basic pH. The tri-iodide was required to be stable for up to 10 min after sonication, allowing enough time for sampling and spectrophotometric analysis. Therefore a preliminary experiment was conducted to determine the stability of tri-iodide over a 10 min period after sonication. Results proved that the tri-iodide formed during sonication was stable for 10 min after sonication and did not revert to I_2 and I^- (Appendix 2.B). It should be noted that the luminol technique indicated localized sites of cavitation, whereas iodine oxidation provided a quantitative estimate of inertial cavitation.

Iodine oxidation findings supported the results obtained from luminol i.e. that when the standard horn was used, a reproducible cavitation field was recorded. After 5 experiments an average OD_{352} of 0.1833 ±0.0017 was measured after 5 min sonication using the standard

horn. Values of 0.1028 ±0.027 and 0.0230 ±0.0141 were measured for the tapered and stepped microtip respectively (Fig. 2.10). All horns were operated at the maximum allowable amplitude. It is therefore suggested that the tapered and stepped horns produced 43.92% and 77.63% less inertial cavitation respectively, than did the standard horn. In addition standard deviation measurements support the observation that the standard horn produced the most consistent inertial cavitation (Fig. 2.10). It was therefore decided to use only the standard horn in subsequent experimentation.

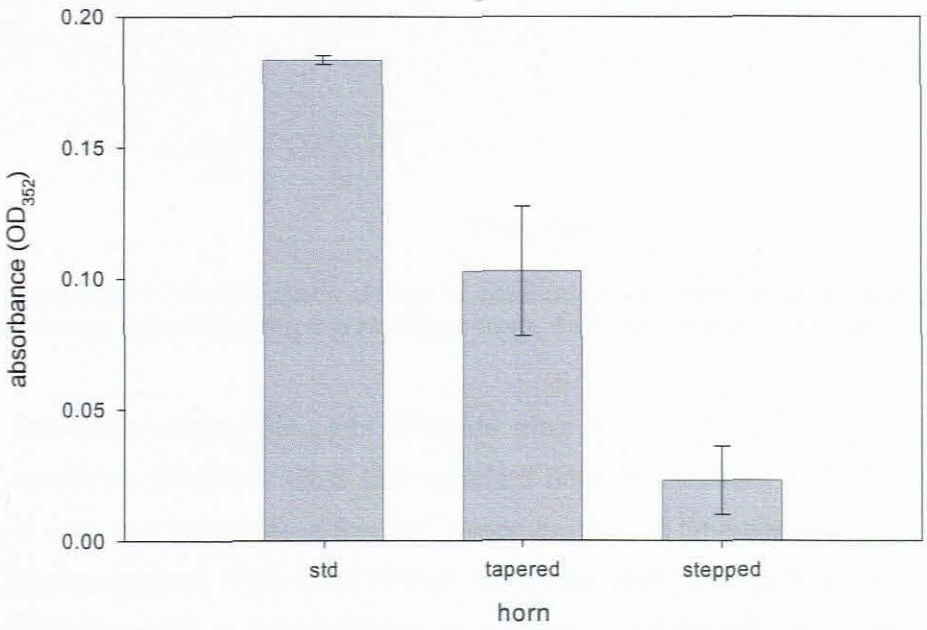

Figure 2.10: Assessment of inertial cavitation as measured by three different horns, using iodine oxidation (std refers to standard)

2.3.2 The effect of the duration of sonication on inertial cavitation

The aim of this experiment was to determine whether the amount of cavitation generated over a 10 min period remained constant. Others have shown that rectified diffusion or fragmentation of mother cells during sonication can change the number of cavitation nuclei available during sonication (Leighton, 1994). Therefore the amount of cavitation generated per unit time may change over time. Knowledge of the rate at which cavitation is generated over time is important when attempting to reproducibly maximize cavitation for microbial studies.

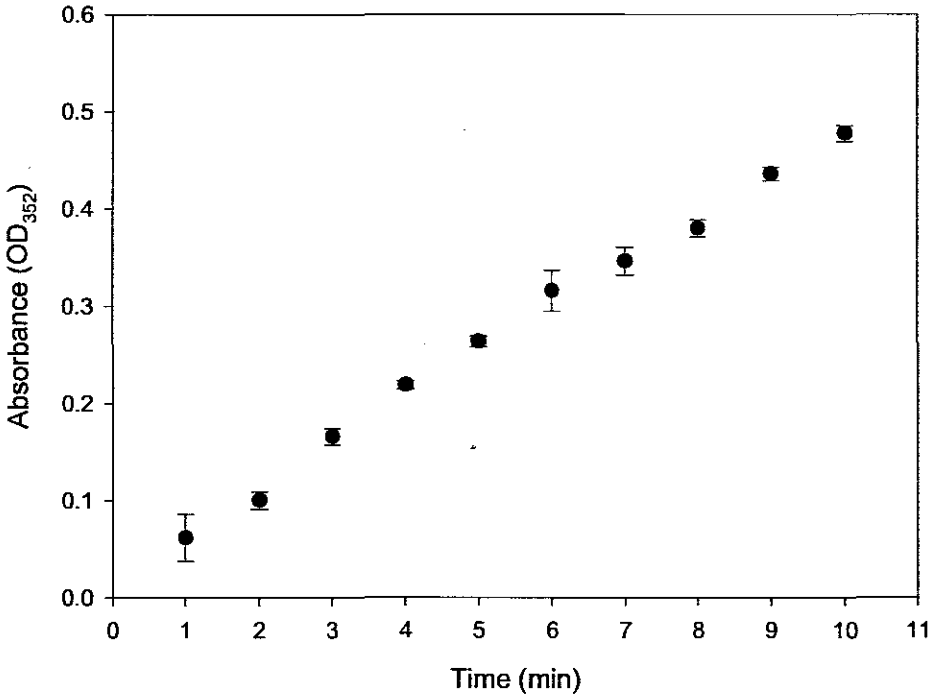

Figure 2.11: The influence of time of sonication on inertial cavitation in a potassium iodide solution (100 ml) using the standard horn. Total sonication time was 10 min

The absorbance (OD_{352}) of tri-iodide after 1, 2, 3, 4, 5, 6, 7, 8, 9 and 10 min ultrasound exposure, using the Vibra-Cell standard horn, is indicated in Figure 2.11. A linear curve, set to intercept the origin of the plot, assuming that at time zero no tri-iodide oxidation occurred, was calculated. The linear curve correlated well with experimental data (R^2 = 0.9943). A linear increase in total tri-iodide as a function of time indicated that the amount of cavitation generated per time unit during a 10 min sonication period remained constant i.e. the similar amount of cavitation that was generated in the first minute was the same amount as generated during the tenth minute.

2.3.3 The effect of volume of treated solution on inertial cavitation

Chemiluminescence caused by luminol demonstrated that the standard horn produced a specific zone of maximum cavitation (Fig. 2.7). The aim of this experiment was to determine if tri-iodide production was influenced by the volume of solution undergoing sonication.

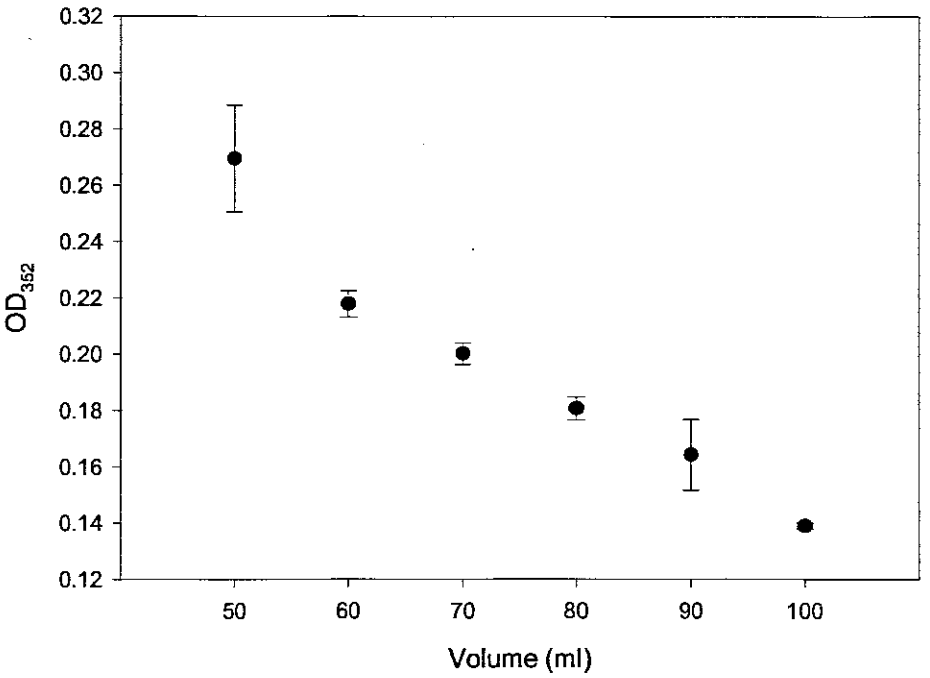

Figure 2.12: The relationship between solution volume and tri-iodine formation (OD_{352})

It was observed (Figure 2.12) that the 50 ml solution (OD_{352} 0.2697 ±0.0192) produced double the tri-iodide than did the 100 ml solution (OD_{352} 0.1390 ±0.0010). A likely explanation is that similar amounts of tri-iodide were generated in both solutions; however, the 50 ml solution was half the volume of the 100 ml solution. Therefore the concentration of the tri-iodide was effectively doubled. This suggested that the cavitation zone below the horn, (Fig. 2.7), generated a fixed amount of cavitation, in sonication volumes between 50 and 100 ml.

It follows that for microbial populations, decreasing the test volume would enhance the passage of microbes suspended in the solution through the cavitation zone. However, during experimentation, it was found that micro-streaming produced a vortex, centred around the horn. Vortexing became more frequent when volumes of 50 ml or less were tested. At times, this caused the level of the water to dip below the emitting tip of the horn. This is damaging to the equipment, as there is a large impedance mismatch between the horn and air-water mixture. The air sucked into the solution adversely affects the number of cavitation nuclei and increases dissolved gases. Therefore it was decided that further experimentation was not to be conducted at 50 ml volumes but at 60 ml.

2.3.4 The effect of horn placement in the treatment solution on inertial cavitation

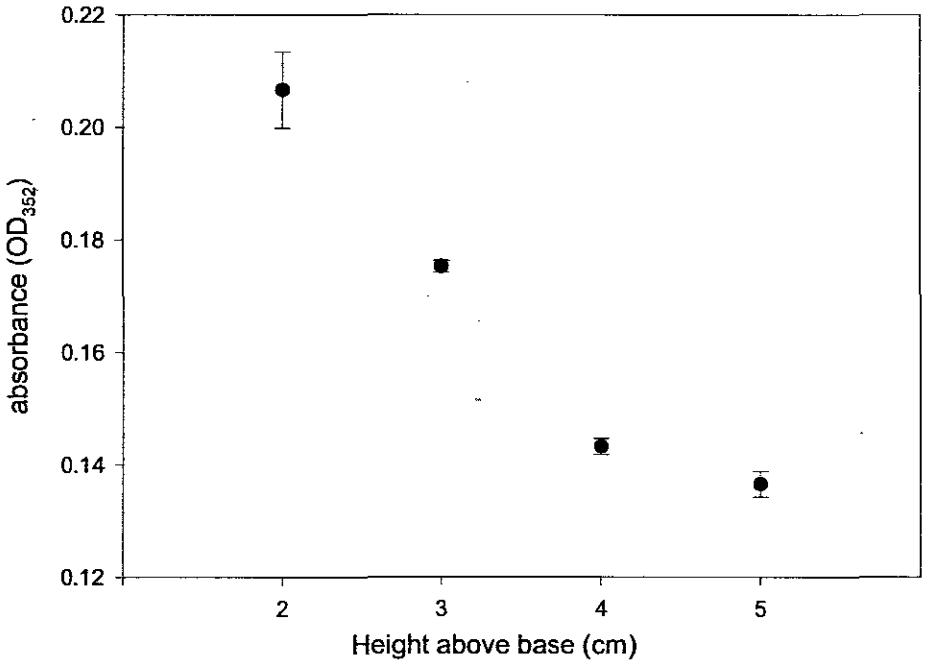

Figure 2.13: The recorded absorbance OD_{352} as influenced by horn immersion depth

It was clear that the closer the horn was to the base of the container, the more tri-iodide was produced (Fig. 2.13). A possible explanation is that when the horn is located nearer to the base, the bubbles impinge against the base with a greater force, due to the strength of micro streaming. The force of the impact fragments the cavitation bubbles into more daughter "cells". Each of these bubbles will form cavitation nuclei when re entering the cavitation zone (Leighton 1994). The effect would be an overall increase in cavitation bubbles thereby increasing tri-iodide formation.

2.3.5 Effect of pulsed vs. continuous wave application on inertial cavitation

It has been reported that enhanced cavitation results from pulsing the ultrasound waves when compared to a continuous wave (CW) (Leighton 1994). Therefore, for microbicidal applications, it may be beneficial to subject microbes to pulsed sound waves and not a continuous wave. In this study, solutions of KI were subjected to various pulsed sound waves. Tri-iodide yield was measured (OD_{352}) to determine the influence of pulsed sound waves cavitation.

A pulse is defined by two properties: the pulse length and the duty cycle (Fig. 2.14).

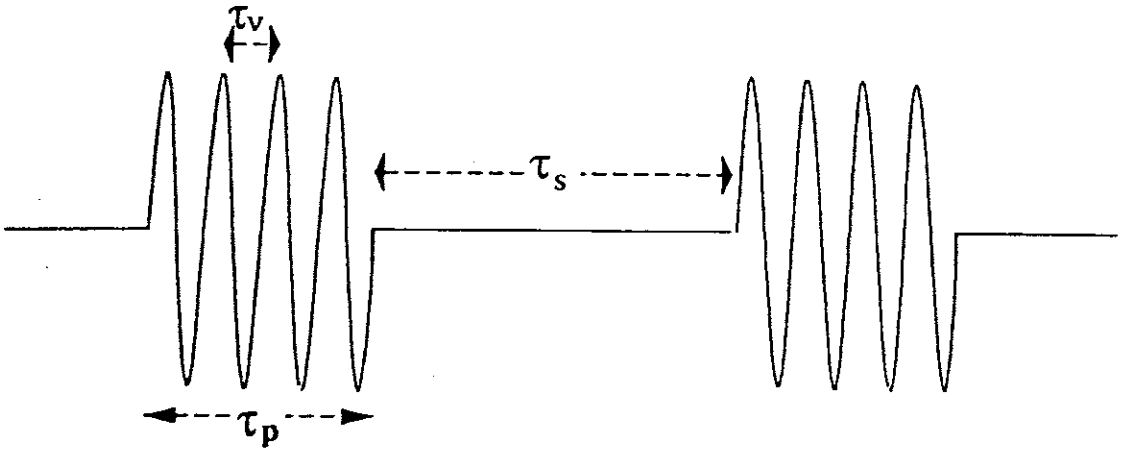

Figure 2.14: Idealized pulsed acoustic waves. τp represents the time that the pulse persists, the 'on' time. τs represents the 'off' time, separating the pulses. The duty cycle is the ratio of τp:τs. τv represents the carrier period

(Adapted from Leighton, 1994)

The pulse length is the length of time that the pulse persists (τp). It is also known as the 'on time'. The pulse will be followed by an 'off time', a period where no sound waves are generated (τs). The ratio of the 'on' time to the 'off' time is known as the duty cycle (τp:τs)(Fig. 2.14). The duty cycle is often expressed as the percentage of on time in a full on / off cycle. For example a 40% duty cycle means that if the on / off time was a total 10 s, the 'on' time was 4 s.

Another term that should be defined is the 'pulse repetition frequency'. This is a measure of how many 'on' times there are in one second. For example a pulse repetition frequency of 50 Hz means that there are 50 'on' times every second (Leighton, 1994). The pulse repetition frequency should not be confused with the acoustic frequency.

In the literature reviewed for this study on pulse enhancement, all frequencies used were within the megahertz range (Hill, Clarke, Crowe & Hammick, 1969; Clarke & Hill, 1970; Buldakov *et al.*, 2009). Hill *et al.*, (1969) showed that a 30 ms pulse at 1 MHz was optimal, while Clarke and Hill, (1970) found 10 ms and 100 ms at 1 MHz to be optimal. These findings were used as a benchmark for this study. A 10 ms, 30 ms and 100 ms pulse at 1 MHz has 10 000, 30 000 and 100 000 cycles per pulse respectively. This corresponds to pulse lengths of 0.5 s, 1.5 s, and 5 s respectively at 20 kHz, as calculated by Equation 2.4. Therefore total on / off times of 0.5 s and 1 s followed by a 10 fold increase to 5 s and 10 s were selected for this study. The duty cycles used in this study were 20, 40, 60, and 80%.

$$\tau p = f / cycles$$

Where: τp = the 'on' time'
f = frequency

Equation 2.4

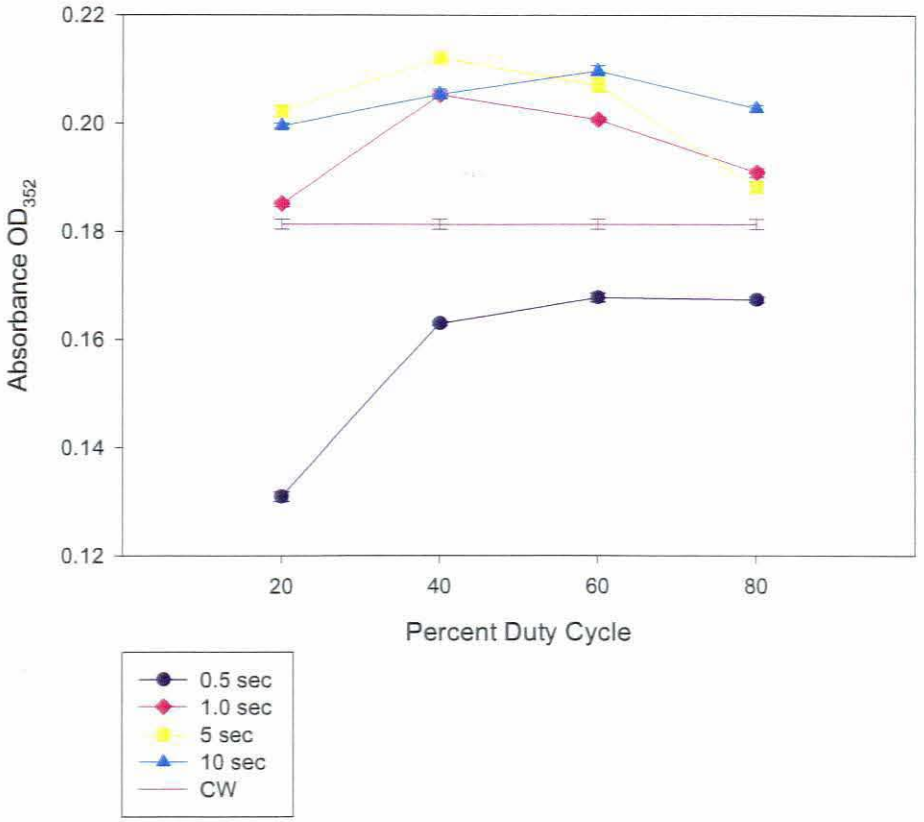

Fig. 2.15: Absorbance measurements (OD_{352}) for lengths of 0.5, 1, 5 and 10 s at duty cycles of 20, 40, 60 and 80%. A continuous wave absorbance reading (OD_{352}) was also included as a control

Results showed that, under certain pulse conditions, inertial cavitation can be enhanced at 20 kHz (Fig. 2.15). An on / off pulse length of 0.5 s decreased cavitation at all duty cycles (blue). The three longer on / off pulse lengths of 1, 5, and 10 s all increased absorbance OD_{352} (Fig. 2.15). Maximum cavitation activity for all on / off pulse lengths occurred at a ~50% duty cycle. Despite this increase in tri-iodide formation, Buldakov *et al.* (2009) found no improvement in cavitation microbial lethality when comparing pulsed ultrasound to a continuous wave.

Various theories have been proposed as to why pulsing enhances inertial cavitation. These theories are beyond the scope of this study and may be found in Leighton (1994).

2.3.6 The effect of dissolved gases (O_2, N_2,or Ar) on inertial cavitation

Two fundamental processes that occur when a cavitating bubble expands and collapses are the flux of dissolved gas and water vapour across the bubble / liquid interface (Leighton 1994). The flux of water vapour is considered to be quasi-static, i.e. the phase change between water and water vapour is so rapid that the vapour pressure in the bubble is unaffected by the bubble oscillations. However the flux of gas does not occur as rapidly and therefore influences the cavitating bubble (Leighton 1994). The solubility, thermal conductivity as well as the concentration of dissolved gases in solution can either oppose or enhance cavitation (Leighton, 1994).

The influence of gas solubility in the liquid undergoing cavitation is marked. An ideal gas would flux across the bubble wall in an adiabatic[2] manner, having very little effect on the cavitating bubble. Gases with low solubility, dissolved in a solution being sonicated, readily migrate from the solution into the cavitation bubble during the bubble growth phase. During bubble collapse, a gas with low solubility in water is slow to redissolve into the solution. The result is that the gas within the bubble resists collapse and therefore exerts a cushioning effect on this collapse. (Leighton, 1994).

By contrast, a gas that dissolves readily in a solution has less of a cushioning effect on cavitation, as it rapidly dissolves back into solution during the collapse phase. Therefore for optimum cavitation to occur, the liquid undergoing sonication should be saturated with a high solubility gas (Leighton 1994).

Alternatively, the removal of all dissolved gases from the solution can also enhance cavitation. In degassed solutions there are fewer gases available to migrate into the bubble during the expansion phase. Therefore there is less gas in the cavitation bubble to cushion the collapse during the collapse phase. (Leighton 1994).

Another property of dissolved gases in a solution undergoing sonication to consider is the thermal conductivity. When a bubble collapses, and the internal gas is compressed, the gas temperature increases. A high thermal conductivity of a gas results in improved heat conduction into the surrounding liquid when compared to gases with a low thermal conductivity. Therefore the temperature inside the collapsing bubble is increased when the gas inside has a low thermal conductivity. Such a gas inside the bubble can both cushion the collapse and simultaneously increase the temperature reached inside the bubble. This result in an increase in the free radicals formed during the collapse (Leighton, 1994).

[2] Adiabatic: when the gas fluxes across the bubble wall there is no exchange of energy as heat (Halliday *et al.*, 2001)

In this study, degassed water and three aqueous solutions saturated with argon, oxygen or nitrogen were subjected to equal ultrasound exposure, as described (Section 2.2.6). Luminol photography and KI oxidation were used to determine the influence on cavitation.

The thermal conductivity and solubility of Ar, O_2 or N_2 and normal atmospheric gas (i.e. air) can be seen in Table 2.2. Argon was considered to be a gas with a low thermal conductivity and nitrogen was considered to have a low solubility in water.

Table 2.2: Thermal conductivity and solubility of oxygen, nitrogen and argon (Lemmon & Jacobsen, 2004)

	Argon	Oxygen	Nitrogen	Atmospheric gases
Thermal conductivity (300 K) ($mW.m^{-1}.k^{-1}$)	23.23	32.55	32.77	32.61
Solubility (20°C) (ml/100 g H_2O)	3.3	3.16	1.54	NA

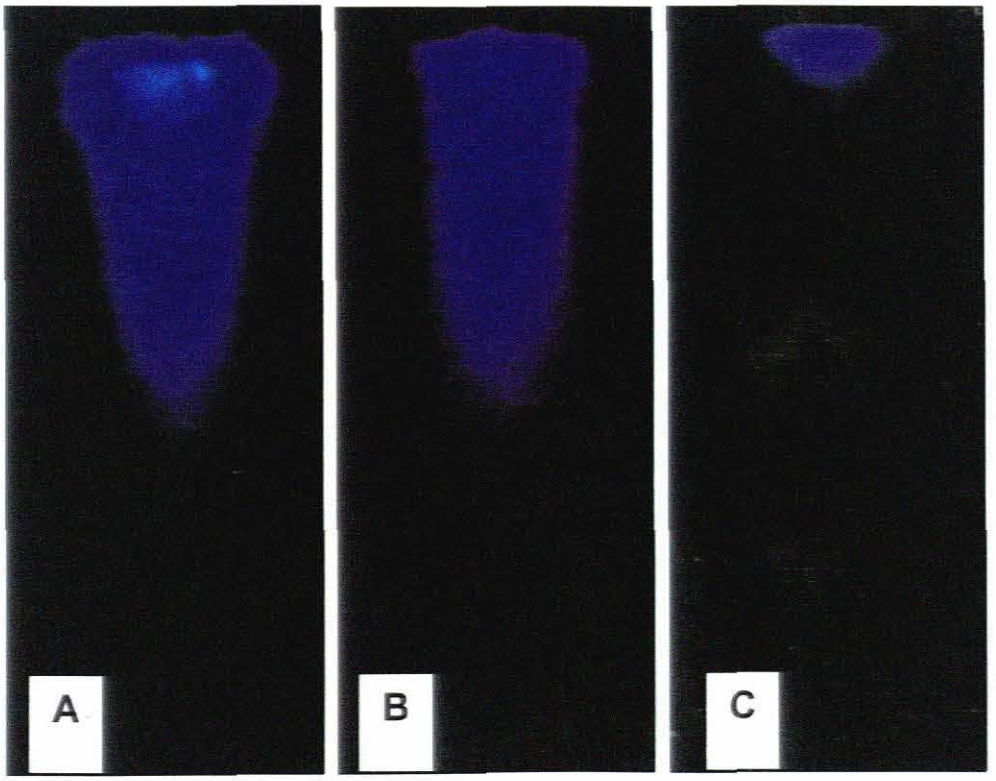

Figure 2.16. Cavitation zones produced by the standard horn in the presence of luminol. (A) – Argon saturated solution (B) – oxygen saturated solution (C) nitrogen saturated solution

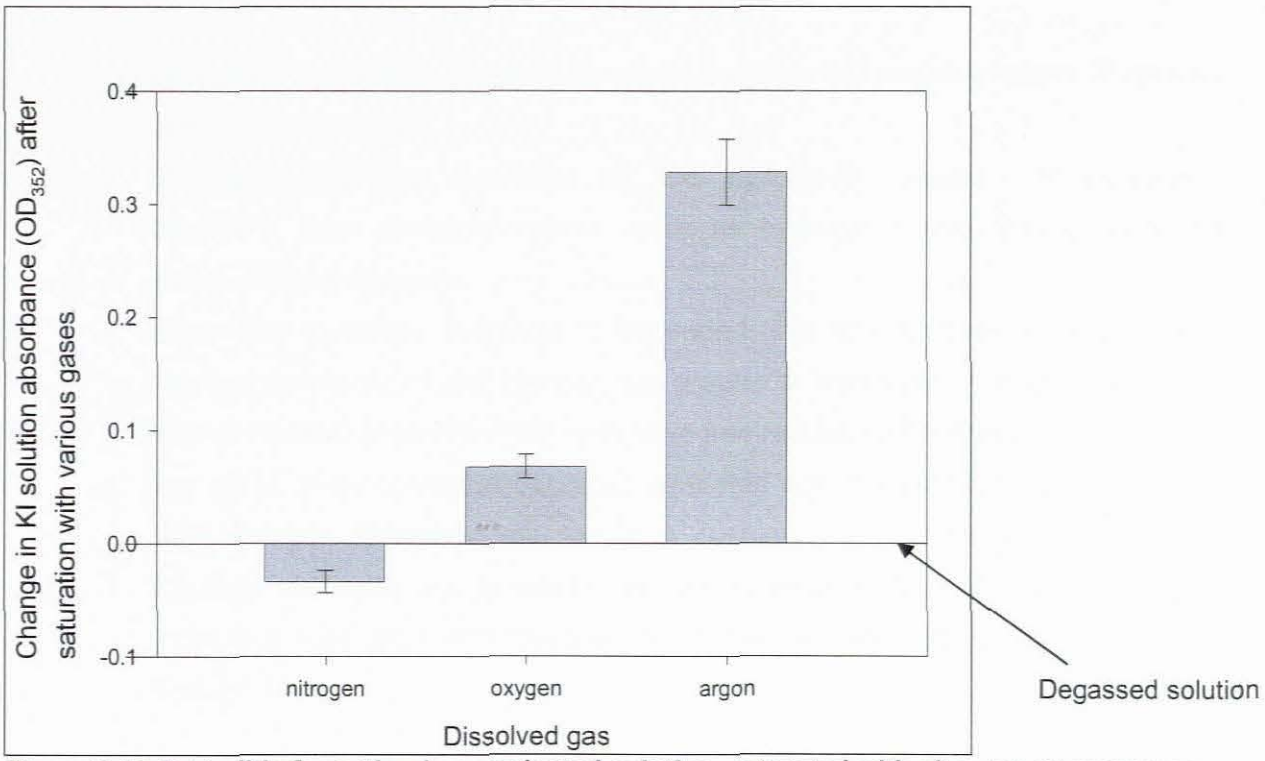

Figure 2.17: Tri-iodide formation in a sonicated solution, saturated with nitrogen or oxygen or argon. The results shown here indicate the increase or decrease in fluorescence as compared to a degassed solution baseline.

Results obtained using either luminol or potassium iodide oxidation, showed that oxygen or argon-saturated solutions enhanced free radical formation when compared with nitrogen (Figs. 2.16 & 2.17). This is due to the relatively high solubility of argon and oxygen in water compared to that of nitrogen (Table 2.2). Furthermore the thermal conductivity of argon is less than that for oxygen and nitrogen (Table 2.2). Therefore the temperature reached within the bubble during collapse is increased, producing more free radicals.

2.3.7 The effect of hydrostatic pressure on inertial cavitation

Hydrostatic pressure directly affects cavitating bubbles. The size of a bubble (not necessarily a cavitating bubble) in solution is determined by the balance of internal bubble pressure and the external pressure acting on the bubble. The external pressure results from the hydrostatic pressure in the liquid. However when a sound wave transverses the solution, the external pressure is the sum of the hydrostatic pressure and acoustic pressure amplitude. The hydrostatic pressure influences the cavitation threshold as well as the force at which cavitating bubbles collapse (Section 1.1.7).

In the pressure experiments conducted during this study, pressure was increased from ambient to 500 kPa in 100 kPa units by pressurizing with nitrogen gas (Afrox, Cape Town, South Africa). Increasing the hydrostatic pressure with nitrogen affects cavitation as follows (Povey and Mason, 1998; Pagan *et al.*, 1999):

1. Increasing hydrostatic pressure dissolves a portion of cavitation nuclei. Therefore less cavitation occurs.
2. Cavitation threshold increases as the hydrostatic pressure is increased. Therefore, less cavitation events occur as hydrostatic pressure is increased above ambient pressure.
3. When the cavitation threshold is exceeded, the temperatures and pressures reached during an inertial collapse are greater at increased hydrostatic pressure than at ambient pressure. Therefore more free radicals are formed
4. The liquid to be sonicated becomes saturated with the pressurizing gas, in this case nitrogen. Dissolved gas tends to cushion the collapse of a bubble and therefore decrease the temperatures and pressures reached during collapse. (note that saturation with nitrogen decreased tri-iodide formation, as shown in Section 2.3.6)

Tri-iodide formation was measured at 3 different displacement amplitudes (31, 62 & 124 µm) for each pressure. The aim was to determine how pressure influenced tri-iodide formation.

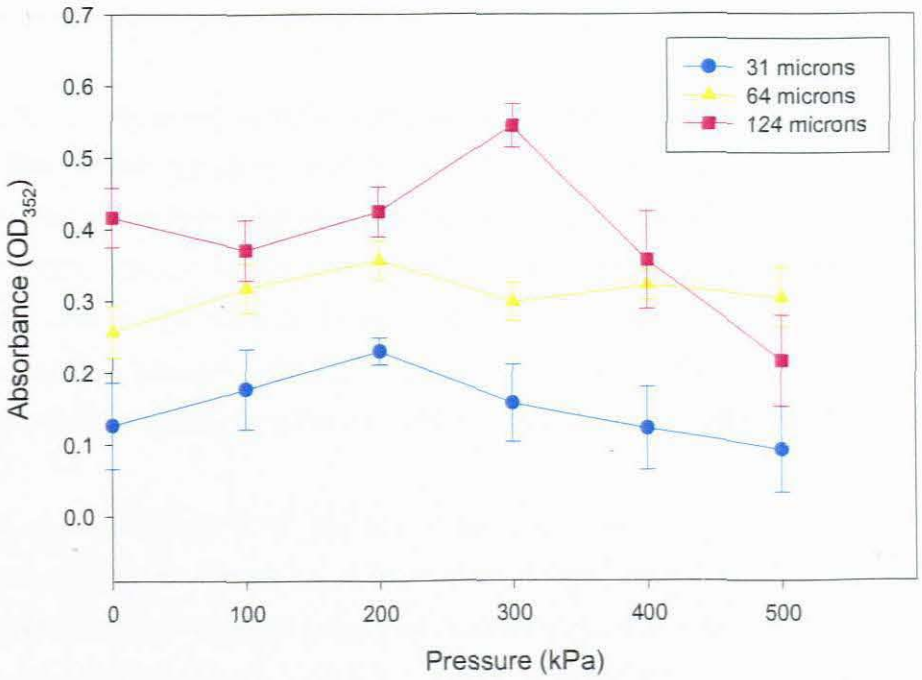

Figure 2.18: Absorbance (OD_{352}) of tri-iodide after 5 min sonication at 0, 100, 200, 300, 400 and 500 kPa. Three displacement amplitudes were tested: 31, 62 & 124 µm (standard horn)

It was evident that 124 μm displacement amplitude produced more free radicals than did 62 μm displacement amplitude, which in turn, produced more free radicals than 31 μm displacement amplitude. An exception was noted between 400 and 500 kPa where 64 μm displacement amplitude produced more tri-iodide than did 124 μm displacement amplitude.

A distinct peak of maximum cavitation was noted for the three amplitudes tested (31, 62 and 124 μm). This peak represented the pressure where the temperature of the collapse and the number of collapses were at a maximum. As the displacement amplitude was increased from 31 μm to 62 μm to 124 μm respectively, the pressure required to reach this maximum peak increased from 200 kPa to 300 kPa (Fig. 2.18)

The increased tri-iodide generation under hydrostatic pressure may improve the microbicidal effect on micro-organisms. However damage to the horn tip was severe at pressures above ambient, resulting in more titanium fragments released into the solution. Visual observation clearly showed that corrosion of the horn was markedly intensified when used under pressure. Titanium alloy fragments released into a liquid would be undesirable in any beverage due to the adverse affect on the quality of the beverage. In addition, pressurized ultrasonic applications, such as the one used in the study in a single container, would limit applications to batch processing. Therefore it was decided that a pressurised system was not suitable for microbicidal application for beverage production.

2.4 *Ultrasonic experimental setup for biological testing*

The iodine oxidation and luminol fluorescence experiments identified the experimental parameters that enhanced inertial cavitation. It also indicated which parameters did not notably impact on inertial cavitation. The experimental parameters tested were: horn type, volume of test solution, location of horn within test solution, pulsed sound waves, effect of dissolved gas and effect of hydrostatic pressure. The data gathered were used to establish the experimental conditions for the biological study reported in Chapter 4.

It is important to note that iodine oxidation and luminol fluorescence measured free radical production, associated with inertial cavitation. An increase in tri-iodide formation or luminol fluorescence indicated either an increased number of inertial cavitation bubbles and / or an increased force with which the bubbles collapsed. The results gave no indication of how other physical effects (Section 1.1.5) associated with inertial cavitation were influenced. Furthermore tri-iodine formation and luminol fluorescence yield no information on phenomena associated with non-inertial cavitation (Section 1.1.6).

The microbicidal action of cavitation is complex and is attributed to a combination of mechanisms (Gogate & Kabadi, 2009). While it is well documented that free radicals such as H_2O_2 are microbicidal (Prescott *et al.*, 1996), it is generally not considered the principal mode of cell death of sonicated microorganisms (Tsukamoto *et al.*, 2003). Therefore, optimised experimental conditions based on tri-iodine formation and luminol fluorescence do not necessarily equate to optimal killing conditions for microorganisms. However, the data do provide a useful guide for the potential utilisation of ultrasound for beverage disinfection.

One of the principal aims of this study was to measure the effect of ultrasound and heat (55 and 60°C) on *S. cerevisiae*, and to determine if a synergy occurred between the two. Therefore it was important that the biological studies were conducted under constant conditions. Whilst this was easily achieved for the heat applications, the standardisation of optimal ultrasonic experimental design was important. It was clearly indicated in Chapter 1 (Section 1.1.7) that variations in ultrasound equipment and experimental setup influence microbicidal/static results. The data obtained from the iodine oxidation and luminol fluorescence were used as indicators to select the ultrasonic conditions considered optimal for the biological testing. The criteria for selecting sonication experimental conditions, where possible, were based on the location of the cavitation zone and on increased free radical production. It was also important to consider the practicality for large scale industrial applications.

Based on the results obtained, conditions selected for the biological tests were:

1. The standard 13 mm horn was used throughout. Both the iodine oxidation and the luminol fluorescence indicated that the standard horn generated more cavitation than did the microtips. The standard 13 mm horn also produced consistent results when compared to the microtips.

2. Maximum amplitude was used throughout. It was apparent that at an amplitude of 124 µm, inertial cavitation was optimum.

3. The concentration of free radicals increased as the treatment volume decreased. This was probably because the same amount of cavitation was generated, regardless of the treatment volume. Therefore, a greater percentage of solution was exposed to cavitation within smaller volumes. It follows that microorganisms undergoing sonication will pass through the cavitation zone more frequently in smaller volumes. The minimum volume tested was 50 ml. It was decided to use a volume of 60 ml for the biological applications as excessive vortexing occurred at 50 ml when 100% power was applied(Section 2.3.3).

4. Results indicated that inertial cavitation was enhanced by locating the horn tip closer to the base of the treatment vessel. Therefore the horn was always used at the closest tested distance to the base i.e. 20 mm above the base of the 100 ml treatment vessel. However, a disadvantage of this was that the closer the horn tip was to the base of the treatment vessel, the more disintegration of the container base and horn tip occurred. This would impact negatively on equipment maintenance as well as introducing impurities into the beverage being treated.

5. The pulsing experiments were conducted such that each KI solution tested underwent a total of 5 min sonication. The total experimental time therefore had to be increased beyond 5 min to compensate for the 'off' times between pulses. When tested as such, it was found that the pulsed sound waves increased tri-iodide formation, compared to 5 min of continuous wave application. The greatest increase in tri-iodide formation (12 – 16%) was recorded for duty cycles of ~50% (Fig. 2.15). A total of 10 min experimental time was required to achieve 5 min of 'on' time at 50% duty cycle. If a continuous wave was applied for 10 min, such that the total experiment time was the same as the 50% pulse experiment, the tri-iodide formation could double. Experiments reported in section Section 2.2.2 showed a linear relationship between time and tri-iodide formation and effectively double sonication time doubles tri-iodide formation). Compared to the 12 – 16% improvement in tri-iodide yield noted during pulsing, the continuous wave was considered more effective when comparing the total sonication time.

   With respect to industrial applications, production times are kept to a minimum. Therefore the increased experimental time required for pulsing was undesirable. In addition Buldakov *et al.*, 2009 reported that cell viability was less impacted when treated with pulsed ultrasound compared to a continuous wave, for the same total 'on' time. Overall, results showed that continuous waves were more advantageous, and were used throughout the biological experiments.

6. Degassed solutions generated more tri-iodide than did solutions saturated with nitrogen or atmospheric air. Solutions saturated with oxygen or argon increased tri-iodide generation. The increase in tri-iodide is solely attributed to the increased temperature of the bubble collapse (Leighton, 1994). The temperature of bubble collapse is not considered microbicidal (Gogate & Kabadi, 2009); however, in our laboratories, argon was shown to enhance the killing of *Escherichia coli*, (van Wyk, 2004). This could be due to the increased content of free radicals exerting a microbicidal effect on a Gram negative organism. However, it would be both a logistical and economic challenge for industrial

applications to pre-saturate solutions with gas during food production. Therefore, it was decided to treat *S. cerevisiae* in degassed solutions.

7. Sonicating solutions under increased hydrostatic pressure markedly increased tri-iodide formation. However, increase in the corrosion of the horn tip was noted. This was as a result of cavitation bubbles collapsing with a greater force (Refer Appendix 2.B which shows an image of removable pitted horn tips). This was a major disadvantage with the system. Clearly, the dissolution of the Ti-Al-Va alloy tip in a beverage is hazardous to consumers and therefore pressure could not be used in the system applied in this study. Although sonication under high hydrostatic pressure (manosonication) has been used successfully to improve the microbicidal action of ultrasound (Pagan *et al.*, (1999)(Section 1.2.4), it is well known that increased hydrostatic pressure can only be applied as a batch process. Batch processing of large volumes of beverages under pressure is impractical for industrial applications. In addition, sonication has the potential to be applied continuously. Therefore, the biological studies conducted in this study were done at atmospheric pressure, at sea level.

CHAPTER THREE

PREPARATION OF FLUORESCENCE FLOW CYTOMETER TO DETECT *SACCHAROMYCES CEREVISIAE*

3.1 General overview of fluorescent flow cytometry

Fluororescent flow cytometry is the process of detecting cells and measuring cellular attributes and was used in this study to measure four characteristics of *Saccharomyces cerevisiae* cells. These were: relative cell size, relative cytoplasmic complexity and the fluorescent intensity of the fluorescent dyes thiazole orange (TO) and propidium iodide (PI) bound to DNA. The addition of Liquid Counting Beads (BD™ Liquid Counting Beads) added to the *S. cerevisiae* suspension enabled immediate quantitation of *S. cerevisiae* populations ($CFU.ml^{-1}$). A Becton Dickson FACScan flow cytometer along with Becton Dickson Cell Quest software was used throughout this study (BD Biosciences, San Jose, CA).

The four above-mentioned characteristics were measured using a 14 mW, 488 nm argon ion laser and various detectors. As particles (including yeast cells) move through the path of the laser, a voltage pulse is detected by a diode opposite the laser (180°). The pulse height, width and area are relative to the size of the particle moving through the laser. This signal is referred to as a forward scatter signal (FSC-H) (BD Biosciences, 2002).

The laser (488 nm) is also reflected at 90° by cellular constituents. The extent of reflection is directly proportional to the granularity of the cytoplasm. A second diode situated at 90° to the laser beam detects voltage pulses relative to the cytoplasmic complexity of the yeast cell. This signal is referred to as side scatter signals (SSC-H) (BD Biosciences, 2002).

Propidium iodide and thiazole orange fluorochromes were added to the *S. cerevisiae* suspension. Both fluorochromes intercalate in the DNA of the cell (Malacrino Zapparoli, Torriani & Dellaglio, 2001). The fluorochromes absorb the incident laser energy (488 nm) and release the excess energy at wavelengths of 617 nm for propidium iodide and 530 nm for thiazole orange (Boyd, Gunasekera, Attfield, Simic, Vincent & Veal, 2003). This emitted light is detected by any one or all of the three diodes sensitive to wavelengths of 530 ±30 nm (FL1-H[3]), 585 ±42 nm (FL2-H) and 570 LP (FL3-H) (BD Biosciences,2002).

The detected particles, referred to as 'events', are displayed as "plots", using BD Cell Quest software (BD Biosciences, San Jose, CA). The axes of the plots can incorporate any of the five possible attributes listed above (FSC-H, SSC-H, FL1-H, FL2-H, FL3-H). The two plots selected for use in this study incorporated four channels, i.e. FSC-H vs. SSC-H and FL1-H

[3] FL1-H, FL2-H and FL3-H, refers to the fluorescent signals detected by channel 1, 2 or 3

vs. FL3-H. Each event detected is displayed as a dot on the plot. Therefore the plots are referred to as 'dot plots'.

Analysed particles, or cells, with similar properties form dense populations of events on the plots as shown in Figure 3.1. A population of *S. cerevisiae* cells composed of cells of similar size and cellular complexity is seen. Likewise a separate and distinct population of beads is visible as all beads are of a similar size and optical complexity.

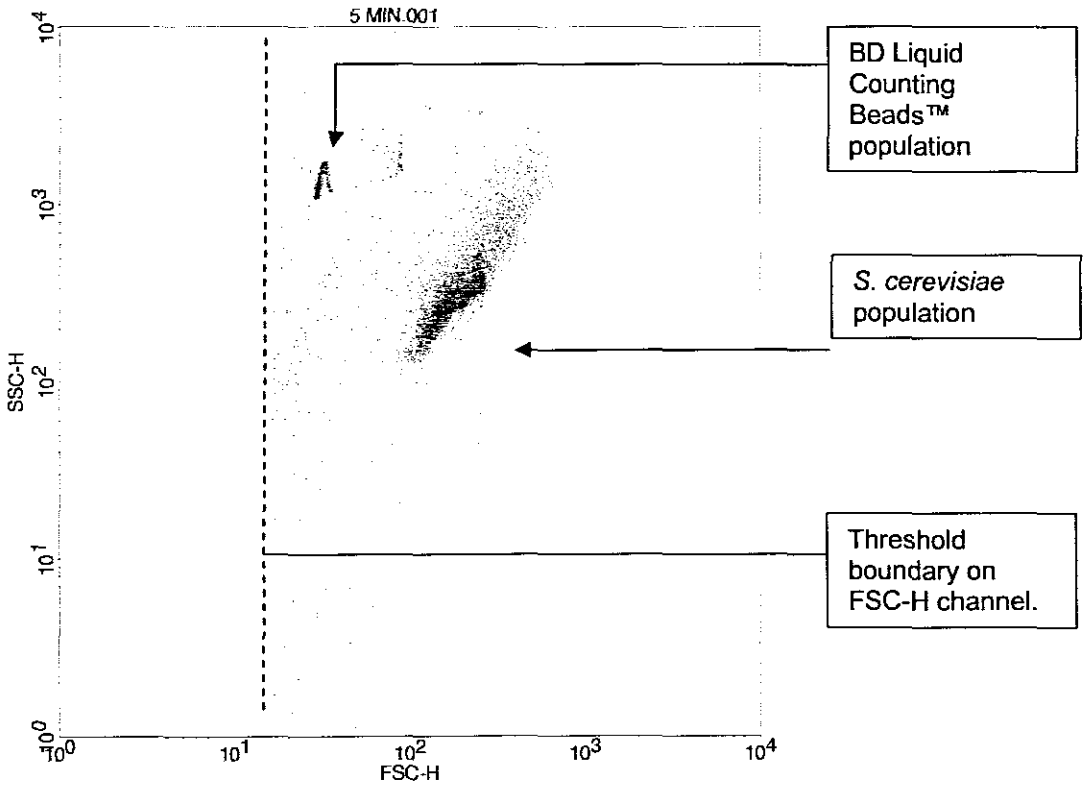

Fig. 3.1 BD Cell Quest FSC-H vs. SSC-H dot plot showing separate populations of BD Liquid Counting Beads™ and *S. cerevisiae* population. The majority of 'noise' events are detected as low FSC-H values. Therefore a threshold on the FSC-H channel was set to prevent the noise events being detected.

Data is obtained by using two modes in flow cytometry: an 'acquisition' mode and an 'analysis' mode. In the acquisition mode, real time manipulation of the plots can be made as events are acquired. Acquisition mode was used to set up the BD Cell Quest software such that desired particles were displayed on a 4 log scale in both the FSC-H vs. SSC-H and FL1-H vs. FL3-H dot plots (Fig. 3.1).

Analysis mode was used to perform functions and calculations once all the events had been acquired. In analysis mode, populations of *S. cerevisiae* and BD Liquid Counting Beads™ identified in the FSC-H vs. SSC-H dot plot were isolated by 'gating'[4] (Fig. 3.2).

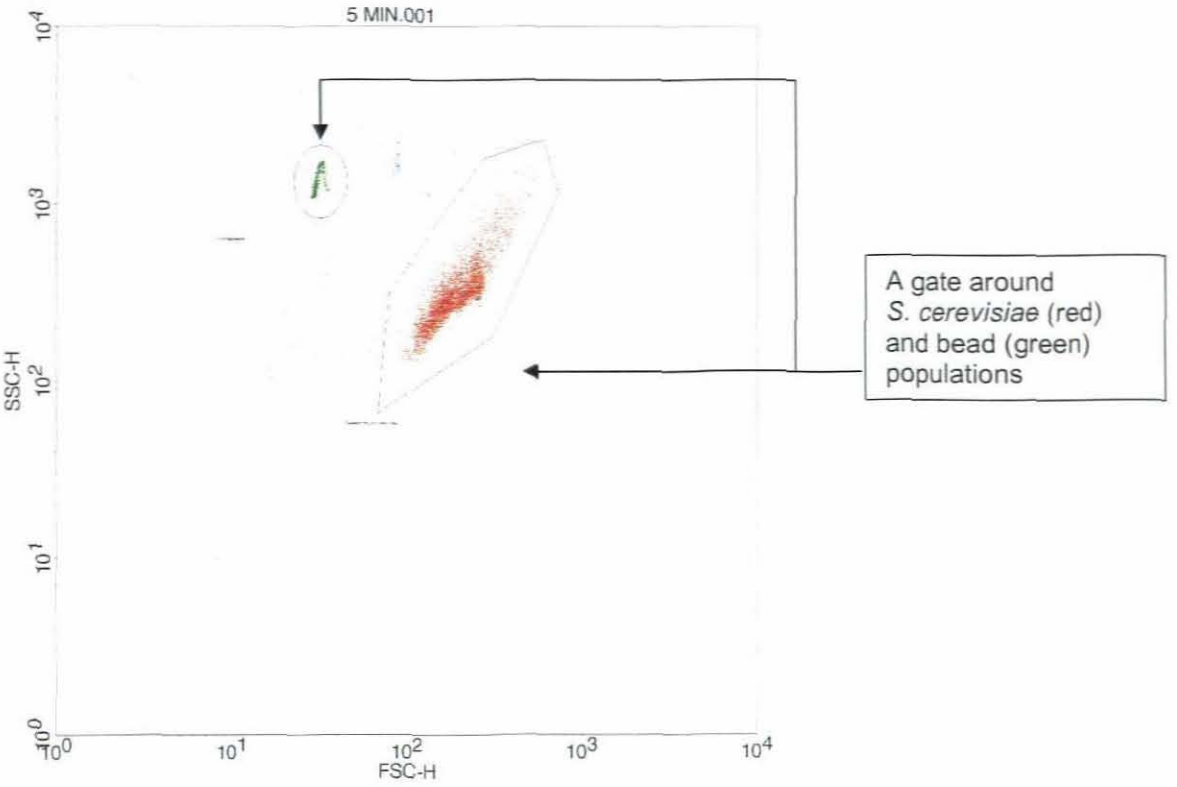

Fig. 3.2: BD Cell Quest FSC-H vs. SSC-H dot plot with gated *S. cerevisiae* and a gated bead populations. The events within the gates are displayed as red dots for the *S. cerevisiae* population and green dots for the bead population.

The gate around *S. cerevisiae* was set to capture all the events within the gate and display it on a separate plot, thereby minimising the presence of non-*S. cerevisiae* "noise" events. This separate plot was set up for the analysis of fluorescent cells, where the x-axis represented the FL1-H channel and the y-axis represented the FL3-H channel. The events were displayed as contour plots instead of dot plots. Contour plots display confluent regions of identical cell concentrations. Figure 3.3 shows an example of a contour plot used in this study. Fluorescing cells were generally considered to be those with x axis (FL1-H) or y-axis (FL3-H) values greater than 10^1.

[4] Gating is the process of enclosing a region of a plot within a border thereby separating this population from other events (Fig. 3.2).

3.2 Methods and Materials

3.2.1 Maintenance *Saccharomyces cerevisiae* GC210 (*MATα lys2*)

Saccharomyces cerevisiae GC210 (*MATα lys2*) with a genetic background congenic to *S. cerevisiae* ∑1278b was used throughout this study (Cunningham and Cooper, 1991). A 60 ml yeast peptone dextrose broth (YPDB) (Biolab Diagnostics, Midrand, South Africa) was inoculated with 1 ml *S. cerevisiae*, and incubated at 25°C in a thermostatically controlled water bath (Thermomix 1440, B, Braun Melsungen AG, Germany) for 17 – 19 h until OD_{600} 0.8 – 1.1 was reached, indicating late exponential phase cells. The OD_{600} was determined using a *GeneQuant Pro spectrophotometer (Biochrom Cambridge, United Kingdom).* Pure cultures of *S. cerevisiae* were maintained on malt extract agar slants (MEA) (Biolab Diagnostics, Midrand, South Africa). The stock of yeast inocula was prepared from a 16 h culture (YPDB) of *S. cerevisiae*. A known volume of cells (1 ml) was removed from this culture and mixed with sterile glycerol, AR grade, (Biolab Diagnostics) to a final concentration of 15%. This was stored by freezing at -70°C.

3.2.2 Initial calibration of the BD FACScan using CaliBRITE™ beads and FACScomp™ software

Becton Dickinson CaliBRITE™ beads and Becton Dickinson FACScomp™ software were used to automatically calibrate the Becton Dickinson FACScan flow cytometer (BD Biosciences, San Jose, CA).

Four separate types of CaliBRITE™ beads were used. One type was comprised of non-fluorescent beads and the remaining three were supplied labelled with fluorescein or isothiocyanate (FITC), or phytoerythrin (PE) or peridinin chlorophyll protein (PerCP). Following manufacturer's instructions, two suspensions were prepared from the four types of beads. The suspensions were prepared by adding 50 µl non-fluorescent beads to 1 ml FACSflow solution (BD Biosciences, San Jose, CA) and, to a separate 3 ml of FACSflow, 50 µl each of FITC, PE and PerCP fluorescent beads. The two CaliBRITE™ bead suspensions were homogenised by gentle mixing.

Calibration of the BD FACScan flow cytometer was done by first acquiring the non-fluorescent CaliBRITE™ bead suspension, followed by acquiring the CaliBRITE™ fluorescent bead mixture. During these procedures, the FACScomp™ software automatically calibrated the FACScan flow cytometer to compensate for overlapping fluorescent wavelengths.

3.2.3 Setting up of BD Cellquest software for the acquisition of *Saccharomyces cerevisiae*

Photomultiplier tube (PMT) voltages and thresholds levels for each diode were determined by acquiring suspensions of *S. cerevisiae* and BD Liquid Counting Beads™ in 0.1 mM phosphate-buffered saline (PBS) (BD Biosciences, San Jose, CA).

3.2.3.1 Preparation of the *Saccharomyces cerevisiae* suspension for flow cytometry

A *S. cerevisiae* suspension grown to late exponential phase, as described in Section 3.2.1, was removed from the YPDB growth medium by centrifuging 1.5 ml at 9 000 rpm (Spectrafuge 16M centrifuge, Labnet International, Woodbridge) for 5 min. The supernatent was discarded and the *S. cerevisiae* pellet was re-suspended in 400 µl, 0.1 mM PBS such that the final concentration was ~10^7 CFU.ml^{-1}.

A volume of 50 µl BD Liquid Counting Beads™ (BD Biosciences, San Jose, CA) was added to the 400 µl of *S. cerevisiae* in 0.1 mM PBS. The beads were supplied at a concentration of 969 beads.ml^{-1}.

Tween-90 (50 µl) (Merck, Darmstadt) and ethylenediaminetetraacetic acid (EDTA) (50 µl) (Merck, Darmstadt) were added to the 400 µl *S. cerevisiae* 0.1 mM PBS suspension such that final concentrations of 0.01% Tween-90 and 0.1 mM EDTA were achieved.

The resultant *S. cerevisiae* suspension was non-fluorescent. If a fluorescing *S. cerevisiae* suspension was required, an additional 5 µl TO (final concentration 420 nM) and 5 µl PI (final concentration 43 nM) fluorescent dyes were added. The final suspension was stored in a dark room for 10 – 15 min prior to acquisition.

The final solution volume was 510 µl, which represented a 1.28x dilution of the initial 400 µl sample.

The suspension of 0.1 mM PBS containing *S. cerevisiae* and BD Liquid Counting Beads™ was mixed before being connected to the FACScan flow cytometer.

3.2.3.2 Optimisation of the FSC-H and SSC-H channels to detect non-fluorescent *Saccharomyces cerevisiae* cell

A non-fluorescent *S. cerevisiae* sample was prepared for FACScan flow cytometer and acquired using CellQuest™ software (BD Biosciences, San Jose, CA). A FSC-H vs. SSC-H dot plot was used to display detected events. During acquisition, the FSC-H and SSC-H PMT

voltages were adjusted such that the *S. cerevisiae* and BD Liquid Counting Beads™ populations were positioned entirely on a FSC-H vs. SSC-H dot plot. A threshold of 302 V was set for the PMT voltage of the forward scatter channel such that events with PMT voltages below the threshold were not recorded. It was necessary to ensure that the threshold did not exclude any of the *S. cerevisiae* and bead events from being detected (Refer Fig. 3.1)

The following PMT and threshold settings were used for this study:

Threshold – FSC 302 V

FSC – E01 logarithmic amplification

SSC – 295 V logarithmic amplification

3.2.3.3 The use of non-fluorescent *Saccharomyces cerevisiae* to optimise FL1-H and FL3-H channels for the detection of yeast cells

The *S. cerevisiae* and BD Liquid Counting Beads™ populations on the FSC-H vs. SSC-H dot plot were gated (Refer Fig. 3.2, Section 3.1). The gated events were set to be displayed on an FL1-H vs. FL3-H dot plot. During acquisition, the PMT voltages of the FL1-H & FL3-H channels were set such that the non-fluorescent *S. cerevisiae* population was situated near the origin of a FL1-H vs. FL3-H dot plot, indicating no fluorescence (Fig. 3.3).

The following PMT settings were used for this study:

FL1-H – 500 V logarithmic amplification

FL3-H – 427 V logarithmic amplification

Compensation – none

3.2.3.4 The use of fluorescence to optimise the FL1-H and FL3-H channels to enable differentiation of viable, injured and dead *Saccharomyces cerevisiae* cells

A fluorescent 400 µl *S. cerevisiae* (0.1 mM) PBS suspension of actively growing late exponential phase cells was prepared as described in Section 3.2.3.1. The suspension was acquired and gated on an FSC-H vs. SSC-H dot plot and displayed on a FL1-H vs. FL3-H dot plot.

A gate was set around the population of viable cells in the FL1-H vs. FL3-H plot and labelled as 'V'. A second gate was set around a population of non fluorescing noise events that formed near the origin of the plot. This gate was labelled 'N'.

The location of a dead *S. cerevisiae* population on FL1-H vs. FL3-H dot plot was determined by acquiring a fluorescent 0.1 mM PBS suspension of dead *S. cerevisiae* cells. The dead cells were prepared by submerging a 1.5 ml suspension of actively growing exponential phase cells for 20 min in a waterbath (Thermomix 1440, B, Braun Melsungen AG, Germany) preheated to 70°C. The suspension was then cooled in an ice / water mix. The actively growing cells were prepared as described in section 3.2.3.1. A 400 µl volume was removed and prepared for fluorescent flow cytometry as described in section 3.2.3.1.

The suspension was acquired and gated on the FSC-H vs. SSC-H dot plot and displayed on a FL1-H vs. FL3-H dot plot. The position of the dead *S. cerevisiae* population was gated and labelled as 'D'. The injured cells were considered to be those that occurred between the gates of the viable and dead populations and did not occur within the noise gates.

The instrument and software settings established in this section (Section 3.2.3) were saved as a template to use in all further experimentation.

3.2.4 Setting up of BD Cellquest software for analysis of acquired data

After acquisition, the instrument was set to 'analysis' mode, such that data could be viewed and analysed subsequent to acquisition. In this mode, FL1-H vs. FL3-H *contour* plots were used, and not FL1-H vs. FL3-H *dot* plots.

Contour plot parameters were set as follows:

Scale:	probability, 20%
Smoothing:	1
Contour threshold:	0.5%

All gates created as described above in acquisition mode remained unchanged throughout all experiments (Section 3.2.3). Contour lines were used as a guide for defining gated population boundaries.

The number of *S. cerevisiae* was expressed as CFU.ml^{-1}. The CFU.ml^{-1} of the viable and dead populations was calculated by applying Equation 3.1 to the events detected within the 'viable' and 'dead' gates. The CFU.ml^{-1} of the total population was calculated by applying Equation 3.1 to the total number events displayed on the FL1-H vs. FL3-H plot, less the gated 'noise' events. The injured population CFU.ml^{-1} was calculated by applying Equation 3.1 to the total number of events displayed on the FL1-H vs. FL3-H plot, less the gated 'living', 'dead' and 'noise' events. BD Liquid Counting Beads™ was supplied at a specific concentration thus enabling the estimation of cells per ml (BD Biosciences, San Jose, CA).

$$\frac{\#\text{ of events in gate containing cell population}}{\#\text{ of events in bead population}} \times \frac{(\#\text{ of beads per } \mu l)(50\ \mu l)}{\text{test volume}} \times \text{dilution} = \text{concentration of } S.\ cerevisiae \text{ population}$$

where: # = number
dilution factor was 1.28

Equation 3.1
(BD Biosciences, San Jose, CA)

3.2.5 Further tests conducted to optimise the FACScan flow cytometer for detection of *Saccharomyces cerevisiae*.

3.2.5.1 Identification of noise events introduced by fluids used for FACScan flow cytometer for various analysis

Reagents and solutions added to the *S. cerevisiae* suspension during experimentation for flow cytometry were individually acquired by the FACScan flow cytometer, and the associated interference of noise populations was established and eliminated where possible. The 400 µl solutions were: 0.1 mM EDTA, 0.01% Tween-90 and 0.8% w/v NaCl. The solutions were made using pre-filtered water (Nucleopore, pore diameter 0.22 µm). The 0.1 mM PBS solution supplied by BD Biosciences was also acquired. All solutions (400 µl) were individually connected to the FACScan flow cytometer and acquired 3 times.

Instrument settings were as described in Section 3.2.3. Noise events were recorded on an FSC-H vs. SSC-H plot using BD Cell Quest software (BD Biosciences, San Jose, CA). The settings of the BD Cell Quest software used (BD Biosciences, San Jose, CA) were those given in Section 3.2.3. After each analysis, the location and magnitude of the noise population in the FSC-H vs. SSC-H plot was recorded.

3.2.5.2 Tests used determine the reproducibility of the FACScan flow cytometer

A) Multiple acquisition from a single 400 µl non-fluorescent *S. cerevisiae* suspension

A heterogeneous population of non-fluorescent *S. cerevisiae* cells suspended in 400 µl 0.1 mM PBS was used to test the accuracy of the FACScan flow cytometer. The 400 µl non-fluorescent *S. cerevisiae* PBS suspension was prepared as described in Section 3.2.3.1.

A single 400 µl sample was acquired six times using the BD FACScan flow cytometer. Instrument settings were as described in Section 3.2.3. Each sample was mixed before acquisition. *S. cerevisiae* cells and liquid counting beads were recorded on a FSC-H vs. SSC-H plot using BD cell Quest software (BD Biosciences, San Jose, CA). The settings of the BD Cell Quest software (BD Biosciences, San Jose, CA) are those given in Section 3.2.3. After each analysis the number of *S. cerevisiae* cells was determined by using Equation 3.1.

B) Acquisition of six different 400 µl *S. cerevisiae* suspensions, sampled from a single *S. cerevisiae* culture (OD_{600}, 0.8)

Six separate 400 µl PBS (0.1 mM) suspensions of non-fluorescent *S. cerevisiae* cells were prepared as described in Section 3.2.3.1. All six *S. cerevisiae* samples were taken from a single 100 ml *S. cerevisiae* culture (OD_{600} 0.8 – 1.1).

Instrument settings were as described in Section 3.2.3. Each sample was mixed before acquisition. *S. cerevisiae* cells and liquid counting beads were recorded on a FSC-H vs. SSC-H plot using BD cell Quest software (BD Biosciences, San Jose, CA). The settings of the BD Cell Quest software (BD Biosciences, San Jose, CA) are those given in Section 3.2.3. After each analysis the number of *S. cerevisiae* cells was determined using Equation 3.1.

3.2.5.3 Optimal suspension flow rate for acquisition of *Saccharomyces cerevisiae* cell counts using the BD FACScan

Ten 400 µl PBS (0.1 mM) volumes containing non-fluorescent *S. cerevisiae* were prepared as described in Section 3.2.3.1. All *S. cerevisiae* samples were taken from a single 100 ml culture (OD_{600} 0.8 – 1.1).

Five 400 µl samples were acquired using the FACScan flow cytometer. Instrument settings were as described in Section 3.2.3. The flow rate of *S. cerevisiae* suspended in 400 µl 0.1 mM PBS was set at 12 µl per min ('low' setting). The remaining five *S. cerevisiae* suspensions were acquired using a flow rate of 60 $\mu l.min^{-1}$ ('high' setting). Each sample was mixed before acquisition. The *S. cerevisiae* cells and liquid counting beads were recorded on

an FSC-H vs. SSC-H plot using BD Cell Quest software (BD Biosciences, San Jose, CA). The settings of the BD Cell Quest software (BD Biosciences) are those given in Section 3.2.3. After each analysis the number of *S. cerevisiae* cells was determined using Equation 3.1.

3.2.5.4 Determination of the optimal endpoint of *a Saccharomyces cerevisiae* acquisition when using the BD FACScan

Five separate 400 µl PBS suspensions containing non-fluorescent *S. cerevisiae* were prepared as described in Section 3.2.3.1. All *S. cerevisiae* samples were taken from a single 100 ml culture (OD_{600} 0.8 – 1.1).

All five 400 µl suspensions were acquired twice. The first acquisition was set to automatically terminate after 180 s of acquiring, and the second acquisition was set to terminate after 20 000 total events (comprised of *S. cerevisiae* cells, beads, and noise) were detected.

Instrument settings were as described in Section 3.2.3. Each sample was mixed before acquisition. *S. cerevisiae* cells and liquid counting beads were recorded on a FSC-H vs. SSC-H plot using BD cell Quest software (BD Biosciences, San Jose, CA). The settings of the BD Cell Quest software (BD Biosciences, San Jose, CA) are those given in Section 3.2.3. After each analysis the number of *S. cerevisiae* cells was determined using Equation 3.1.

3.2.6 Statistical analysis of results

The arithmetic mean (average) and standard deviation were estimated by using Microsoft Office Excel™ 2003. The standard deviation was calculated using the "unbiased" or "n-1" method (Microsoft Office Excel™ 2003).

3.3 Results and Discussion

3.3.1 Maintenance *Saccharomyces cerevisiae* GC210 (*MATα lys2*)

It was decided to use *Saccharomyces cerevisiae* GC210 (*MATα lys2*), as this yeast strain does not form spores. The response of spores to heat and ultrasound would differ from that of vegetative cells. Frozen *S. cerevisiae* samples containing similar CFU.ml^{-1}, all taken from a single culture, are often used in research as standard inocula. It is thought this represents a convenient practice to ensure that similar numbers of cells are "metabolically homogeneous". In this study, fluorescent flow cytometry was used to examine the condition of frozen stock cultures after thawing. This showed that these *S. cerevisiae* GC210 (MATα lys2) cells were comprised of a large portion injured cells (40 – 60%), and some cells were dead (5 – 30%). Furthermore, the degree to which the population was injured was variable. At the time of freezing, cytometry had shown that the cells were homogeneous. Therefore freezing at -70°C damaged the cells. As a result, frozen cultures (1 ml) were used to inoculate 500 ml YPDB and were incubated overnight to an OD_{600} ~1. Subsequent fluorescent flow cytometry showed that this practice reduced injury and produced a more homogeneous yeast cell population suitable for experimental use (Refer Chapter 4; contour plots).

3.3.2 Initial calibration of the BD FACScan using CaliBRITE™ beads and FACScomp™ software

Each fluorochrome has a specific wavelength of maximum fluorescence, known as the peak emission wavelength. Thiazole orange and PI used in this study has a maximum peak emission wavelength of 533 and 617 nm respectively (BD Biosciences, San Jose, CA). For optimal detection, the fluorochromes should have a peak fluorescence similar to one of the three light detecting diodes i.e. FL1-H = 530 ±30 nm, FL2 = 585 ±42 nm and FL3-H = 570 nm LP.

Even though there is a peak emission wavelength, the fluorochromes also emit light at wavelengths higher and lower than the peak wavelength. Therefore a fluorochrome may have a wavelength peak detected by FL1-H channel. However the FL2-H and FL3-H may also detect less intense signals. These signals may interfere with the fluorescence of other fluorochromes detected by the other two detectors. The FACSComp™ software (BD Biosciences, San Jose, CA) automatically corrected for this such that the overlap in fluorescence was compensated for. CaliBRITE™ Beads (BD Biosciences, San Jose, CA) were used as standard particles of detection for the calibration.

The beads used were:

a) Non-Fluorescent beads i.e. no fluorochromes
b) Fluorescein isothiocyanate (FITC) fluorescent beads
c) Phytoerythrin (PE) fluorescent beads
d) Peridinin chlorophyll protein (PerCP) fluorescent beads

Calibration measurements are automatically documented (Refer Fig. 3.4) and indicate whether the calibration was successful or not.

3-Color Lyse/Wash FACSComp Report

Institution: CPUT
Director: *Dr. K Meehan*
Operator: facs

Date: Thu, Nov 3, 2005 1:10 PM
Software: *FACSComp 5.1.1*
Cytometer: FACSC[illegible]81827R

A — B

Parameter	High	Low	Separation	Minimum	Result	Lot ID
FSC	187	74	113	100	Pass	65533I
SSC	236	7	229	210	Pass	65533I
FL1	180	63	117	85	Pass	60789P
FL2	187	51	136	128	Pass	65529I
FL3	187	46	141	128	Pass	60839M

Parameter	Detector	Amplifier	Threshold
FSC	E00	2.00	52
SSC	343	1.00	
FL1	561	Log	
FL2	642	Log	
FL3	588	Log	

Blue Laser Current 5.86 Amps
Blue Laser Power 15.00 mWatts

Compensation	FL1-%FL2	FL2-%FL1	FL2-%FL3	FL3-%FL2
	1.3	18.5	0.0	13.1

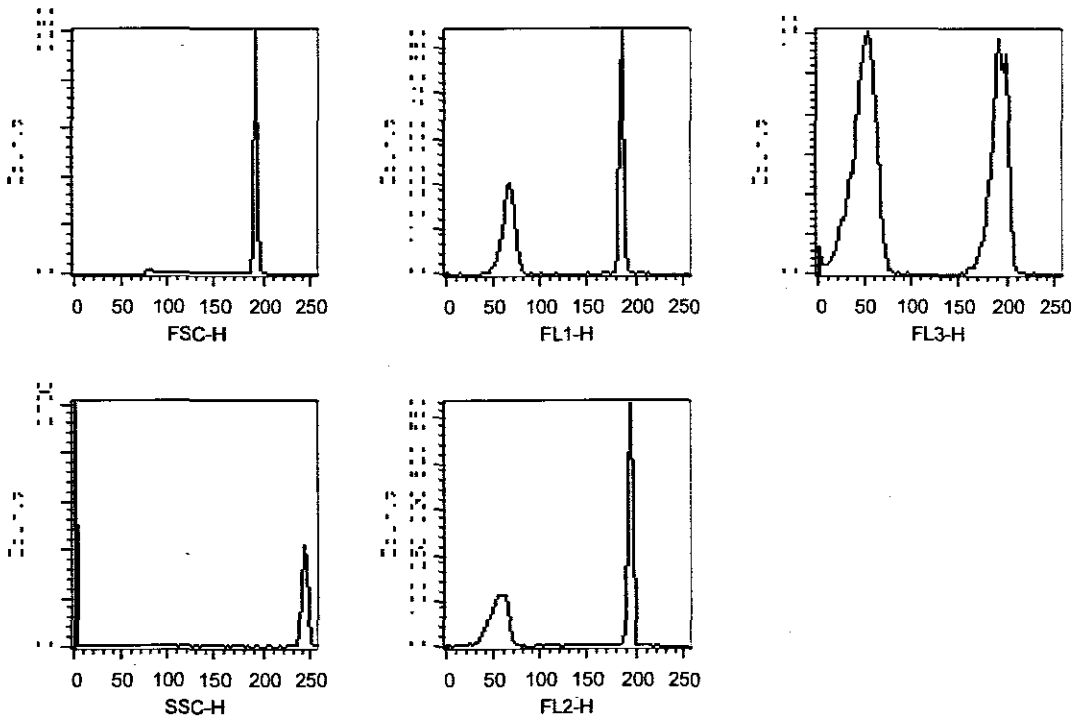

Comments:

Figure 3.4. A typical report issued after calibration of the FACScan using using beads supplied by the manufacturer. 'A' indicates the channel (i.e. forward scatter, side scatter, etc) and 'B' depicts the test result

3.3.3 Setting up of BD Cellquest software for the *acquisition* of *Saccharomyces cerevisiae*

The optimal instrument settings for detecting *S. cerevisiae* and BD Liquid Counting Beads™ were established before experimentation was conducted. This was achieved by acquiring 0.1 mM PBS containing *S. cerevisiae* (final concentration ~10^7CFU.ml^{-1}) and BD Liquid Counting Beads™ (final concentration of 969.ml^{-1}) in *acquisition* mode. The optimal instrument settings for the FSC-H, SSC-H, FL1-H and FL3-H channels were determined in two successive stages. In the first stage, the FSC-H and SSC-H channel PMT voltages were adjusted to display the *S. cerevisiae* and BD Liquid Counting Beads™ populations on a FSC-H vs. SSC-H dot plot. The two populations of events were required to be readily distinguishable from each other and from the interfering noise events (Fig.3.1).

Secondly, separate gates were then drawn around the two populations of events on the FSC-H vs. SSC-H dot plot (Fig.3.2). The gate around the *S. cerevisiae* population was set such that all the events within the gate were displayed on a separate FL1-H vs. FL3-H dot plot. Further acquisition was required to optimise the FL1-H and FL3-H channels. The FL1-H and FL3-H channels needed not only to be optimised to display the *S. cerevisiae* population but also to differentiate between viable, injured and dead sub-populations.

A *non*-fluorescent population of *S. cerevisiae*, cultured in YPDB to late exponential phase (Section 3.2.3.1), was used to establish the optimal settings for FSC-H and SSC-H channels. The settings for FSC-H and SSC-H channels were: (Section 3.2.3.2)

- FSC-H – E01 (logarithmic amplification)
- SSC-H – 295 V (logarithmic amplification)

A threshold was set on the FSC-H channel such that any event with a PMT voltage less than 302 V would not be recorded and displayed (Fig.3.1)(Section 3.2.3.2). This reduced noise events, thereby enhancing resolution of the *S. cerevisiae* and BD™ Liquid Counting Beads populations.

The gated *non*-fluorescing *S. cerevisiae* population was set to display on a FL1-H vs. FL3-H dot plot. The FL1-H and FL3-H channel settings were adjusted during further acquisition such that non-fluorescing *S. cerevisiae* were located near the origin of the plot, this representing the area where lowest PI (FL3-H) and TO (FL1-H) fluorescence was measured.

Thereafter, a PBS solution containing *fluorescent* late exponential phase *S. cerevisiae* cells, stained with TO and PI (Section 3.2.3.1), were acquired in acquisition mode. The TO and PI bound to DNA, therefore cells were detected as fluorescent events.

The FSC-H and SSC-H channels do not detect PI or TO fluorescence. Therefore the channel settings did not require adjustment for the acquisition of fluorescent cells. The detected fluorescent population was gated and set to display on a FL1-H vs. FL3-H dot plot, as was the non-fluorescent population.

The FL1-H and FL3-H channels respectively detect TO and PI bound to DNA. Therefore the position of individual fluorescent *S. cerevisiae* cells on a FL1-H vs. FL3-H plot depends on the amount of TO or PI that entered a cell. Thiazole orange enters all cells. However, PI is only capable of entering cells with compromised cell boundaries (Malacrino *et al.*, 2001). Therefore *fluorescent S. cerevisiae* cells are separated over the FL3-H axis according to the extent of cell boundary integrity. As a result, three sub-populations of cells are formed on a FL1-H vs. FL3-H plot: viable, injured and dead.

The location of viable and dead populations was identified by acquiring PBS containing either fluorescent viable *S. cerevisiae* cells or fluorescent pasteurised *S. cerevisiae* cells. *Saccharomyces cerevisiae* was pasteurised by heating at 70°C for 20 minutes (Refer 3.2.3.4). The FL1-H and FL3-H PMT voltages were adjusted such that both populations were adequately displayed on the FL1-H vs. FL3-H dot plot.

Gates were applied around the viable and dead populations once located on a FL1-H vs. FL3-H dot plot. A separate gate was placed around the noise population which was always located near the origin of the FL1-H vs. FL3-H contour plot. Injured cells were considered to be those that did not occur within any of the viable, dead or noise gates. The final PMT voltage settings used were:

- FL1-H – 500 V (TO)
- FL3-H – 427 V (PI)
- Compensation – none

3.3.4 Setting up of BD Cellquest software for *analysis* of acquired data

Once an acquisition of a 400 µl sample was complete, all the data collected was analysed in 'analysis mode'. In analysis mode, the FL1-H vs. FL3-H plots were displayed as 'contour plots' and not 'dot plots'. Instead of a series of dots representing each event, contour lines represent areas of the same event concentration. A typical contour plot is shown in Fig. 3.3.

The contour plot criteria used in this study were: (Refer 3.2.4)

- Scale: probability set at 20%
- Smoothing: 1
- Threshold: 0.5%

The scale of the contour lines was set to 'probability' with 20% intervals. This meant that each contour line represented a percentage of the total population. The outermost contour represented 10% and increased sequentially by 20% to a maximum of 90%. The area between each contour represented an equal percent (20%) of the total population (BD Biosciences, 2002).

A smoothing factor of '1' was applied to the contour lines. This decreased irregularities of the contour profiles but did not affect calculated statistics on the contour plot (BD Biosciences).

A contour threshold of 0.5% was applied to the contour lines. This provided a level of discrimination to eliminate unwanted data. The threshold did not affect statistics on the contour plot (BD Biosciences, 2002).

The viable and dead population did not occur in precisely the same location when different samples were acquired. Therefore the position of the gates was adjusted to fit around the population satisfactorily. The advantage of contour plots over dot plots is that contour lines can be used as definitive boundaries of populations, thus making placement of gates objective.

The BD Liquid Counting Beads™ were added to 400 µl PBS at a known concentration (969.ml^{-1}). Therefore the concentration of *S. cerevisiae* cells.ml^{-1} was calculated by relating the number of BD Liquid Counting Beads™ detected during the acquisition to the number of *S. cerevisiae* cells detected during the same acquisition. Equation 3.1 was used to calculation the CFU.ml^{-1} of the *S. cerevisiae*. (BD Biosciences 2002).

3.3.5 Optimisation of flow cytometer and flow cytometry solutions for *Saccharomyces cerevisiae* detection

3.3.5.1 Identification of noise events introduced by fluids used in flow cytometry

Contaminant particles in solutions undergoing flow cytometric analysis are detected as noise events. Noise particles may be positioned amongst populations of yeast cells or BD Liquid Counting Beads™, and are therefore included in gates and calculations. Therefore contaminant particles in solutions were kept to a minimum and the inclusion of noise events within any analysed gated areas was avoided. In this section, the location of noise populations associated with reagents and solutions added to the *S. cerevisiae* suspension during experimentation were determined on a FSC-H vs. SSC-H dot plot. This was to ensure it did not occur in the area where *S. cerevisiae* or BD Liquid Counting Beads™ population was located. All FL1-H vs. FL3-H dot plots showed less noise events than did FSC-H vs. SSC-H dot plots, as only the events gated around the *S. cerevisiae* population were

displayed on a FL1-H vs. FL3-H dot plot. In addition, most noise events do not fluoresce and therefore were readily separated from fluorescent *S. cerevisiae* cells on a FL1-H vs. FL3-H plot.

Yeast cells may form clumps in a solution, which are detected as a single event by the FACScan flow cytometer. The addition of 0.01% Tween 90 and 1 mM EDTA to the solution aided the separation of the clumps thereby improving the accuracy of cell counts (Boyd *et al.* 2003). However, both Tween 90 and EDTA were a potential source of noise particles.

Filtering a solution through a 0.22 µm Nucleopore filter reduced the number of noise signals but did not eliminate these. To overcome this, solutions of 0.01% Tween 90 or 1 mM EDTA were acquired as described in Section 3.2.5.1 to locate the precise position of this noise on an FSC-H vs. SSC-H dot plot. The location of the associated noise populations is shown in Fig. 3.5 for 0.01% Tween 90 and Fig. 3.6 for 1 mM EDTA.

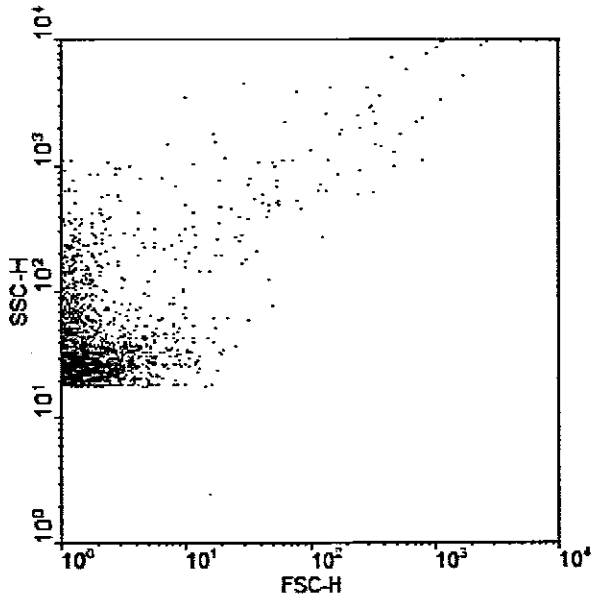

Fig. 3.5: BD Cell Quest dot plot showing the location of the noise population associated with a Tween 90 (0.01%) solution

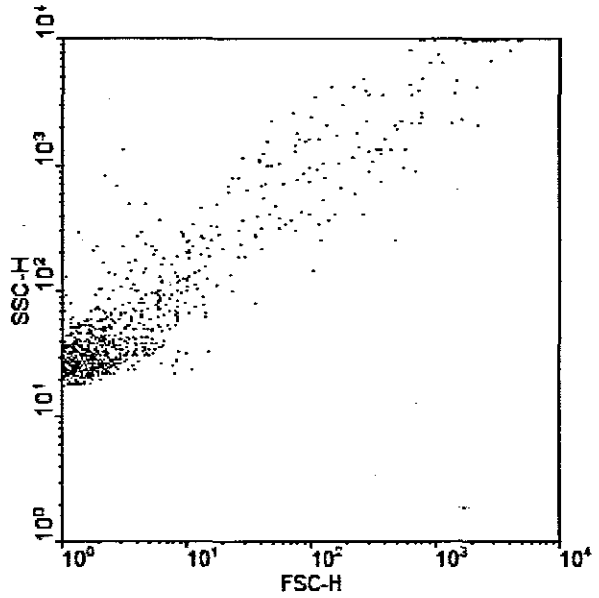

Fig. 3.6: BD Cell Quest dot plot showing the location of the noise population associated with an EDTA (1 mM) solution

The recommended solution in which *S. cerevisiae* was suspended for flow cytometry analysis was 0.1 mM PBS (Malacrino *et al* 2001). The PBS solution was supplied by the manufacturer and was pre-filtered through a 0.22 µm filter. However, noise particles were still visible on a FSC-H vs. SSC-H dot plot (Fig. 3.7). Therefore a 0.1 mM PBS solution supplied by the manufacturer was acquired as described in Section 3.2.5.1 to determine where on FSC-H vs. SSC-H dot plot the noise population occurred (Fig. 3.7).

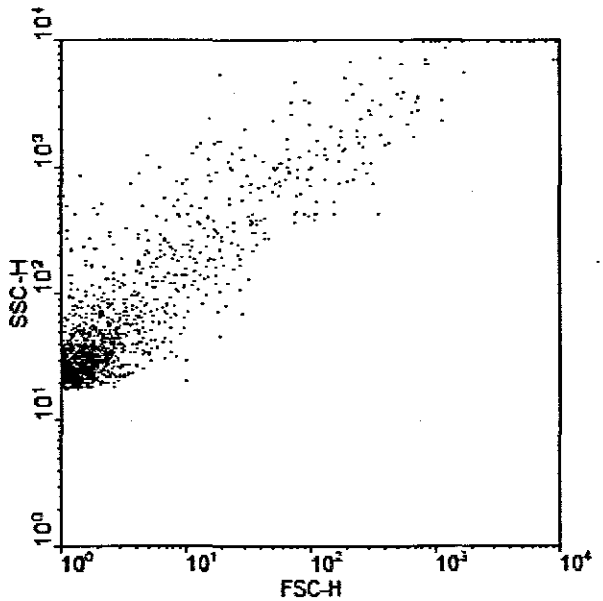

Fig. 3.7: BD Cell Quest dot plot showing the location of the noise population associated with the supplied PBS solution

Boyd, *et al* (2003) recommended that yeast cells acquired by flow cytometry should be suspended in a PBS solution. However, throughout this study, ultrasound and heat experiments were conducted using *S. cerevisiae* suspended in physiological saline. Therefore, it was considered advantageous for *S. cerevisiae* cells to be acquired in the saline solution. Sterile, filtered (0.22 µm) 0.8% w/v NaCl solution was acquired to determine the extent and location of noise on a FSC-H vs. SSC-H dot plot (Fig. 3.8) and compared to a solution of PBS (Fig. 3.7)

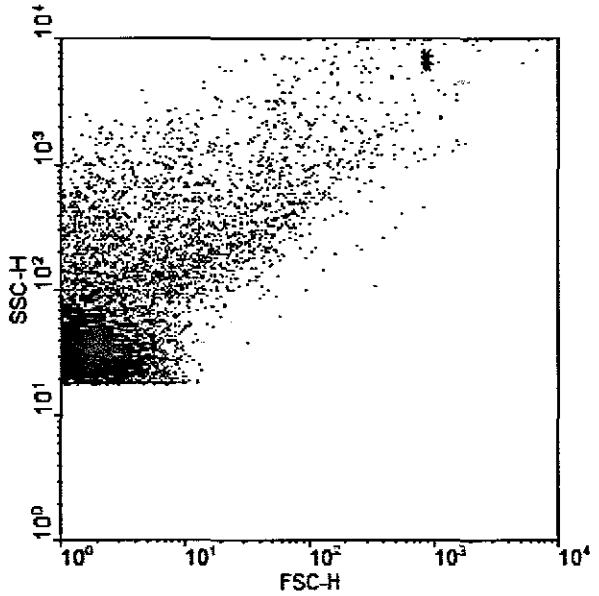

Figure 3.8: BD Cell Quest dot plot showing the location of the noise population associated with a saline solution (0.8%)

It was apparent that the PBS solution was more suited for the acquisition of data than was the 0.8 (w/v) saline. The latter was characterised by an intense level of interfering noise (Fig. 3.8). Based on these results, all *S. cerevisiae* cells were suspended in PBS for flow cytometric analysis.

Each solution tested was characterised by noise events. These events were situated at low FSC-H values, on the x axis of a dot plot. A threshold was therefore set on the FSC-H channel such that any events detected at low FSC-H PMT voltages would not be recorded. This improved the resolution of the yeast and bead populations.

3.3.5.2 Tests used to determine the reproducibility of the FACScan flow cytometer

The reproducibility of the FACScan flow cytometer was tested using two methods:

1. a single 400 µl aliquot of non-fluorescing *S. cerevisiae* cells suspended in 400 µl PBS was acquired 6 times (Section 3.2.5.2)
2. six 400 µl aliquots from a 1 L PBS suspension of non-fluorescing *S. cerevisiae* cells were all acquired once (Section 3.2.5.2)

Events obtained from these analyses were recorded on a FSC-H vs. SSC-H dot plot. The *S. cerevisiae* populations were gated as described in Section 3.2.3 and enumerated using equation 3.1

The CFU.ml^{-1} values for *S. cerevisiae* cells acquired from the same 400 µl sample are shown in Table 3.1. The average *S. cerevisiae* concentration of the six acquisitions of the same sample was 1.58 x10^5 CFU.ml^{-1}.

Table 3.1: *Saccharomyces cerevisiae* counts (CFU.ml^{-1}) of a single 400 µl PBS *S. cerevisiae* suspension, measured six consecutive times, as determined by the flow cytometer

Sample A (CFU.ml^{-1})					
First acquisition	Second acquisition	Third acquisition	Forth acquisition	Fifth acquisition	Sixth acquisition
1.61 x10^5	1.56 x10^5	1.58 x10^5	1.52 x10^5	1.59 x10^5	1.60 x10^5

Results obtained for the acquisition of six different 400 µl PBS *S. cerevisiae* suspension samples, taken from the same 1 l stock culture are shown in Table 3.2. Results were reproducible with the average *S. cerevisiae* concentration of the stock solution, calculated from six separate 400 µl samples was 1.55 x10^5 CFU.ml^{-1}.

Table 3.2: *Saccharomyces cerevisiae* counts (CFU.ml^{-1}) of six different 400 µl PBS *S. cerevisiae* suspension from the same 1 l stock solution, as determined by the flow cytometer

(CFU.ml^{-1})					
Sample B	**Sample C**	**Sample D**	**Sample E**	**Sample F**	**Sample G**
1.57 x10^5	1.55 x10^5	1.60 x10^5	1.54 x10^5	1.54 x10^5	1.52 x10^5

Overall, results showed that in the absence of noise from the acquisition, flow cytometry represented an accurate real time analytical method for enumeration of a *S. cerevisiae* suspension as used in this study.

3.3.5.3 Optimal suspension flow rate for acquisition of *Saccharomyces cerevisiae* cell counts using the BD FACScan

The rate at which the FACScan flow cytometer acquires events is determined by the flow rate of sheath fluid passing the laser. Two flow rates, of 12 or 60 µl per min, can be selected when acquiring data. It was therefore necessary to determine which of the two flow rates was optimum for determining *S. cerevisiae* cell numbers.

Five 400 µl 0.1 mM PBS solutions containing non-fluorescent *S. cerevisiae* from a single culture suspension were acquired at both flow rates to determine whether these influenced the number of CFU.ml^{-1} detected (Section 3.2.5.3). The *S. cerevisiae* was cultured as described in Section 3.2.3.1. The recorded concentrations of *S. cerevisiae* are shown in Table 3.3. Results showed that the recorded CFU.ml^{-1} were similar for both flow rates of the samples A – E.

Table 3.3: *Saccharomyces cerevisiae* counts (CFU.ml^{-1}) of five 0.1 mM PBS *S. cerevisiae* suspensions determined by flow cytometry at high (60 µl.min^{-1}) and low (12 µl.min^{-1}) flow rates.

Flow rate	Sample A (CFU.ml^{-1})	Sample B (CFU.ml^{-1})	Sample C (CFU.ml^{-1})	Sample D (CFU.ml^{-1})	Sample E (CFU.ml^{-1})	**AVE (CFU.ml^{-1})**
12 µl. min^{-1}	1.57 x10^5	1.55 x10^5	1.52 x10^5	1.54 x10^5	1.54 x10^5	**1.54 x10^5**
60 µl. min^{-1}	*1.60 x10^5*	*1.62 x10^5*	*1.62 x10^5*	*1.59 x10^5*	*1.55 x10^5*	**1.60 x10^5**

3.3.5.4 Determination of the optimal endpoint of *a Saccharomyces cerevisiae* acquisition when using the BD FACScan

The FACScan flow cytometer can be set to acquire suspensions for a specified time period, or until a specified number of events are detected. The specified number of events can be the total events detected, or alternatively the events detected within a specified gate. It was decided to determine if both end point criteria yielded similar CFU.ml^{-1} when acquiring a 400 µl 0.1 mM PBS *S. cerevisiae* suspension.

For this test, five PBS (400 µl) suspensions containing BD Liquid Counting Beads™ and unstained *S. cerevisiae* were prepared (Section 3.2.3.1). These samples were acquired for either 180 s or until a total events of 20 000 was detected.

Table 3.4: Concentration of *S. cerevisiae* (CFU.ml^{-1}) calculated using data obtained by using two different end points of acquisition: at 180 s or 20 000 total events

End point	A	B	C	D	E	AVE
20 000 events	1.47 x10^5	1.44 x10^5	1.46 x10^5	1.45 x10^5	1.47 x10^5	1.45 x10^5
180 s	1.39 x10^5	1.44 x10^5	1.43 x10^5	1.45 x10^5	1.47 x10^5	1.43 x10^5

Table 3.4 shows the calculated number of *S. cerevisiae* per millilitre was similar, regardless of the method used for the endpoint of acquisition. Boyd *et al.*, (2003) recommended that a

minimum of 1 000 beads should be detected in order to assure accurate calculation of the number of CFU.ml^{-1}.

These results suggested that the criteria for the endpoint did not influence calculation of the number of CFU.ml^{-1}. Therefore it was decided to set acquisitions to automatically cease after 180 s through all experimentation.

3.4 Conclusion

Overall, these preliminary studies showed that once calibrated to detect *S. cerevisiae* events, fluorescent flow cytometry, using TO and PI as the fluorophores was a highly reproducible method for real time analyses of *S. cerevisiae*. These analyses were quantitative and qualitative, enabling precise measurements of viable, membrane-injured and dead cell populations. The most commonly encountered problem was one of "noise", but by the setting of correct thresholds, this was eliminated from interfering with event readings.

CHAPTER FOUR

FLOW CYTOMETRIC EVALUATION OF CULTURES TREATED WITH HEAT AND/ OR ULTRASOUND

4.1 Introduction: Background to hurdle technology and the use of flow cytometry to evaluate the efficacy of such applications

Moist heat, such as pasteurisation of beverages, is commonly used in the food industry to reduce the microbial load on food items and thereby extend the shelf life (Jay, 1997). However heat as a single pasteurisation parameter can impact negatively on the flavour and colour of the beverages. Therefore there is a commercial need for newer "near to natural" approaches (hurdle technology) that may reduce microbial load whilst maintaining acceptable food quality.

Ultrasound has been investigated as an alternative to heat pasteurisation. While ultrasound has been reported to reduce microbial loads in beverages, it need not inactivate all the microorganisms (Piyasena, *et al.*, 2003). Therefore it is possible that ultrasound be used as a hurdle in combination with other disinfection techniques, such as heat or pressure (Pagan *et al.*, 1999). In this study, heat and ultrasound were investigated either separately or combined, to reduce the number of *Saccharomyces cerevisiae* suspended in physiological saline. A synergistic combination of ultrasound and heat could shorten times and decrease the temperatures required to disinfect liquids, therefore maintaining organoleptic properties of that liquid. Since the two disinfection techniques work in synergistic combination, it is not required that either hurdle kills a large fraction of the population. Instead, the individual treatments are only required to injure the cells but the additive effect of injuries of different origins results in cell death (Leistner, 1994).

A difficulty encountered with any microbicidal / static effects on microbes has been the accurate and rapid assessment of cell viability before, during and after treatment. The serial dilution and plate count technique is commonly used to determine the lethality of a microbicidal treatment. However it is limited in that results are retrospective as they are only determined after 72 h or more after incubation. Furthermore, injured cells may recover or die during incubation on the nutrient agar (Ray, 2003). Therefore, plate counts yield little information regarding the physiological state of injury sustained by the micro-organism during antimicrobial treatment.

Various research groups have suggested that metabolic changes consistent with possible injury occurred in microorganisms after ultrasonic treatment. (Ciccolini *et al.*, 1997; Lorincz, 2004; Tsukamoto *et al.*, 2004, Borthwick, Coakley, Mc Donell, Nowtony, Benes, and Groschl,

2005) It would therefore be preferable to use a cell measurement technique that provides a quantitative real time measurement of cell viability, death and injury.

Fluorescent flow cytometry allows for real time enumeration of *S. cerevisiae* as well as determining the metabolic state of the cell. (Sorensen & Jakobsen, 1997; Malacrino, *et al.*, 2001; Boyd *et al.*, 2003; Muller & Losche, 2003; Martinez-Esparza, Sarazin, Juoy, Poulain & Jouault, 2006; Cipollina, Val, Porro & Hatzis, 2007; Simonin, Beney & Gervals, 2007). For the purposes of this study, fluorescent flow cytometry was assessed and then used to monitor the effect of heat and/or ultrasound on *S. cerevisiae* populations in a physiological saline solution.

The metabolic state of the cell was determined by the use of the two fluorescent dyes, propidium iodide (PI) and thiazole orange (TO). Thiazole orange is permeant in all cells whereas PI only enters cells when the integrity of the membrane has been compromised (BD Biosciences, 2002). Propidium iodide uptake therefore indicates both cell membrane injury and death (Boyd *et al.*, 2003)(Section 3.1). Boyd *et al.*, (2003) demonstrated that colony forming units (CFU) counts obtained for yeasts correlated well with counts obtained using a flow cytometer or a haemocytometer.

The effects of heat (55°C and 60°C) and ultrasound on the *S. cerevisiae* cell boundary were first separately determined. Thereafter the effects of a combined ultrasound and heat treatment were investigated. Many authors have commented on the synergy between sonication and heat to inactivate microorganisms (Munkacsi & Elhami 1976; Garcia *et al.*, 1989; Ciccolini *et al.*, 1997; Petin *et al.*, 1998; Pagan *et al* 1999; Guerrero, *et al.*, 2001; Joyce, *et al.*, 2003; Lorincz, 2004) (Section 1.2.4). This study represents the first report on the use of fluorescent flow cytometry to determine yeast cell metabolic state as influenced by heat and ultrasound.

4.2 Methods and Materials

4.2.1 Maintenance and growth of *Saccharomyces cerevisiae* GC210 (*MATα lys2*) (Refer to 3.2.1)

Saccharomyces cerevisiae GC210 (*MATα lys2*) was used throughout the study and is a haploid non-sporulating laboratory strain with a genetic background congenic to *S.cerevisiae* Σ1278b (Cunningham & Cooper, 1991). Throughout this study the organism is referred to as *S. cerevisiae*. Pure cultures were maintained on malt extract agar (MEA) (Biolab Diagnostics, Midrand, South Africa).

To culture cells for heat treatment, 100 ml sterile Yeast Peptone Dextrose Broth (YPDB) (Biolab Diagnostics) were inoculated with the stock *S. cerevisiae* prepared as described in section 3.2.1, and incubated at 25°C in a thermostatically controlled water bath (Thermomix 1440, B, Braun Melsungen AG, Germany) for 12 - 20 h until an OD_{600} ~0.15 - 1.5 were variously attained. The optical density was measured using a *GeneQuant Pro* spectrophotometer (Biochrom, Cambridge, United Kingdom).

Thereafter, cells were harvested by centrifugation of 1.5 ml YPDB culture using a Spectrafuge 16M centrifuge (ManSci Inc, Tonawanda, NY, USA), at 9000 rpm for 5 min. The cell pellet was re-suspended in 1.5 ml sterile 0.8% NaCl (w/v). The 0.8% (w/v) NaCl solution was filtered through a 45 mm Nucleopore filter (Whatman Ltd, New York, United States of America) pore diameter 0.22 µm, prior to use.

4.2.2 Heat application at 55°C to *Saccharomyces cerevisiae* cultures

Two 0.5 ml samples of the 1.5 ml *S. cerevisiae* suspension prepared in accordance with the procedure outlined in Section 4.2.1, were added to two 4.5 ml 0.8% (w/v) sterile saline solution. Prior to inoculation, the 4.5 ml saline solution was preheated to 55°C, using a Heidolph Laborota 4000 water bath (Sigma Aldrich, Aston Manor, South Africa). These suspensions remained at 55°C for 20 min. Samples (400 µl) were removed after 5, 10, 15 and 20 min of heating at 55°C and placed in a water / ice mixture. As a control, the remaining 0.5 ml *S. cerevisiae* saline suspension from the 1.5 ml (as prepared in section 4.2.1) was added to 4.5 ml of 0.8% (m/v) saline solution and held at ambient temperature (22°C) for 20 min and then placed in the ice-water bath. A 400 µL sample was removed and placed on ice. This was the untreated control sample. The 400 µl samples were centrifuged at 9 000 rpm for 5 min. The resultant pellets of cells were re-suspended in 400 µl of 0.1 mM phosphate buffered saline (PBS) and prepared for flow cytometry (Section 4.2.6).

4.2.3 Heat application at 60°C to *Saccharomyces cerevisiae* cultures

Procedures followed were identical to those outlined in Section 4.2.2 above, except that treatment temperature was maintained at 60°C.

4.2.4 Application of ultrasound to *Saccharomyces cerevisiae* cultures

Cells, cultured as described in section 4.2.1, were harvested by centrifugation of 6 ml YPDB culture using a Spectrafuge 16M centrifuge, at 9 000 rpm for 5 min. The cell pellet was re-suspended in 6 ml sterile 0.8% NaCl (w/v). The 0.8% (w/v) NaCl solution was filtered through a 45 mm Nucleopore filter, pore diameter 0.22 µm, prior to use. The 6 ml *S. cerevisiae* saline suspension was added to 54 ml of 0.8% (w/v) sterile saline solution. The saline solution was degassed and sterilised prior to sonication by autoclaving at 121°C, 10^4 kg.m^{-2} for 15 min (Model HA-300D, Hirayama Manufacturing Corporation), as described in Section 2.2.1.

A 20 kHz horn type sonicator (Vibracel VCX 750 Sonics and Materials Inc, Connecticut, USA) was used (Section 2.1.1). The standard titanium alloy (Ti-6Al-4V) horn had a tip diameter of 13 mm (Materials and Sonics Inc, Connecticut, USA). Displacement amplitude was maintained at 124 µm for all treatments. All 60 ml samples were sonicated using a supplied cylindrical 100 ml glass vessel (Materials and Sonics, Inc, Connecticut), cooled by 10°C water circulating through the outer jacket from a Thermomix 1440, B, Braun Melsungen AG waterbath (Fig. 2.2). The temperature of the sample undergoing sonication did not exceed 35°C. The glass cooling cell and contents were placed on a jack platform (Materials and Sonics, 2002) (Fig. 2.2). The height of the cooling vessel was adjusted such that the horn was centrally positioned in the *S. cerevisiae* suspension and the tip was 20 mm above the base of the container.

Before sonication commenced, a 400 µl sample was removed from the 60 ml *S. cerevisiae* suspension and used as an untreated control. Thereafter, for a 5 min treatment, samples (400 µl) were removed after 1, 2, 3, 4 and 5 min. In the case of a 20 min treatment, sampling was done at 0, 5, 10, 15 and 20 min. All samples were centrifuged at 9 000 rpm for 5 min. The resultant pellet of cells was re-suspended in 400 µl of 0.1 mM PBS and prepared for flow cytometry.

4.2.5 Application of hurdle technology to *Saccharomyces cerevisiae* cultures

A *S. cerevisiae* suspension was cultured as described in section 4.2.1 and prepared for sonication as described in section 4.2.4.

The Vibracell VCX 750 was assembled as described in section 4.2.4. Before the commencement of ultrasound, a 400 µl aliquot was removed as an untreated control sample. The remaining *S. cerevisiae* suspension was sonicated for 1 min. Thereafter 10 ml were removed and centrifuged at 9000 rpm for 5 min using a Spectrafuge 16M centrifuge. The resultant *S. cerevisiae* cell pellet was re-suspended in 1.5 ml 0.8% (w/v) saline solution.

Two 0.5 ml volumes of this suspension were added to two 4.5 ml of 0.8% (w/v) sterile saline solution preheated to either 55 or 60°C, using a Heidolph Laborota 4000 waterbath. Samples were incubated for 5 min at the respective temperatures. The remaining 0.5 ml aliquot was added to 4.5 ml of 0.8% (w/v) saline solution at room temperature (22°C). This was the ultrasound-only control. Samples (400 µl) were removed after 1, 2, 3, 4 and 5 min of heating at either 55 or 60°C and placed in a water / ice mixture.

The samples (400 µl) were centrifuged at 9 000 rpm for 5 min. The resultant pellet of cells was resuspended in 1 ml of 0.1 mM PBS and prepared for flow cytometry as described in Section 4.2.6. After staining, all samples of *S. cerevisiae* cells were analysed using a BD FACScan™ flow cytometer (BD Biosciences, San Jose, CA, USA) to determine living, membrane-injured and dead fractions of the *S. cerevisiae* population. Experiments were repeated at least twice.

4.2.6 Preparation of *Saccharomyces cerevisiae* samples for flow cytometry (Section 3.2.3)

The following reagents were added to each 400 µl *S. cerevisiae* 0.1 mM PBS suspension, following manufacturer's recommendations:

- BD Liquid Counting Beads™ (50 µl), supplied concentration of 969 beads.ml^{-1}
- Tween-90 (50 µl) (Merck, Darmstadt), to a final concentration of 0.01%
- EDTA (50 µl) (Merck, Darmstadt), to a final concentration of 0.1 mM
- BD™ thiazole orange (TO) (5 µl), to a final concentration, 420 nM
- BD™ propidium iodide (PI) (5 µl), to a final concentration, 43 nM

The final mixture was stored in a dark room for 10 – 15 min after adding TO and PI, prior to flow cytometric analysis. These were mildly mixed before being connected to the flow cytometer.

4.2.7 Flow cytometry data acquisition and analysis (Refer to 3.2.4)

The FACScan™ flow cytometer and BD™ Cell Quest software (BD Biosciences, San Jose, CA, USA) was optimised for the acquisition and analysis of *S. cerevisiae* as described in Chapter 3. All Photomultiplier tube (PMT), threshold settings, gates and parameters of the BD™ Cell Quest forward scatter (FSC-H) vs. side scatter (SSC-H) dot plots and fluorescent channel 1 (FL1-H) vs. fluorescent channel 3 (FL3-H) contour plots were calculated as described in Section 3.2.3.

Two 0.5 ml volumes of this suspension were added to two 4.5 ml of 0.8% (w/v) sterile saline solution preheated to either 55 or 60°C, using a Heidolph Laborota 4000 waterbath. Samples were incubated for 5 min at the respective temperatures. The remaining 0.5 ml aliquot was added to 4.5 ml of 0.8% (w/v) saline solution at room temperature (22°C). This was the ultrasound-only control. Samples (400 µl) were removed after 1, 2, 3, 4 and 5 min of heating at either 55 or 60°C and placed in a water / ice mixture.

The samples (400 µl) were centrifuged at 9 000 rpm for 5 min. The resultant pellet of cells was resuspended in 1 ml of 0.1 mM PBS and prepared for flow cytometry as described in Section 4.2.6. After staining, all samples of *S. cerevisiae* cells were analysed using a BD FACScan™ flow cytometer (BD Biosciences, San Jose, CA, USA) to determine living, membrane-injured and dead fractions of the *S. cerevisiae* population. Experiments were repeated at least twice.

4.2.6 Preparation of *Saccharomyces cerevisiae* samples for flow cytometry (Section 3.2.3)

The following reagents were added to each 400 µl *S. cerevisiae* 0.1 mM PBS suspension, following manufacturer's recommendations:

- BD Liquid Counting Beads™ (50 µl), supplied concentration of 969 beads.ml^{-1}
- Tween-90 (50 µl) (Merck, Darmstadt), to a final concentration of 0.01%
- EDTA (50 µl) (Merck, Darmstadt), to a final concentration of 0.1 mM
- BD™ thiazole orange (TO) (5 µl), to a final concentration, 420 nM
- BD™ propidium iodide (PI) (5 µl), to a final concentration, 43 nM

The final mixture was stored in a dark room for 10 – 15 min after adding TO and PI, prior to flow cytometric analysis. These were mildly mixed before being connected to the flow cytometer.

4.2.7 Flow cytometry data acquisition and analysis (Refer to 3.2.4)

The FACScan™ flow cytometer and BD™ Cell Quest software (BD Biosciences, San Jose, CA, USA) was optimised for the acquisition and analysis of *S. cerevisiae* as described in Chapter 3. All Photomultiplier tube (PMT), threshold settings, gates and parameters of the BD™ Cell Quest forward scatter (FSC-H) vs. side scatter (SSC-H) dot plots and fluorescent channel 1 (FL1-H) vs. fluorescent channel 3 (FL3-H) contour plots were calculated as described in Section 3.2.3.

4.2.8 Collation and interpretation of data

When heated, the event count of the *S. cerevisiae* subpopulations (viable, injured, and dead) detected at each time interval was expressed as fraction of the total start up population (Equation 4.1).

$$\frac{Vc}{N} = N_V$$

$$\frac{Ic}{N} = N_I$$

$$\frac{Dc}{N} = N_D$$

Where:

N = total population at the time of sampling

Vc = viable cell events

Ic = injured cell events

Dc = dead cell events

N_V = viable fraction

N_I = injured fraction

N_D = dead fraction

Equation 4.1

When calculating the population fractions obtained after *ultrasound* treatment, each population fraction was calculated using the *S. cerevisiae* total cell count at start-up rather than the total population at each sampling time interval as was done for the heat experiments. This was done as sonication treatment fractured the cells, whereas heat did not. In addition the total population at each sampling time was calculated as a fraction of the total population CFU at start-up to estimate the rate of cell fractionation (Equation 4.2).

$$\frac{Tc}{N_0} = N_T$$

$$\frac{Vc}{N_0} = N_V$$

$$\frac{Ic}{N_0} = N_I$$

$$\frac{Dc}{N_0} = N_D$$

Where:

N_0 = the total population at time zero / start-up.

Tc = total population at the time of sampling

Vc = viable cell events

Ic = injured cell events

Dc = dead cell events

N_T = the total population fraction at the time of sampling, compared to the start up total population fraction.

N_V = viable fraction

N_I = injured fraction

N_D = dead fraction

Equation 4.2

The mean and standard deviation of cell fractions from repeated experiments were calculated using Microsoft Office Excel™ 2003. Microsoft Office Excel™ (2003) was used to construct 'xy scatter' line graphs. The x axis displayed time from 0 – 20 min, in 5 min increments, for 55 °C experiments. For 60 °C, ultrasound and hurdle experiments, the x axis displayed time from 0 – 5 min, in 1 min increments. The y axis displayed the population fraction from 1 x 10^{-3} to 1 x 10^{-1}, increasing in 1 $\log_{10}$ increments. The notation of the population fractions on the y axis was displayed as 'scientific' notation. Hence 1 x 10^{-3} was displayed as '1.E-03', where 'E' denoted 'x10' to the exponent of. Likewise, 1 x 10^{-2} and 1 x 10^{-1} were displayed as 1.E-02 and 1.E-01 respectively.

The $\log_{10}$ decrease of viable cells between two sample times was calculated using Equation 4.3:

$$\Delta N_V = \mathrm{Log}_{10} N_{V\,0\,\mathrm{min}} - \mathrm{Log}_{10} N_{V\,y\,\mathrm{min}}$$

Where:

ΔN_V = $\log_{10}$ change in viable cells

N_V = viable cell fraction

y = the difference in minutes between the two sampling times

Equation 4.3

The $\log_{10}$ increase of injured cells between two sample times was calculated using Equation 4.4

$$\Delta N_I = \mathrm{Log}_{10} N_{I\,y\,\mathrm{min}} - \mathrm{Log}_{10} N_{I\,0\,\mathrm{min}}$$

Where:

ΔN_I = $\log_{10}$ change in dead cells

N_I = dead cell fraction

y = the difference in minutes between the two sampling times

Equation 4.4

The $\log_{10}$ increase of dead cells between two sample times was calculated using Equation 4.5:

$$\Delta N_D = \mathrm{Log}_{10} N_{D\,y\,\mathrm{min}} - \mathrm{Log}_{10} N_{D\,0\,\mathrm{min}}$$

Where:

ΔN_D = $\log_{10}$ change in dead cells

N_D = dead cell fraction

y = the difference in minutes between the two sampling times

Equation 4.5

The decimal reduction time (D value) was calculated using Equation 4.6

$$D = \mathrm{Ln}\ 0.1 / m$$

Where:

D = Decimal reduction time

m = gradient of an exponential curve between population fractions at two different time intervals

Equation 4.6

The decimal reduction time symbol, *'D'*, was differentiated between 55 and 60°C heating, ultrasound and 55 and 60°C hurdle treatments using the following subscripts:

D_{ht55}	=	55°C heat
D_{ht60}	=	60°C heat
D_{us}	=	ultrasound
D_{hd55}	=	55°C hurdle
D_{hd60}	=	60°C hurdle

4.2.9 Scanning Electron Microscopy (SEM) of *Saccharomyces cerevisiae* cells

Saccharomyces cerevisiae cells (1 ml) were removed from various samples to be visualised and were then centrifuged as described in Section 4.2.1. The supernatant was discarded and the cells were re-suspended in 1 ml 1% glutaraldehyde (Biolab Diagnostics, Midrand, South Africa). For scanning electron microscopy (SEM), these cells were collected on 12 mm diameter Nucleopore or Millipore membranes (Millipore Ltd, Massachusetts, United States of America), pore diameter 0.2 µm. These then went through a series of dehydrating ethanol (Biolab Diagnostics, Midrand, South Africa) washes, (35%, 50%, 70%, 80%, 90%, 95% and 100%). The cells remained for 10 min in each ethanol solution. Samples were fixed onto aluminium stubs, using carbon glue. Three 100 µL hexamethyldisilazane (Sigma Aldrich, Aston Manor, South Africa) volumes were added to each of the membranes, which were left to dry in a fume hood. Finally, the specimens were coated with a gold/palladium alloy (40:60) to a thickness of 10-20 nm, using the SEM coating unit E5 100 (Polaron Equipment Ltd, United Kingdom). The samples were viewed with a LEO S440 fully analytical SEM (Leica, Gauteng, South Africa) using the secondary detector at 10.00 kV, with a working distance of 15 mm.

4.3 Results and Discussion

4.3.1 Effects of 55°C heat on *Saccharomyces cerevisiae*

Saccharomyces cerevisiae cultures were grown as described in Section 4.2.1, to various OD_{600}, ranging from early (12 h) to late exponential phase (20 h) (Table 4.1). Heat treatment was performed by maintaining duplicate samples at 55°C for 20 min for all cultures. Samples (1 ml) were removed every 5 min and prepared for fluorescent flow cytometry, using TO and PI as described in Section 4.2.

Table 4.1: Age of *S. cerevisiae* cultures measured as optical density and associated growth phase

Culture optical density (OD_{600})	Growth Phase
OD_{600} 0.152	Early exponential
OD_{600} 0.216	Early exponential
OD_{600} 1.058	Late exponential
OD_{600} 1.482	Late exponential/stationary

Based on TO and PI uptake, three populations of cells were identified (viable, membrane-injured and dead) and gated in all *S. cerevisiae* cultures. These three populations were expressed as a fraction of the total population (N), where N had a value of 1. The viable (N_V), injured (N_I) and dead (N_D) fractions were expressed as *Vc/N; Ic/N* and *Dc/N* respectively (Methods 4.2.8).

Experimentation performed in Chapter 2 indicated that cavitation is sensitive to intrinsic parameters of the solution undergoing sonication. In order to maintain a controlled test medium throughout heat and ultrasound experimentation, physiological saline was used for all experiments.

4.3.1.1 Influence of 55°C heat on *Saccharomyces cerevisiae* presented graphically, as contour plots

A typical series of FL1-H vs. FL3-H contour plots analysed by using fluorescence is shown in Figs. 4.1 and 4.2. These represent early exponential (OD_{600} 0.216) and late exponential/stationary (OD_{600} 1.482) *S. cerevisiae* cultures exposed to 55°C and labelled using TO and PI as described (Section 4.2). Each of the five contour plots (A - E) depicts results from a single *S. cerevisiae* sample taken after 0, 5, 10, 15 and 20 min respectively at 55°C. In all graphs, the x axis (FL1-H) displays TO fluorescence and the y axis (FL3-H) displays PI fluorescence. The series represents data obtained from a single experiment. Viable, injured or dead *S. cerevisiae* populations are displayed in different areas of a FL1-H vs. FL3-H plot, as a result of varying intensities of TO and PI fluorescence (Chapter 3). The viable and dead populations are located with a 'V' and 'D', respectively. The area in which injured cells are located is indicated within the dashed line, marked 'I'.

Each contour line represents a percentage of the total population. The outermost contour represents 10% and increases sequentially by 20%, to a maximum of 90%. The area between each contour represents an equal percent of the total population (20%) (BD Biosciences, San Jose, CA).

Contour plots illustrate *populations* of events and not individual events as illustrated in dot plots (Chapter 3). Each contour line links areas of similar dot density. Events with similar fluorescent characteristics are densely located on a FL1-H vs. FL3-H plot and therefore form a population of events, depicted by the concentric contour lines. Some areas of a contour plot may contain loosely grouped events that are below the limit of the contour lines (Chapter 3) and are therefore not displayed. As such, any area of a FL1-H vs. FL3-H plot that does not contain any contour lines may still contain singular events that are not displayed.

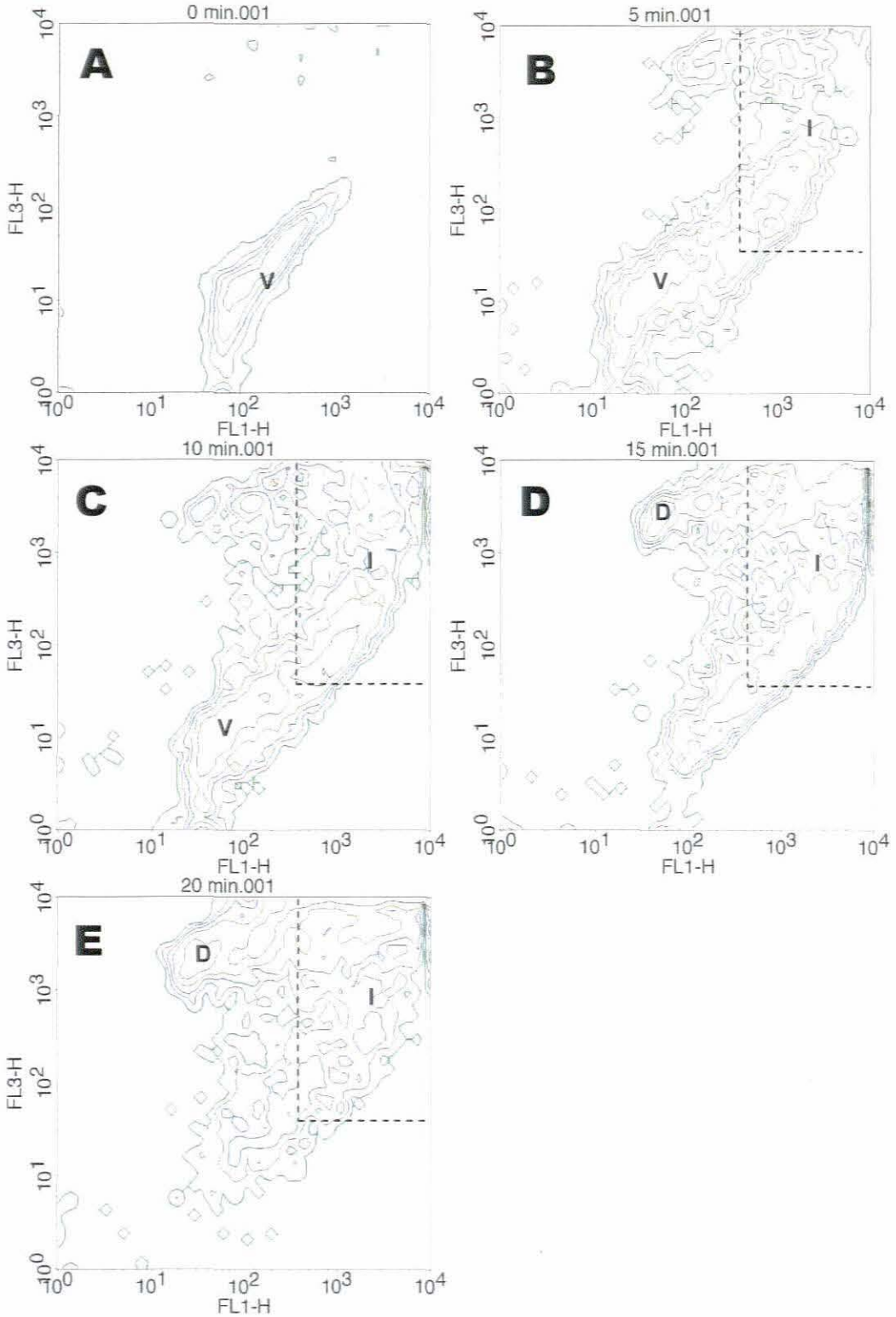

Figure 4.1: A series of BD CellQuest contour plots showing the progression of early exponential (OD_{600} 0.216) *S. cerevisiae* cells from a viable population (V) to injured (I) and dead (D) populations, on exposure to 55°C during a single experiment. Frames A – E represent 0, 5, 10, 15 and 20 min exposure to 55°C. I= injury

The early exponential (OD_{600} 0.216) culture consisted predominantly of viable cells fluorescing mainly in the TO region (FL1-H) at time zero (Fig. 4.1 A). The position of the viable population on a FL1-H vs. FL3-H contour plot shows little PI fluorescence, hence indicating intact cell boundaries (Appendix 4.A).

After 5 min, PI fluorescence increased and was detected by the FL3-H channel. This indicated the presence of dead and membrane-injured cells (Fig. 4.1 D). The formation of a dead population in vertical alignment, above the viable cells was noted, indicating similar TO fluorescence but increased PI fluorescence (Fig. 4.1 D).

Over the course of the experiment, the uptake of PI continued as both N_I and N_D fractions increased (Fig. 4.1 C-E). It was noted that TO uptake simultaneously increased with that of PI uptake. Thiazole orange fluorescence then rapidly decreased at the point of death to a level similar to that of viable cells at start-up (Fig. 4.1 C). The reason for this initial TO uptake is unknown but could be due to alterations in DNA conformation induced by heat altering TO intercalation in the nucleic acid. After 10 min at 55°C, death of injured cells commenced (Figs 4.1D and E); however most of the injured population was still present after 20 min.

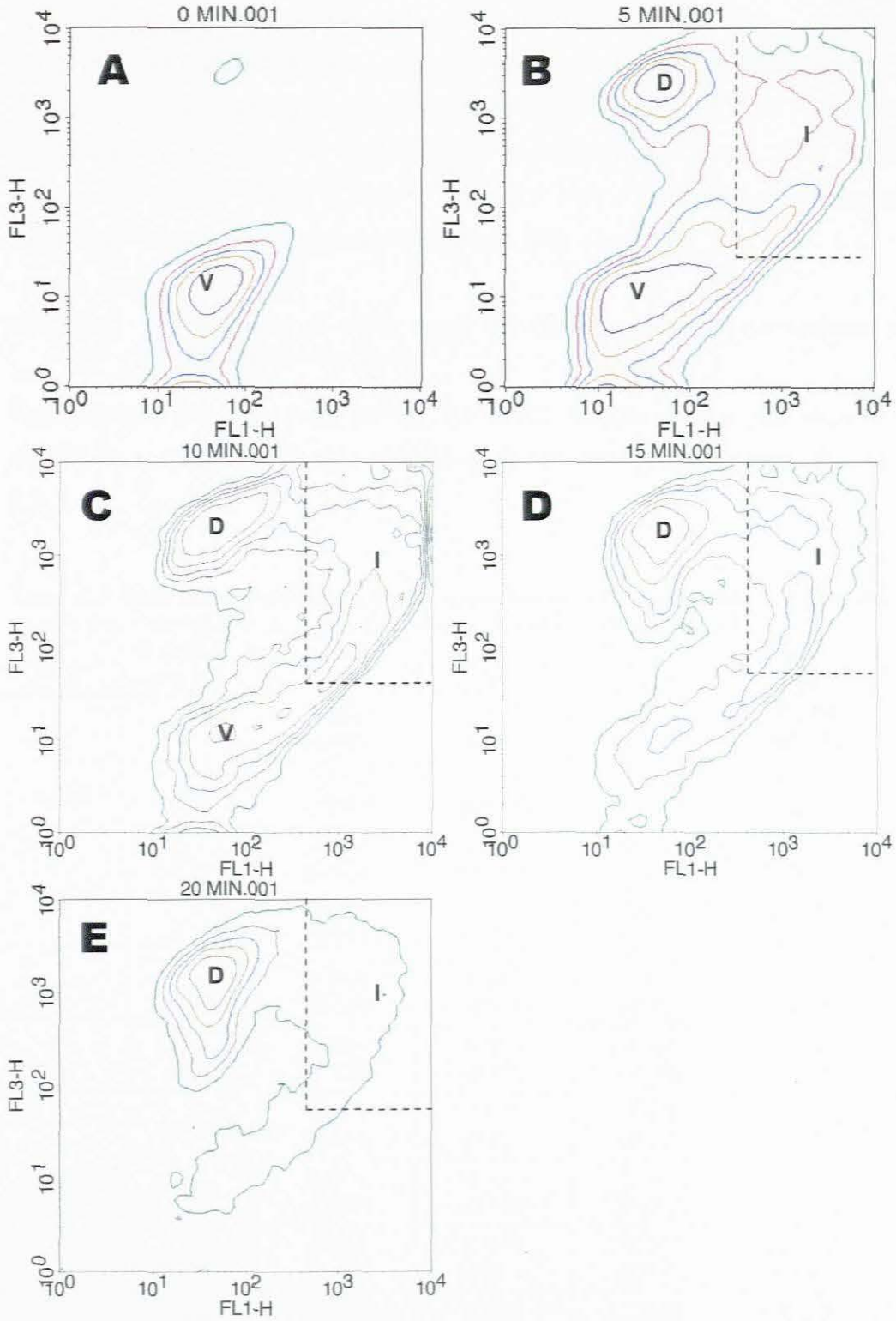

Figure 4.2: BD CellQuest contour plots showing the migration of late exponential/stationary phase (OD_{600} 1.482) *S. cerevisiae* cells from a viable population (V) to injured (I) and dead (D) populations on exposure to 55°C during a single experiment. Frame A – E represents 0, 5, 10, 15 and 20 min exposure to 55°C respectively

The contour plots illustrated that the late exponential culture (OD_{600} 1.482) underwent the same mode of membrane injury as the early exponential culture (OD_{600} 0.216) (Fig. 4.2 B-F). This was characterised by a simultaneous uptake of TO and PI. The TO fluorescence rapidly decreased at the point of death to the same level as viable cells, as did the young exponential culture (OD_{600} 0.216). It was clear that in both cultures a sustained period of injury was induced before cell death occurred (Fig. 4.2 B-F).

4.3.1.2 Influence of 55°C heat on *Saccharomyces cerevisiae*, presented as population fractions

Each contour plot presented in Fig. 4.1 & 4.2 represents a single experiment. However, duplicate samples from all four cultures were run and results obtained are reported in Table 4.2.

Table 4.2: Data obtained from duplicate experiments showing viable, injured and dead population fractions of *S. cerevisiae* of various ages exposed to 55°C

OD_{600}	Population fraction	Time (min)				
		0	5	10	15	20
0.152	(N_V)	0.864 ±0.083	0.526 ±0.001	0.259 ±0.134	0.055 ±0.056	0.008 ±0.004
	(N_I)	0.133 ±0.079	0.464 ±0.006	0.669 ±0.104	0.671 ±0.055	0.599 ±0.019
	(N_D)	0.003 ±0.004	0.009 ±0.005	0.072 ±0.031	0.273 ±0.111	0.393 ±0.022
0.216	(N_V)	0.927 ±0.054	0.732 ±0.048	0.424 ±0.184	0.148 ±0.181	0.065 ±0.085
	(N_I)	0.068 ±0.054	0.245 ±0.035	0.515 ±0.163	0.570 ±0.084	0.500 ±0.066
	(N_D)	0.005 ±0.000	0.023 ±0.013	0.061 ±0.020	0.282 ±0.265	0.434 ±0.151
1.058	(N_V)	0.913 ±0.015	0.573 ±0.005	0.379 ±0.033	0.293 ±0.086	0.150 ±0.013
	(N_I)	0.074 ±0.022	0.161 ±0.189	0.348 ±0.022	0.441 ±0.052	0.396 ±0.060
	(N_D)	0.012 ±0.007	0.146 ±0.014	0.272 ±0.011	0.266 ±0.034	0.454 ±0.047
1.482	(N_V)	0.968 ±0.007	0.696 ±0.122	0.398 ±0.096	0.224 ±0.115	0.066 ±0.035
	(N_I)	0.020 ±0.008	0.148 ±0.060	0.309 ±0.061	0.298 ±0.053	0.247 ±0.099
	(N_D)	0.011 ±0.002	0.156 ±0.062	0.293 ±0.034	0.479 ±0.168	0.687 ±0.135

± = standard deviation

The composition of the *S. cerevisiae* cultures at start-up of the experiments was dependent on age. All the cultures consisted predominantly of viable cells (N_V)(Table 4.2). It was noted that after 20 min the early exponential cultures (OD_{600} 0.152 & 0.216) contained more injured

and less dead cells than did the older cultures (OD_{600} 1.058 & 1.482) (Table 4.2). The precision provided by this real time assessment of the relationship between physiological makeup of the cultures and growth phase is not possible using conventional serial dilution and plating techniques.

In the following sections, the viable, injured and dead population fractions are discussed separately, where the effect of 55°C on each fraction is related and compared to the age of the cultures.

and less dead cells than did the older cultures (OD_{600} 1.058 & 1.482) (Table 4.2). The precision provided by this real time assessment of the relationship between physiological makeup of the cultures and growth phase is not possible using conventional serial dilution and plating techniques.

In the following sections, the viable, injured and dead population fractions are discussed separately, where the effect of 55°C on each fraction is related and compared to the age of the cultures.

4.3.1.2.a The influence of 55°C on viable fractions of *Saccharomyces cerevisiae*

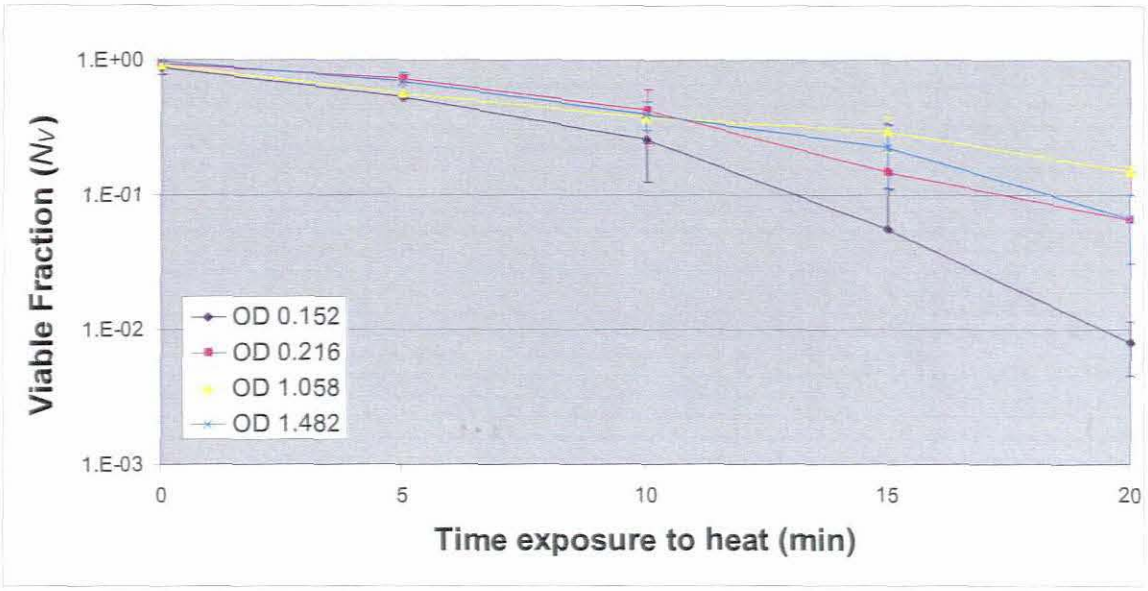

Figure 4.3: The effect of 55°C on N_V of *S. cerevisiae* cultures in different growth phases as a result of heat exposure (55°C) over 20 min. The optical density was measured at 600 nm. The standard deviation is indicated by the T bars (n=2)

Using fluorescent flow cytometry it was possible to show that N_V decreased over 20 min in all cultures and that the sensitivity of *S. cerevisiae* to 55°C varied according to culture age. Hence D_{ht55} values varied (Fig. 4.3; Table 4.2). The D_{ht55} and $\log_{10}$ reduction of the viable cells are shown in Table 4.3. It was noted that a greater $\log_{10}$ reduction of viable cells occurred during the 10 – 20 min heat exposure period than during the 0 – 10 min stage, for all culture ages (Table 4.3).

Table 4.3: Log_{10} reduction and D_{ht55} values of viable *S cerevisiae* cultures subjected to 55°C for 20 min

Culture absorbance (OD_{600})	Log_{10} decrease in N_V		D_{ht55}
	0 - 10 min	0 - 20 min	
0.152	0.523	2.028	9.85 min
0.216	0.340	1.152	17.37 min
1.058	0.382	0.785	>20 min
1.482	0.386	1.169	17.13 min

4.3.1.2.b The influence of 55°C on injured fractions of *Saccharomyces cerevisiae*

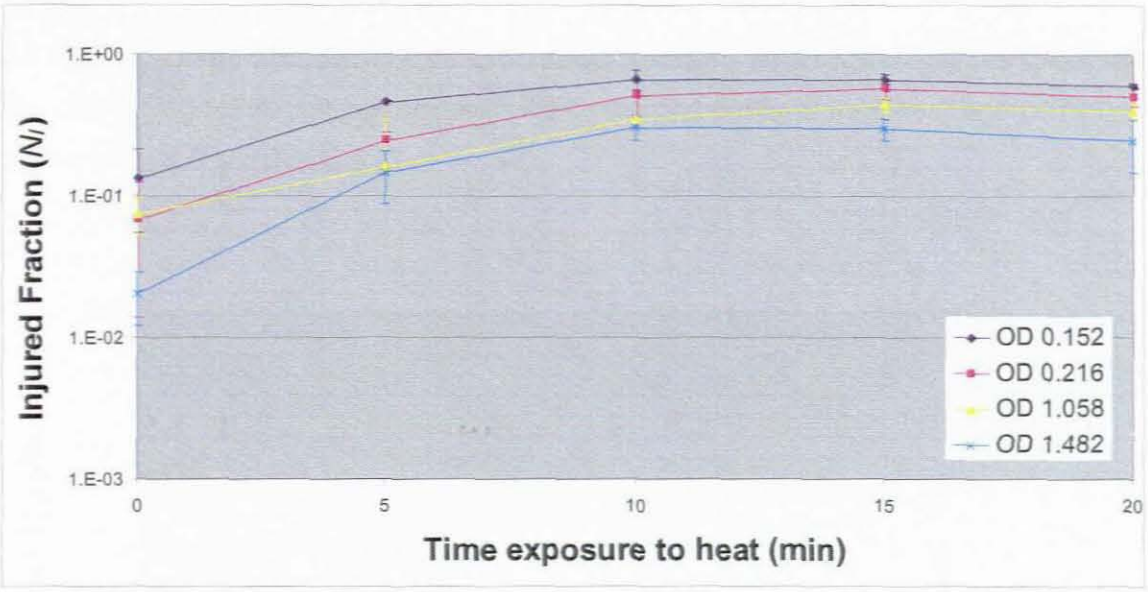

Figure 4.4: The increase in N_I of *S. cerevisiae* cultures in different growth phases as a result of heat exposure (55°C) over 20 min. The optical density was measured at 600 nm. The standard deviation is indicated by the T bars (n=2).

In all culture ages tested, PI uptake showed that membrane injury in S. cerevisiae occurred within 5 min of exposure to 55°C (Fig. 4.4). A maximum N_I was recorded at 10 - 15 min, after which N_I decreased due to cell death (Fig. 4.4 & Table 4.4).

The influence of 55°C on injury differed with cell age. The early exponential culture (OD_{600} 0.152) experienced the least increase in injured cells (log_{10} 0.71) and the late exponential culture (OD_{600} 1.482) experienced the highest increase in injured cells (log_{10} 1.18)(Table 4.4). After 20 min at 55°C, 24 – 60% of the population, depending on culture age, remained injured.

Table 4.4: Injured fraction (N_I) of *S. cerevisiae* at start-up and at maximum injury, when exposed to 55°C heat

Culture age (OD_{600})	Maximum N_I recorded	Log_{10} increase in N_I from initial to maximum injury
0.152	0.67 ±0.06	0.71 (after 15 min)
0.216	0.57 ±0.08	0.91 (after 15 min)
1.058	0.44 ± 0.05	0.79 (after 15 min)
1.482	0.31 ±0.06	1.18 (after 10 min)

± = standard deviation

It was of interest to note that despite the late exponential culture (OD_{600} 1.482) undergoing the greatest increase in cell injury, the maximum injured fraction was only half that of the early exponential phase culture (OD_{600} 0.152) after 20 min (Table 4.4). This was related to

the fact that the early exponential culture (OD_{600} 0.152) consisted of more injured cells at start up than did the older exponential cultures (OD_{600} 1.058 & 1.482) (Table 4.2).

4.3.1.2.c The influence of 55°C on dead fractions of *Saccharomyces cerevisiae*

Cell death (N_D) for all cultures occurred within the first 5 min of treatment and continued over 20 min (Fig. 4.5 and Table 4.2).

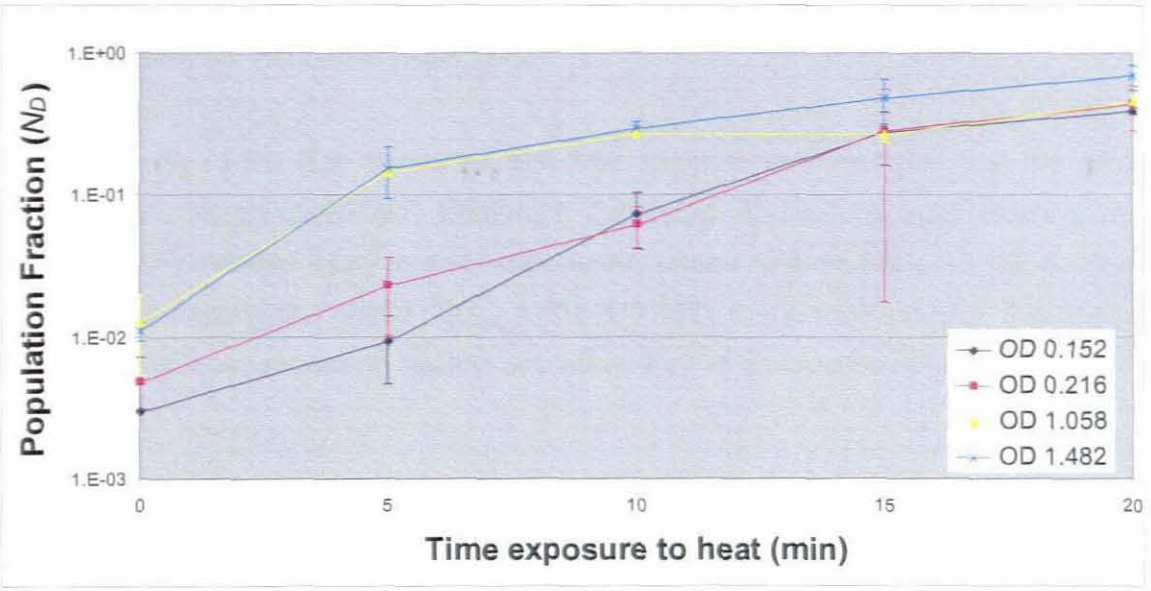

Figure 4.5: The increase in N_D in *S. cerevisiae* cultures in different growth phases as a result of heat exposure (55°C) over 20 min. The optical density was measured at 600 nm. The standard deviation is indicated by the T bars (n= 2)

A comparison of the $\log_{10}$ increase in N_D experienced in all four cultures after 20 min at 55°C shows that cell death was influenced by the age of the culture. This trend was most noticeable within the first 15 min of heat treatment (Fig. 4.5). Regardless, after 20 min exposure, all cultures, irrespective of growth phase, underwent similar $\log_{10}$ increases in the dead population (Fig. 4.5).

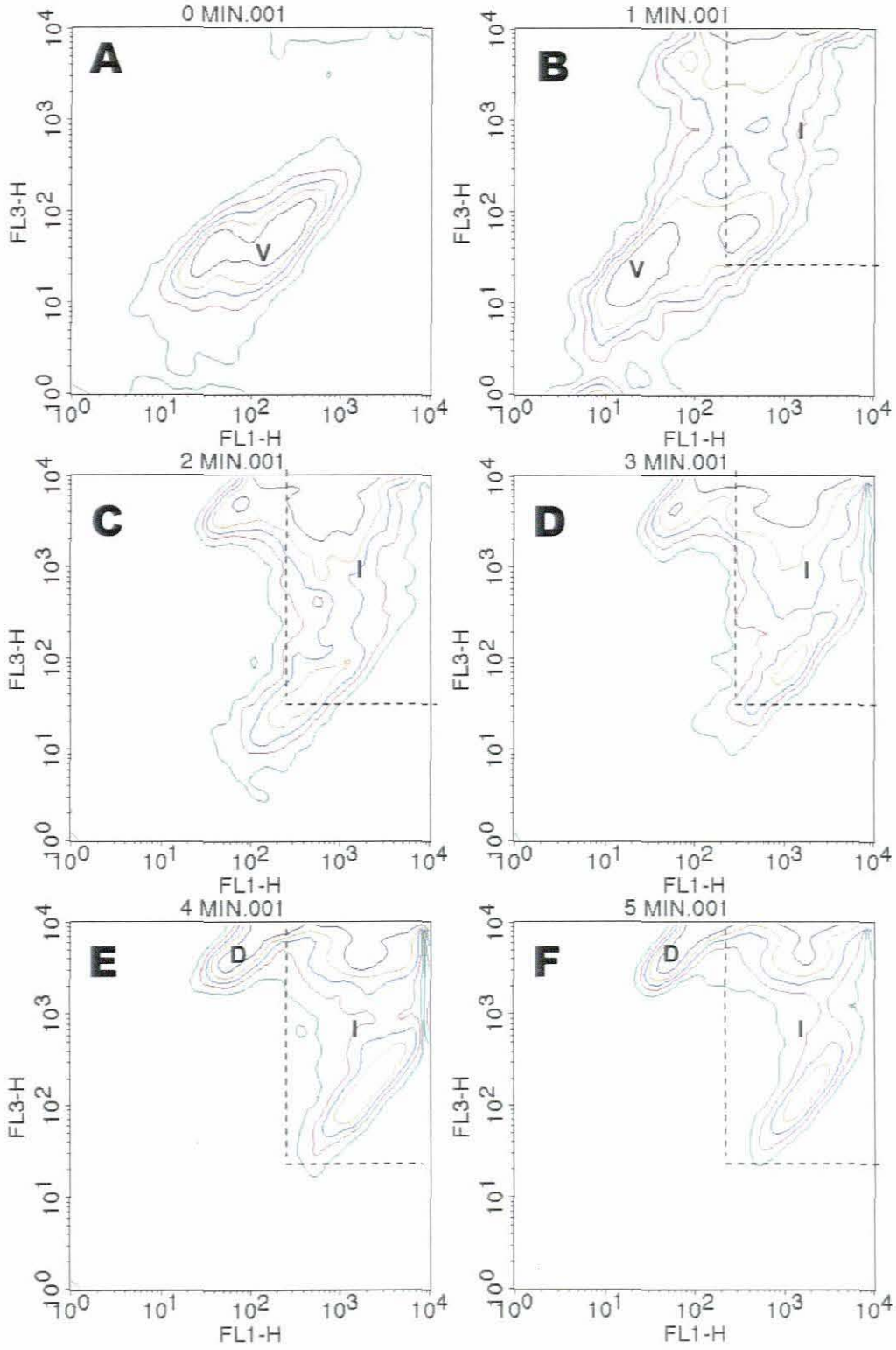

Figure 4.7: BD CellQuest contour plots showing the progression of *S. cerevisiae* cells from a viable population (V), to injury (I), to dead (D) on exposure to 60°C. These contour plots represent a single experiment. Frame A – E represents 0, 1, 2, 3, 4 and 5 min exposure to 60°C.

4.3.1.3 Summary of 55°C heat experiments on *Saccharomyces cerevisiae* cultures

Flow cytometry showed that the application of heat at 55°C heat was capable of inducing much cell boundary injury to *S. cerevisiae* cells. Some of the cells died after a sustained period of injury. The 20 min exposure to 55°C heat was sufficient to reduce the viable fraction by between $\log_{10}$ 0.79 and 2.03, depending on culture age. However it is notable that at this time, the population still consisted of between N_I 0.25 – 0.60 injured cells (Table 4.2). In disinfection processes, cell death is preferable to cell injury, as injured cells may recover during subsequent incubation (Ray, 2003).

The sensitivity of the flow cytometer real time analyses demonstrated that the efficacy of 55°C as a microbi-static/cidal treatment depended on culture age. Heating at 55°C predominantly induced injury in early exponential phase cultures (OD_{600} 0.152 & 0.216) and death in late exponential phase (OD_{600} 1.058 & 1.482). In the food industry, this needs to be accounted for when modelling heating processes for the disinfection of beverages.

4.3.2 Effects of 60°C heat on *Saccharomyces cerevisiae*

Data presented in the foregoing (Section 4.3.1) showed that culture age influenced *S. cerevisiae* response to 55°C. It was decided that for further investigation, only cultures grown to late exponential phase (OD_{600} ~ 1) would be used in an attempt to standardise cell response to heat and ultrasound. Selected volumes of these cultures were exposed to 60°C for 20 min and sampled every 5 min, in a manner identical to that described for the 55°C investigation (Section 4.2.2). Population fractions were determined using TO and PI fluorescent flow cytometry (Section 4.2).

Initial experimentation showed that maximum response of *S. cerevisiae* cells to heat applied at 60°C occurred during the initial 5 min, and thereafter 'stabilised' during the remaining 15 min (Fig. 4.6 and Appendix 4B). It was therefore decided to restrict treatment time to 5 min and to increase frequency of sampling to 1 min intervals during that time.

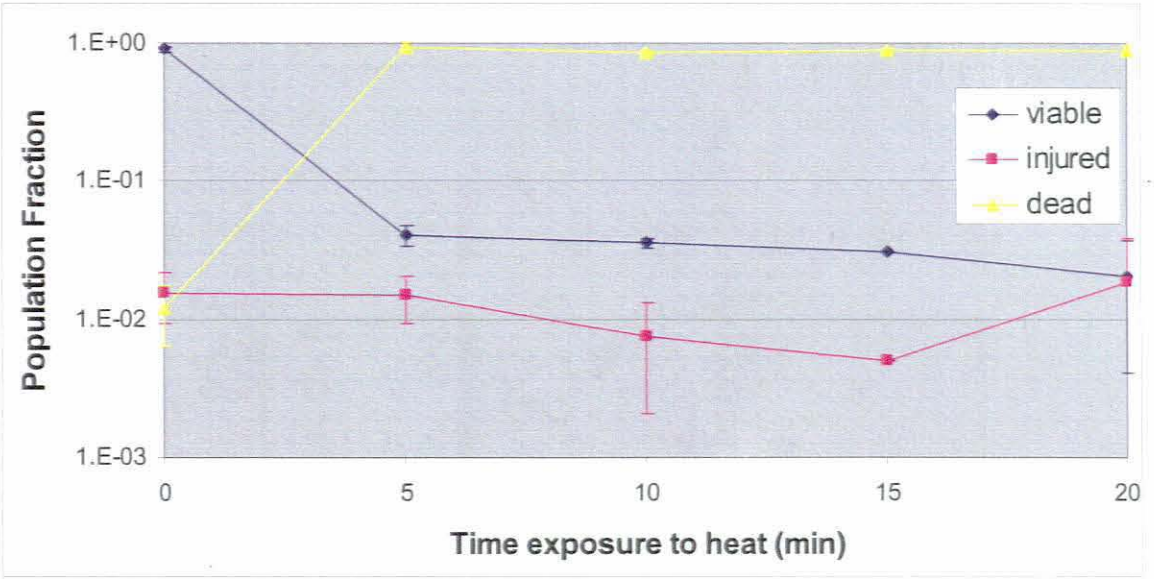

Figure 4.6: The effect of 60°C on late exponential phase (OD_{600}~1.0) cultures of *S. cerevisiae* during 20 min exposure. The standard deviation is indicated by the T bars (n=3)

4.3.2.1 Influence of 60°C on *Saccharomyces cerevisiae* presented graphically, as contour plots

A typical series of contour plots showing 0, 1, 2, 3, 4 and 5 min responses of *S. cerevisiae* cells is shown in Figure 4.7. Viable, injured or dead *S. cerevisiae* populations were located in different areas of the FL1-H vs. FL3-H plots. The figure clearly illustrates that damage occurred to the cell boundary during 60°C heat exposure. The viable and dead populations are indicated by a 'V' and 'D', respectively. The area in which injured cells is located is indicated within the dashed line 'I'. The associated population fractions for each contour are presented in Appendix 4.B.

At start-up the *S. cerevisiae* culture consisted predominantly of viable cells (N_V 0.97)(Fig. 4.7 A). The change in fluorescence of *S. cerevisiae* cells, and therefore the position of injured cells in the contour plots, was similar to cultures heated to 55°C. Initially both TO and PI fluorescence increased during injury, followed by a rapid increase in PI fluorescence. As the cells died, TO fluorescence decreased and a PI-fluorescent dead population was observed and gated in the same location as that identified for the 55°C experiment (Fig. 4.7 C, D & E).

4.3.2.2 Influence of 60°C heat on *Saccharomyces cerevisiae*, presented as population fractions

Viable, injured and dead population fractions collected over 5 min at 60°C are shown in Fig. 4.8 and Table 4.6.

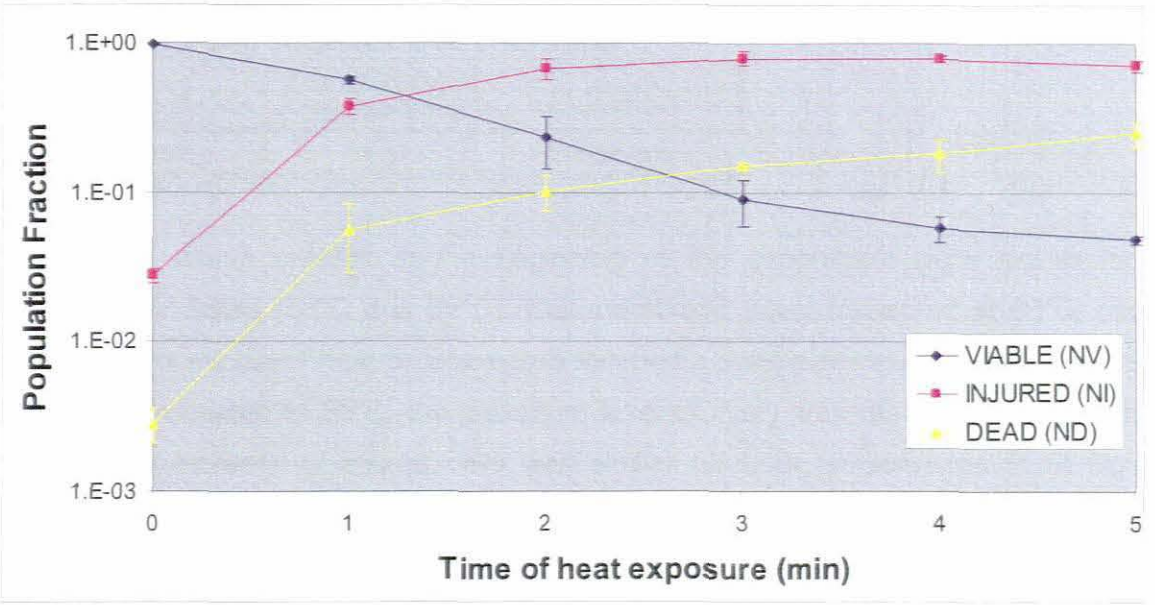

Figure 4.8: The effect of 60°C on late exponential phase (OD_{600}~1.0) cultures of *S. cerevisiae* over 5 min exposure. The standard deviation is indicated by the T bars (n=3)

Table 4.6: The average viable, injured and dead population fractions of *S. cerevisiae* exposed to 60°C, recorded using fluorescent flow cytometry (n=3)

Population fraction	Time (min)					
	0	1	2	3	4	5
(N_V)	0.970 ±0.002	0.569 ±0.035	0.233 ±0.090	0.090 ±0.031	0.057 ±0.011	0.048 ±0.003
(N_I)	0.028 ±0.003	0.375 ±0.045	0.674 ±0.099	0.791 ±0.088	0.779 ±0.041	0.702 ±0.061
(N_D)	0.003 ±0.001	0.056 ±0.027	0.102 ±0.027	0.152 ±0.007	0.183 ±0.045	0.250 ±0.049

± = standard deviation

The cultures were constituted primarily of a viable population at start-up (N_V 0.97 ±0.002, N_I 0.028 ±0.003 and N_D 0.003 ±0.001 (Table 4.6), similar to that recorded for the exponential phase cultures exposed to 55°C (Table 4.2)

Viable cells decreased within the first minute of exposure to 60°C. Within 5 min a $\log_{10}$ 1.31 reduction in viable cells was observed (Fig. 4.8 and Table 4.7). When *S. cerevisiae* cultures were exposed to 55°C, the reduction in N_V ranged between $\log_{10}$ 0.10 – 0.22 after 5 min, depending on culture age. A 1 $\log_{10}$ decrease in viable cells required 2.58 min at 60°C, whereas at 55°C more than 20 min exposure time was required for a similar age culture (Table 4.3). As recorded for the 55°C analyses (Table 4.3) viable cells treated at 60°C underwent a dominant period of membrane injury before death (Table 4.6).

Table 4.7: $\log_{10}$ reduction and D_{ht60} values of viable *S cerevisiae* cultures subjected to 60°C for 5 min

Culture age	Log decrease in N_V after 5 min	D_{ht60}
Late exponential	1.31	2.58 min

Injured cell events present at the beginning of the experiment were similar for both temperatures tested (55°C and 60°C). Cell membrane injury measured at 60°C, occurred within the first minute of heat exposure and reached a maximum value of N_I 0.79 ±0.09 after 3 min. When heated to 55°C, the maximum level of injury was reached after 10 min. The overall $\log_{10}$ increase of injured cells was similar for both temperatures (1.18 $\log_{10}$ late exponential at 55°C and 1.42 $\log_{10}$ late exponential at 60°C) (Tables 4.4 and 4.8).

Table 4.8: The membrane-injured fraction (N_I) of *S. cerevisiae* at start-up and at maximum N_I, recorded when exposed to 60°C heat

Culture age	Maximum N_I recorded	$\log_{10}$ increase in N_I from initial to maximum injury
Late exponential	0.79 ±0.09	1.42 (after 3 min)

± = standard deviation

A population of cells with maximum PI fluorescence on the FL3-H axis represented those inactivated by heat (Fig. 4.8). Dead cell events increased within the first minute of exposure to 60°C. After 5 min, the dead fraction of the population was 0.250 ±0.049, indicating that most of the population remained either viable or injured. Results obtained using TO and PI fluorescence clearly indicated that membrane injury was a prerequisite for death caused by heating. Exposure to 60°C was more effective in increasing both injury and death than at 55°C. (Tables 4.7 and 4.8)

4.3.2.3 Summary of 60°C heat experiments on *Saccharomyces cerevisiae* cultures

The viable *S. cerevisiae* cell fraction was reduced to 4.8 ±0.3% after 5 min at 60°C, representing a reduction of $\log_{10}$ 1.31. The advantage of real time fluorescent flow cytometric analyses in enabling differentiation between injured and dead cells is obvious. At least 70.2 ± 6.1% of the population was comprised of injured cells. The proportion of dead cells after 5 min heating at 60°C did not exceed 25%. This observation for both temperatures tested in this study is that the food industry needs to take cognisance of the fact that *S. cerevisiae* cell injury and not death, accounted for the decrease in the D_v fraction and this needs to be considered when modelling heat processes required to kill. Injured cells may recover after heating. These observations are not as apparent when using serial dilution and plate count techniques or dyes such as resazurin of methylene blue to indicate cells numbers and viability.

4.3.3 Effect of ultrasound on *Saccharomyces cerevisiae*

Initially, as applied in the heat experiments, *S. cerevisiae* cultures were sonicated for 20 min and sampled every 5 min. The preliminary results indicated that the maximum response of cells to sonication occurred within the first 5 min (Appendix 4.C). Therefore, cultures were sonicated for a total of 5 min and sampled every minute. To standardise, it was decided to use cultures in late exponential phase for ultrasonic treatment.

Sonication conditions used were constant and optimised, based on the results obtained using both Luminol and potassium iodide reported on in Chapter 2. Throughout this study, ultrasound generated was at a frequency of 20 kHz, using the maximum displacement amplitude of 124 µm. Sound waves were delivered to 60 ml *S. cerevisiae* saline suspension using the 13 mm diameter tip standard horn, 20 mm above the container base (Section 2.4). Testing in Chapter 2 showed that cavitation was less diluted at volumes less than 100 ml (Section 2.4). During sonication, a 400 µl sample was removed every minute from the cell suspension and prepared for fluorescent flow cytometry, using TO and PI as described (Section 4.2.6).

Viable, injured and dead cell fractions were identified based on TO and PI uptake by cells and were gated in all *S. cerevisiae* cultures, as described in Section 4.2.7. The viable, injured and dead cell counts were expressed as a fraction of the total population at start-up (N_0), where N_0 had a value of 1. The viable (N_V), injured (N_I) and dead (N_D) fractions were expressed as V/N_0; I/N_0 and D/N_0 respectively. Ultrasound reduced the total population (N_0) during sonication due to cell fragmentation. Therefore, the total population at zero min was used for all time intervals when calculating the population fractions gated during sonication. Cell breakage was not observed for heated cells which remained entire.

By using PI and TO uptake, the amount of cell breakage caused by cavitation during sonication was calculated. This was achieved by expressing the total cell counts at each time interval sampled as a fraction of the initial total population (Section 4.2.8).

4.3.3.1 Influence of ultrasound on *Saccharomyces cerevisiae* presented graphically, as contour plots

A typical series of contour plots recorded during a 0 – 5 min sonication period is shown in Figure 4.9. Viable, injured or dead *S. cerevisiae* populations are displayed in different areas of a FL1-H vs. FL3-H plot, as a result of varying amounts of TO and PI fluorescence. The results clearly showed that ultrasound damaged the cell boundary in a lethal manner, as noted by the shift in PI and TO fluorescence indicated by viable and dead populations. The viable and dead populations are located with a 'V' and 'D', respectively. The area in which

ured cells are located is indicated within the dashed line 'l'. The associated pop-
actions for each contour are presented in Appendix 4.C. However, important differences
were noted in the damage mechanism/s caused by ultrasound when compared to the heat
treatments. These are referred to below.

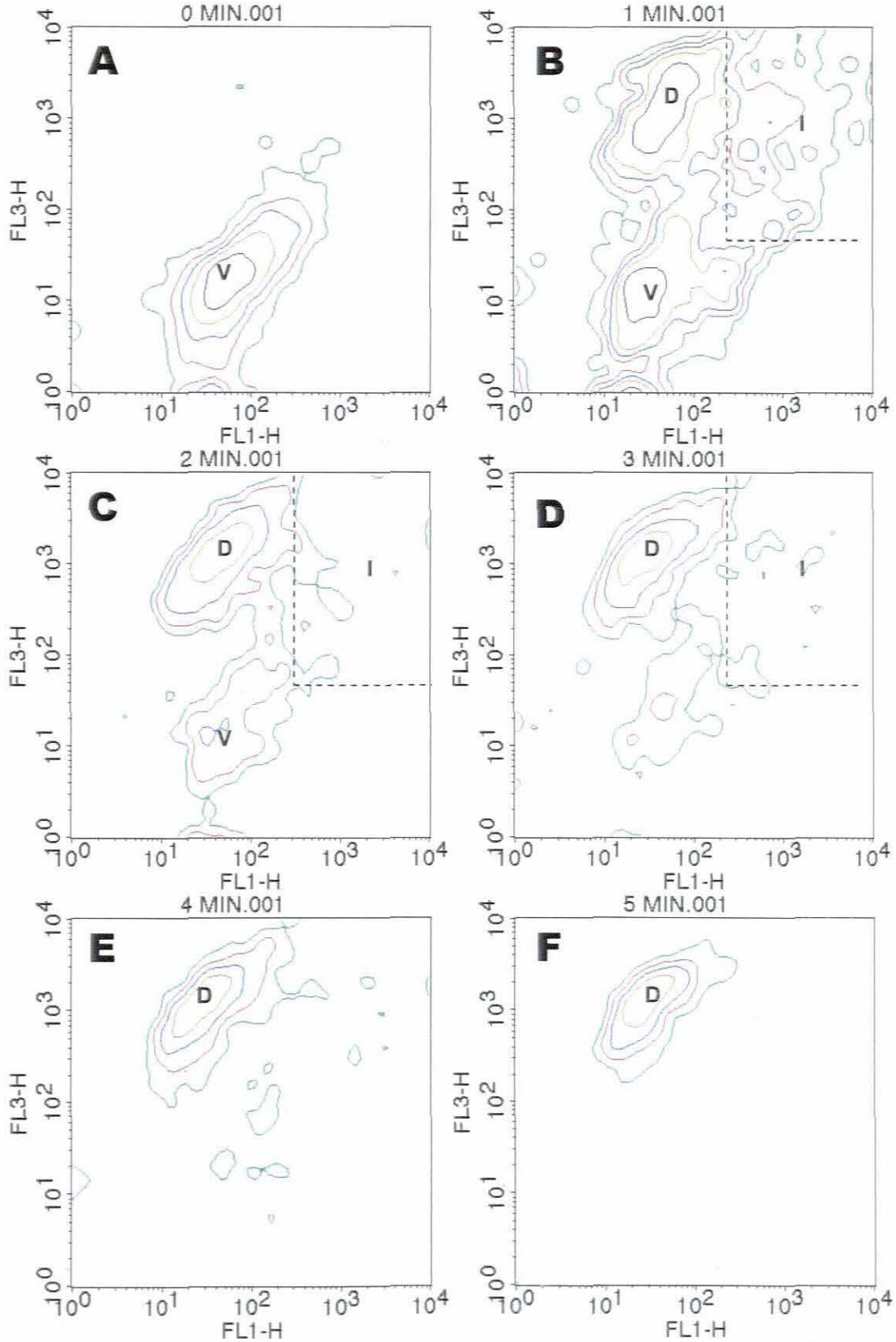

Figure 4.9: A series of BD CellQuest contour plots showing the transition of *S. cerevisiae* cells from a viable to a dead population on exposure to 5 min ultrasound, during a single experiment. The x-axis (FL1-H) indicates TO fluorescence and the y-axis (FL3-H) shows PI fluorescence. Frame A – E represents 0, 1, 2, 3, 4 and 5 min exposure to ultrasound respectively. The viable (V) and dead (D) populations are clearly visible.

The contour plots for ultrasound indicated that, unlike heat, cell boundary damage causing cell injury did not feature. Low numbers of cell boundary injured cells were detected but no distinct population of boundary-injured cells was ever gated at the time intervals tested (Fig. 4.9). Instead, a complex set of diffuse contour lines was located within the injured region of the plot after the first minute (Fig. 4.9B). At times the events were so dispersed that it was not possible to measure these above the threshold of the lowest contour (10%) (Fig. 4.9B). After 1 min, there were few injured cells with damaged boundaries (Fig. 4.9C, D and E). A substantial dead population (D) fluorescing in the same position as the heat-treated dead cells was observed after 1 min sonication (Fig. 4.9 B). After 2 min of treatment, both the zone of diffuse injury and viable population were almost absent (Fig. 4.9 C, D & E). This was in contrast to the heat treated cells (55 & 60°C) where both viable and cell boundary injured populations remained visible after 5 min of heating (55 & 60°C) (Section 4.3.1.1 and 4.3.2.1).

4.3.3.2 Influence of ultrasound on *Saccharomyces cerevisiae*, presented as population fractions

The cell fractions for each population extracted from repeated experiments were calculated over 5 min of sonication. The mean and standard deviations from repeated experiments were collated and graphically presented on a time vs. population fraction graph (Fig. 4.10).

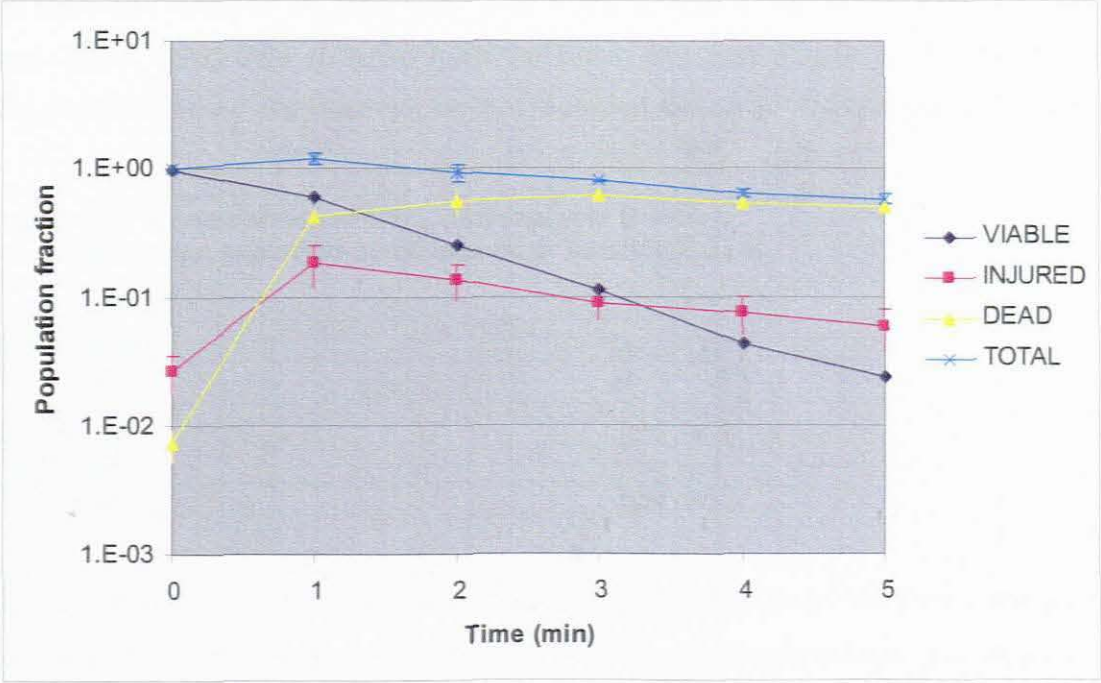

Figure 4.10: The effect of ultrasound on late exponential phase (OD_{600}~1.0) cultures of *S. cerevisiae* recorded during 5 min exposure. The standard deviation is indicated by the T bars (n=3)

Table 4.9: The average viable, injured and dead population fractions of *S. cerevisiae* exposed to ultrasound (20 kHz), recorded using fluorescent flow cytometry

Population fraction	Time (min)					
	0	1	2	3	4	5
(N_V)	0.966 ± 0.007	0.592 ± 0.063	0.253 ± 0.013	0.113 ± 0.003	0.043 ± 0.004	0.024 ± 0.002
(N_I)	0.026 ± 0.008	0.183 ± 0.068	0.133 ± 0.042	0.088 ± 0.023	0.073 ± 0.024	0.059 ± 0.021
(N_D)	0.007 ± 0.002	0.423 ± 0.062	0.552 ± 0.132	0.613 ± 0.010	0.532 ± 0.025	0.499 ± 0.032
(N_T)	1.000 ± 0.000	1.198 ± 0.112	0.939 ± 0.158	0.815 ± 0.016	0.648 ± 0.042	0.582 ± 0.050

± = standard deviation

The late exponential cultures (OD_{600} ~1) were primarily comprised of viable cells at start-up. However injured and dead fractions were also present (Table 4.9). This population composition was similar to that noted for the cultures (OD_{600} ~1) at the commencement of heat experiments (Table 4.2 & 4.6).

The number of viable cells decreased from the onset of sonication, throughout the 5 min treatment (Fig. 4.10). The viable fraction decreased by $\log_{10}$ 1.57 after 5 min, similar to the $\log_{10}$ 1.31 reduction achieved by heat applied at 60°C (Table 4.10). The microbicidal action of ultrasound was superior to that caused by the application of heat at 55°C, where the viable fraction was reduced by $\log_{10}$ 0.20 after 5 min (Table 4.10). A D_{US} value of 3.06 min was calculated, using data obtained from the 5 min exposure (Table 4.10). This was similar to D_{ht60} and a marked improvement on that recorded for the 55°C experiment (Table 4.10).

Table 4.10: A comparison of Log_{10} decrease and D values of cultures when subjected to ultrasound or 60 or 55°C heat for 5 min

Microbicidal treatment	Log_{10} CFU decrease in N_V after 5 min treatment	D value
Ultrasound	1.57	3.06 min
55°C heat	0.20	> 20 min
60°C heat	1.31	2.58 min

As noted in the analysis of the contour plots, cell boundary injury was not evident when *S. cerevisiae* cells were sonicated. Data from repeated experiments presented in Fig. 4.10 and Table 4.9 confirmed that no increase in boundary injured cells was recorded during the 5 min sonication period. It is important to note that the only form of injury measured by PI uptake was membrane injury. It was considered likely that other forms of undetected intracellular injury could be caused by both sonication and heating. This suggests that injury

caused by ultrasound was elsewhere in the cells, by means such as intracellular cavitation occurring within the cell. Radel, McLouglin, Gherardini, Doblhoff-Dier and Benes (2000) examined sonicated (2 MHz) *S. cerevisiae* cells using TEM and observed no damage to the cell boundary. However, damage to cell vacuoles and the nuclear envelope was observed. Such cells could maintain cell boundary integrity, and this type of injury therefore would not be detected by PI uptake (Fig. 4.10 and Table 4.9). After 5 min the dead population increased to N_D 0.499 ±0.032. Hence cells were rapidly killed by the forces of cavitation.

Heating at 60°C resulted in a similar $\log_{10}$ reduction of the viable population (Table 4.10). The critical difference between heating and sonication was that the viable cells were predominantly membrane-injured when heated and not killed as recorded during sonication. Therefore, even though a similar reduction in viable population was observed, sonication was more lethal than 55 or 60°C heat exposures and presented a more effective sterilisation technique.

4.3.3.3 The influence of ultrasound on the total fraction of the population

The total number of cells (N_T), comprised of the sum of N_V, N_I and N_D fractions, decreased $\log_{10}$ 0.24 after 5 min ultrasound. It was calculated that the time required to reduce the total population due to cell fractionation by 1 $\log_{10}$ was 21.26 min. (Tests conducted over 20 min showed a $\log_{10}$ 0.74 reduction in the total cell population after 20 min sonication) (Appendix 4.C). These observations were due to cells being fragmented by the physical forces associated with cavitation. This rapid onset of cell fragmentation noted is supported by Borthwick *et al.*, (2005) who reported *S. cerevisiae* cell fragmentation after 90 s of sonication, using 20 kHz ultrasound at 60 W. The slight increase (0.19 ±0.11) in total population size after 1 min sonication was likely due to cavitation induced breakage of *S. cerevisiae* CFU's (consisting of cells, attached buds and filaments), therefore increasing cell numbers for a brief time (Piyasena *et al.*, 2003). Fluorescent flow cytometry identified that most cells were killed before disintegration occurred. Therefore the mechanism of cell death was not solely due to fragmentation. It should be noted that the strain of *S. cerevisiae* used in this study does not form spores. Had this been the case, it is likely that times recorded for inactivation of the culture would be different.

4.3.3.4 Scanning electron microscope examination of *Saccharomyces cerevisiae* cells after exposure to ultrasound (20 kHz).

Scanning electron microscopy (SEM) was conducted on *S. cerevisiae* cells subjected to sonication. Figure 4.11 shows an image of a typical untreated *S. cerevisiae* cell prior to the commencement of sonication. Figs. 4.12 – 4.18 show images of *S. cerevisiae* cells after

1 - 5 min exposure to ultrasound. Extensive multiple injuries of cell boundaries were detected from the onset of ultrasound. The SEM revealed that boundary injury occurred immediately after sonication commenced, yet PI uptake to form an injured population was not observed (Fig. 4.9). Micrographs suggested that cell contents from *S. cerevisiae* cells were extruded forcefully from the cells, possibly from increased intracellular pressure experienced during sonication. Cells with a single pore were regularly visualised from which it was likely cell contents had been ejected. Many cells appeared empty and flattened. It was also clear the ultrasound did not exert similar injuries on all cells as *S. cerevisiae* cells were damaged in different ways.

Electron micrographs therefore confirmed that *S. cerevisiae* boundaries were compromised by sonication, even after 1 min. Collectively, results presented here suggest that the transition from living to dead in *S. cerevisiae* caused by the mechanical forces of cavitation was too rapid for PI injury detection and cell boundary damage was immediately lethal. Tsukamoto *et al.*, (2004) suggested that *S. cerevisiae* cells situated near to cavitation bubbles could undergo immediate death and work reported on here supports this view.

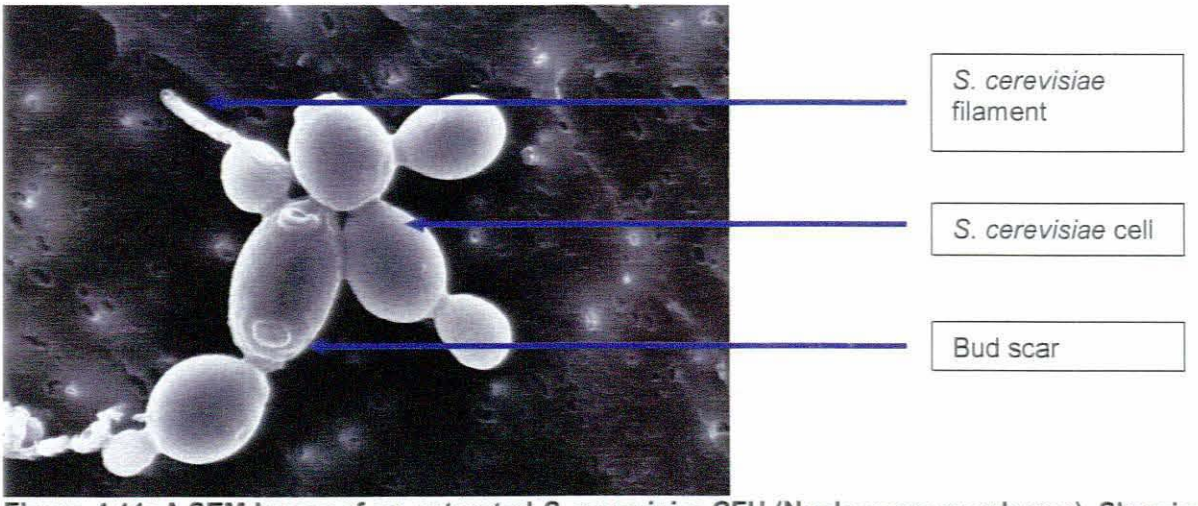

Figure 4.11: A SEM image of an untreated *S. cerevisiae* CFU (Nucleopore membrane). Showing conjoined both oval cells and filaments of cells. note the bud scars (x 18 430)

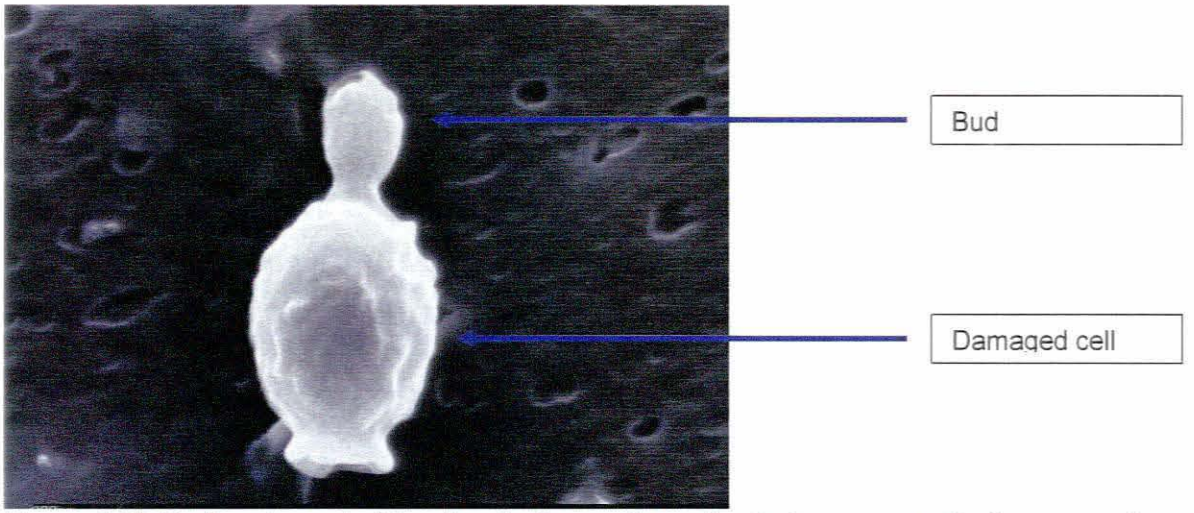

Figure 4.12: Surface irregularities developing on the cell exterior as a result of exposure to cavitation (x 43 540)

Figure 4.12 shows irregularities that developed on the surface of a cell after exposure to cavitation. Note the rough topography when compared with the untreated cells shown in Fig. 4.11. It has previously been reported that small cells are less susceptible to cavitation than large cells (Ahmed & Russell, 1975). The smaller attached bud appears to be more affected than the mother cell.

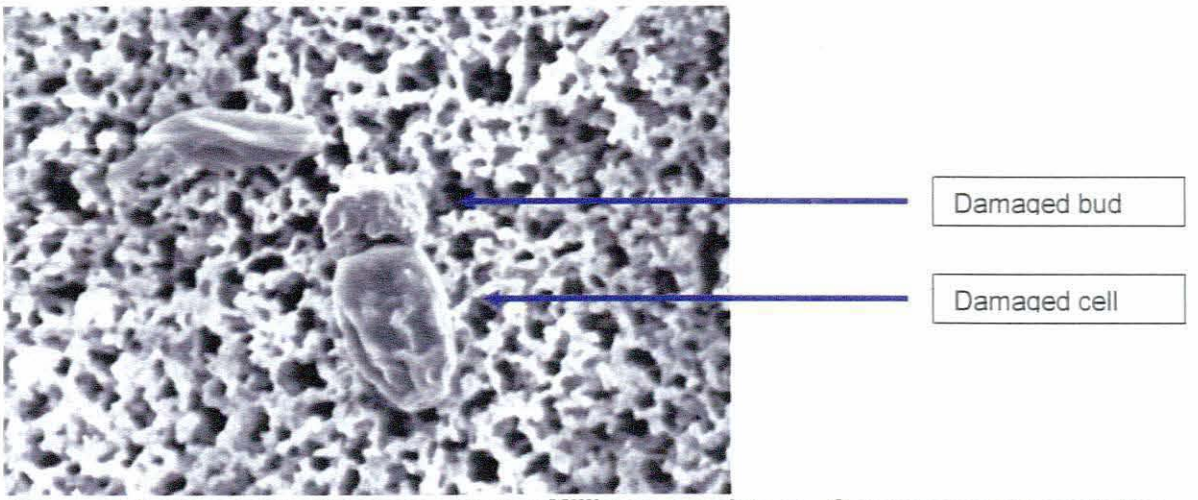

Figure 4.13: Damaged cells observed on a Millipore membrane, after exposure to cavitation (x 20 000)

The cells noted in Fig. 4.13 also displayed surface irregularities, similar to, but more severe, than the cell in Fig. 4.12. The attached bud in this image has undergone an unusual form of cell death / cell injury. The top left cell has shows deformation and appears flattened.

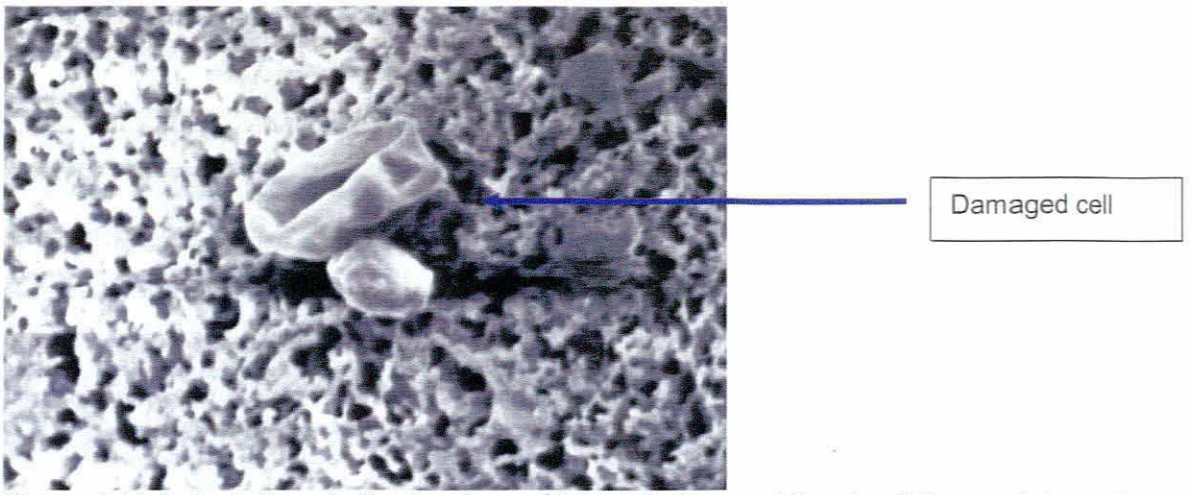

Figure 4.14: Indentations indicating loss of intracellular constituents of *S. cerevisiae* cells on a on a Millipore membrane (x 20 000)

Cells such as those noted in Fig. 4.14 indicate the loss of intracellular constituents as the cells appear indented and collapsed.

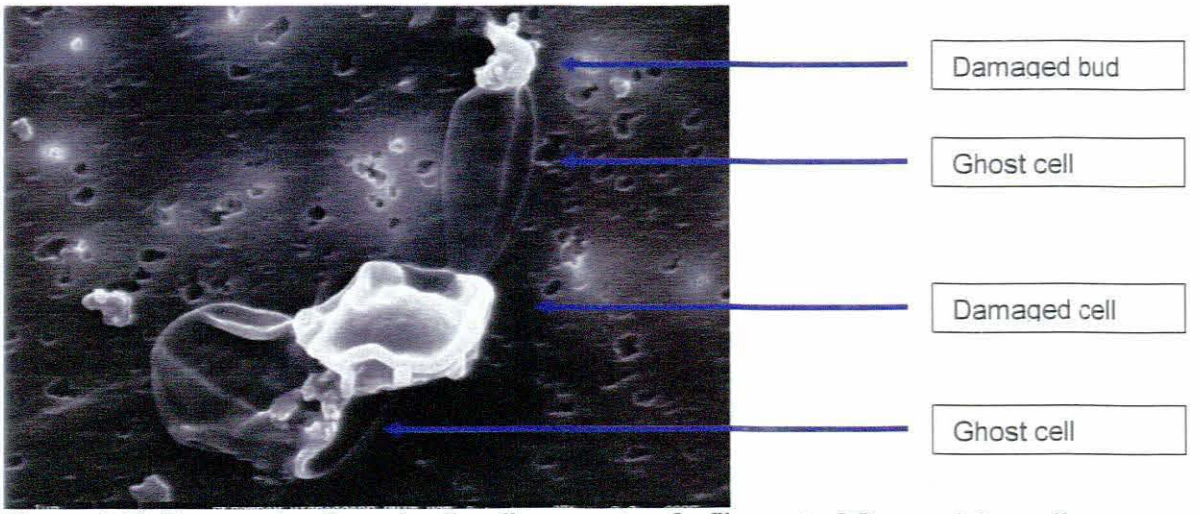

Figure 4.15: Damaged cells and cell wall remnants of a filament of *S. cerevisiae* cells as a result of cavitation (x 23 460)

In Fig. 4.15 two 'ghost cells', which appear to be cell wall remnants of collapsed cells are seen. A highly irregular, flattened cell devoid of cell content is also visible as well as a cell bud that appears to have burst. Cell remnants from fragmented cells were also detected, as illustrated in Fig. 4.15. The Electron Dispersion Spectrophotometry (EDS) function of the SEM confirmed that these particles were organic material. In addition to the cellular constituents observed on the filter, inorganic pieces of titanium alloy from the horn-tip disintegrate during cavitation were also observed (Appendix 4.C).

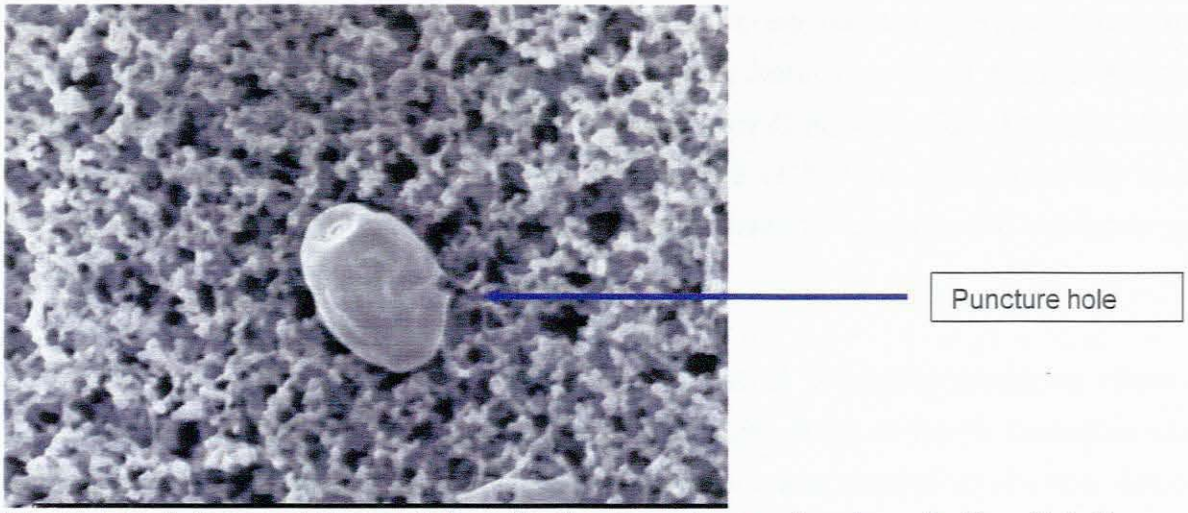

Figure 4.16: A damaged *S. cerevisiae* cells showing minor surface irregularities. Note the puncture hole visible on the side of the cell (x 20 000)

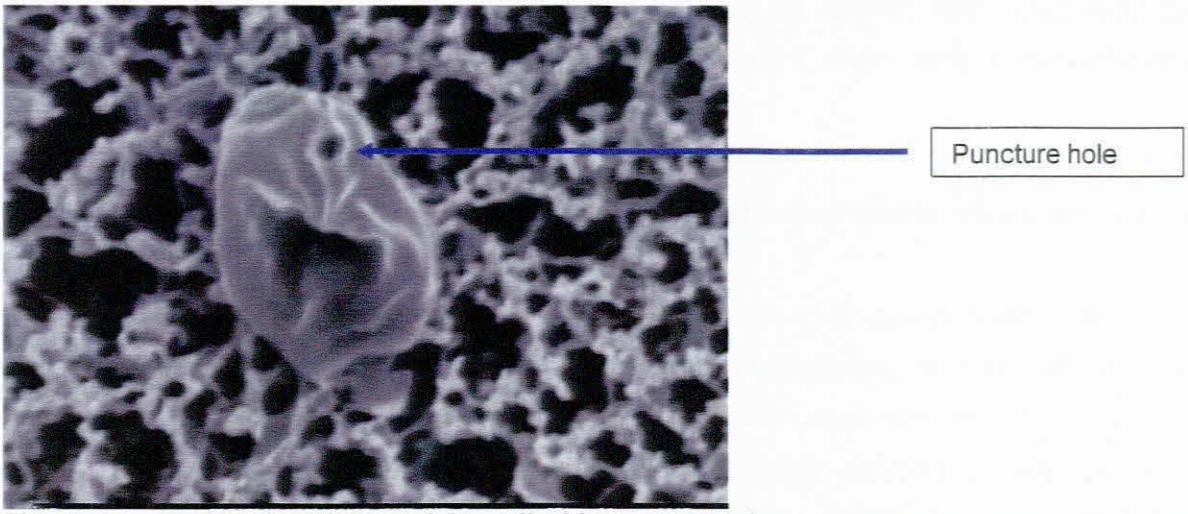

Figure 4.17: A collapsed *S. cerevisiae* cell with a puncture hole, possibly a result of microjets or abrasion forces associated with cavitation (x 30 000)

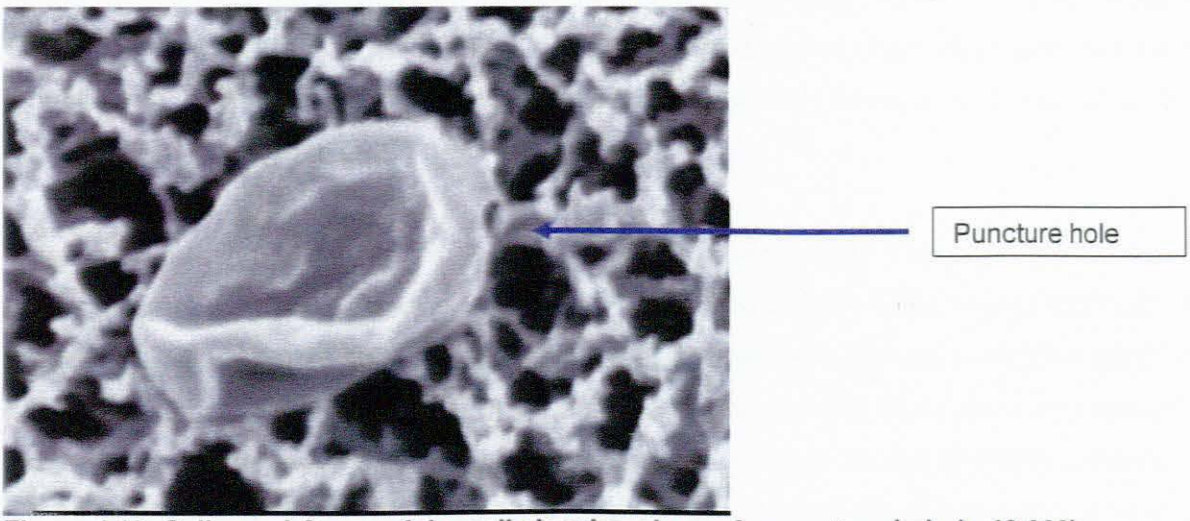

Figure 4.18: Collapsed *S. cerevisiae* cell showing signs of a puncture hole (x 40 000)

Cells visualised in Figs 4.16, 4.17 and 4.18 show single puncture holes in the cell boundary. This was frequently observed. It is likely that PI would enter through the hole therefore

causing the cell to fluoresce as a dead cell. The puncture holes may have been formed during an asymmetrical bubble collapse near to the cell, thereby forming a microjet. Microjets travel up to 300 $m.s^{-1}$ and cause pitting of titanium alloy (Leighton, 1994, Povey & Mason, 1998). It is therefore likely that microjets are capable of forming such punctures in cell boundaries. Alternatively, cells exposed to extreme shearing forces during cavitation may undergo tearing of the cell boundary as a result.

The SEM images illustrate that cavitation has a distinct physically damaging effect on *S. cerevisiae* cells. It is suggested that immediacy of cell death of the *S. cerevisiae* strain GC210 (*MATα lys2*) when subjected to cavitation is primarily caused by physical damage and not to the toxic effects of free radicals formed as a result of sonochemistry

Data presented here clearly indicate that if ultrasound, as applied here, was used as a hurdle, a time exposure of 5 min was unnecessary. Instead a shorter time period sufficient to injure, but not kill cells was used.

4.3.3.5 Summary of findings from the ultrasound experiments on *Saccharomyces cerevisiae* cultures

Ultrasound (20 kHz) was more effective at reducing viable cells due to death than was the application of either 55 or 60°C heat over 5 min. In the heated cells, reduction of viable cells was due predominantly to membrane injury. This is an important observation on the fate of viable cells subjected to heat or ultrasound and was made possible by the use of flow cytometry. This represents the first report on this difference in cell status between the two types of treatments. Fluorescent flow cytometry represented a precise real time analysis of benefit to the the food industry for designing hurdle technology using heat and sonication. Comparing heat and ultrasound microbicidal / static treatments, data presented here clearly indicate that ultrasound is predominately microbicidal when compared to either 55 or 60°C heat for the *S. cerevisiae* strain used in this study.

It was also observed that the results were markedly reproducible. This was attributed to the sonochemistry work conducted in Chapter 2. The sonochemistry experiments identified that experimental parameters needed to be consistent in order to reproduce sonication conditions amongst test samples. The methodology also demonstrated that the culture age influenced microbicidal effectiveness of treatments and therefore the importance of using cultures of a similar age. Clearly, designing successful hurdle technology for the combination of heat and ultrasound is complex.

4.3.4 Effect of the sequential application of ultrasound (20 kHz) and heat (55 or 60°C) on *Saccharomyces cerevisiae*

Saccharomyces cerevisiae cultures were grown to late exponential phase (OD_{600} ~1.0). Ultrasound and heat were administered for 1 min and 5 min respectively using conditions described (Section 4.2.1). During the 5 min of heating, 400 µl samples were removed every 1 min and prepared for fluorescent flow cytometry, using TO and PI as described in Section 4.2.6. Gating and population fraction determination were as described in Section 4.2.8.

4.3.4.1 Influence of sequential ultrasound and heat (55 or 60° C) exposure to *Saccharomyces cerevisiae* presented graphically, as contour plots

A typical series of contour plots from 0 – 5 min is shown in Figs 4.19 and 4.20. This series represents single experiments carried out at either 55 or 60°C. For both, *S. cerevisiae* cells had undergone a 1 min sonication pre-treatment as described (Section 4.2.4). Viable, injured or dead *S. cerevisiae* populations are displayed in different areas of a FL1-H vs. FL3-H plot. The figure illustrates the physiological changes that occurred in the cell boundary during exposure to 55 or 60°C. Frame A – E in Fig. 4.19 represents respectively 0, 1, 2, 3, 4 and 5 min exposure to 55°C. The viable and dead populations are located with a 'V' and 'D', respectively. The area in which injured cells are located is indicated within the dashed line 'I'. The associated population fractions for each contour are presented in Appendix 4.D.

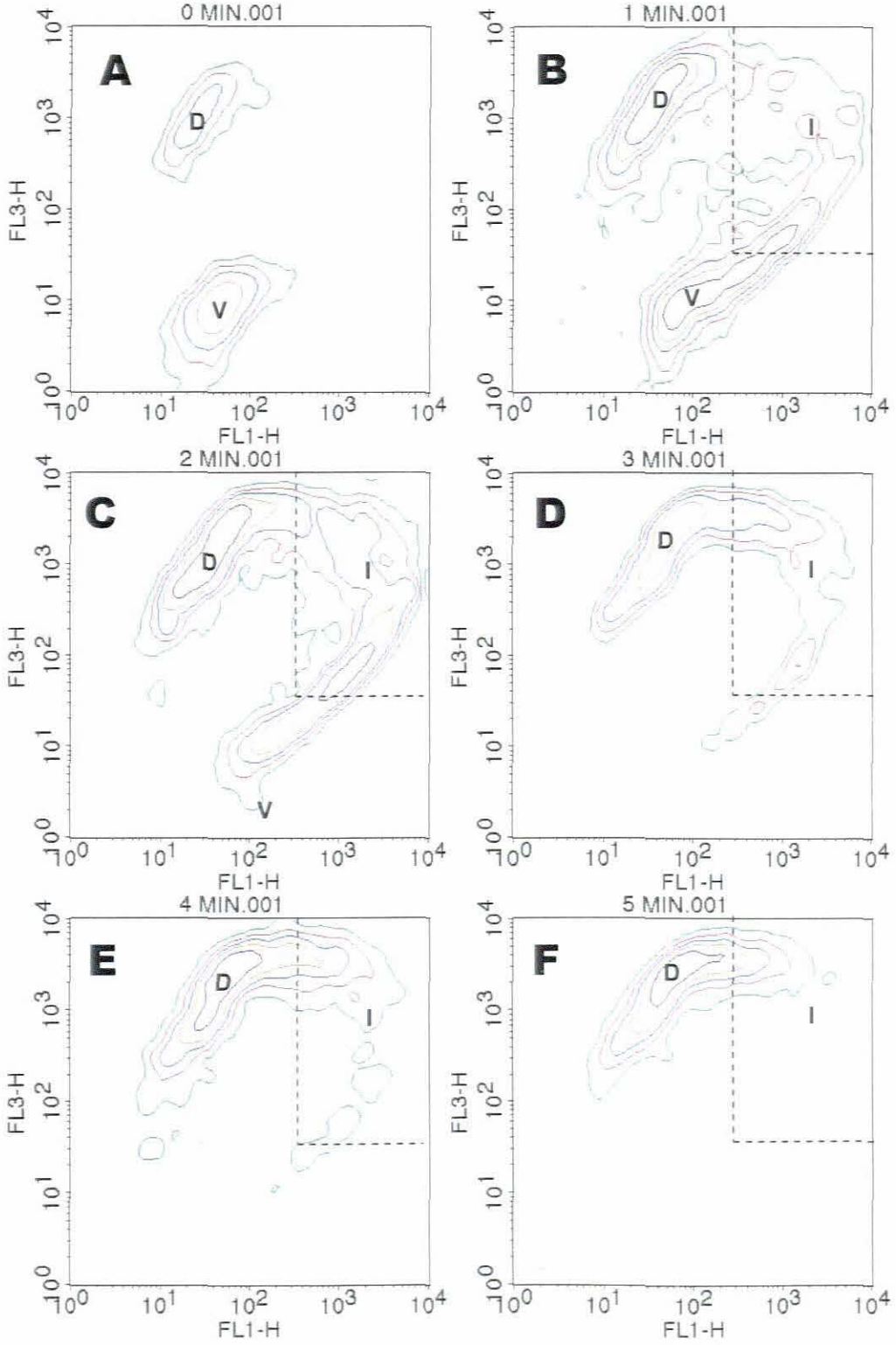

Figure 4.19: BD CellQuest contour plots showing the progression of pre-sonicated late exponential (OD_{600} ~1) *S. cerevisiae* cells from a viable (V), to injured (I), to death (D) when exposed to 55°C for 5 min.

The contour plot represented by Fig. 4.19 A is typical of the *S. cerevisiae* culture subjected to 1 min ultrasound. At this stage, only dead and viable populations were observed. No boundary injured population was observed.

Heat-induced cell boundary injury was observed from the first minute (Fig. 4.19 B). It is likely that the *mechanism* by which cells were injured and killed by heat (55 or 60°C) was not

influenced by the 1 min pre-sonication. This is evident as the progression of fluorescent cells through injury to dead on the contour plots in Fig. 4.19 is similar to the heat-only contour plots (Figs 4.1 and 4.2). However, it is likely that the 1 min pre-sonication caused internal injuries that rendered the population markedly more susceptible to heat membrane-induced injury and subsequent death.

The contour plots representing the 5 min 60°C treatment, are shown in Fig. 4.20. This series represents a single experiment. Frames A – E in Fig. 4.20 represent respectively 0, 1, 2, 3, 4 and 5 min exposure to 60°C. The viable and dead populations are indicated with a 'V' and 'D', respectively. The area in which injured cells are located is indicated within the dashed line 'I'. The associated population fractions for each contour are presented in Appendix 4.D.

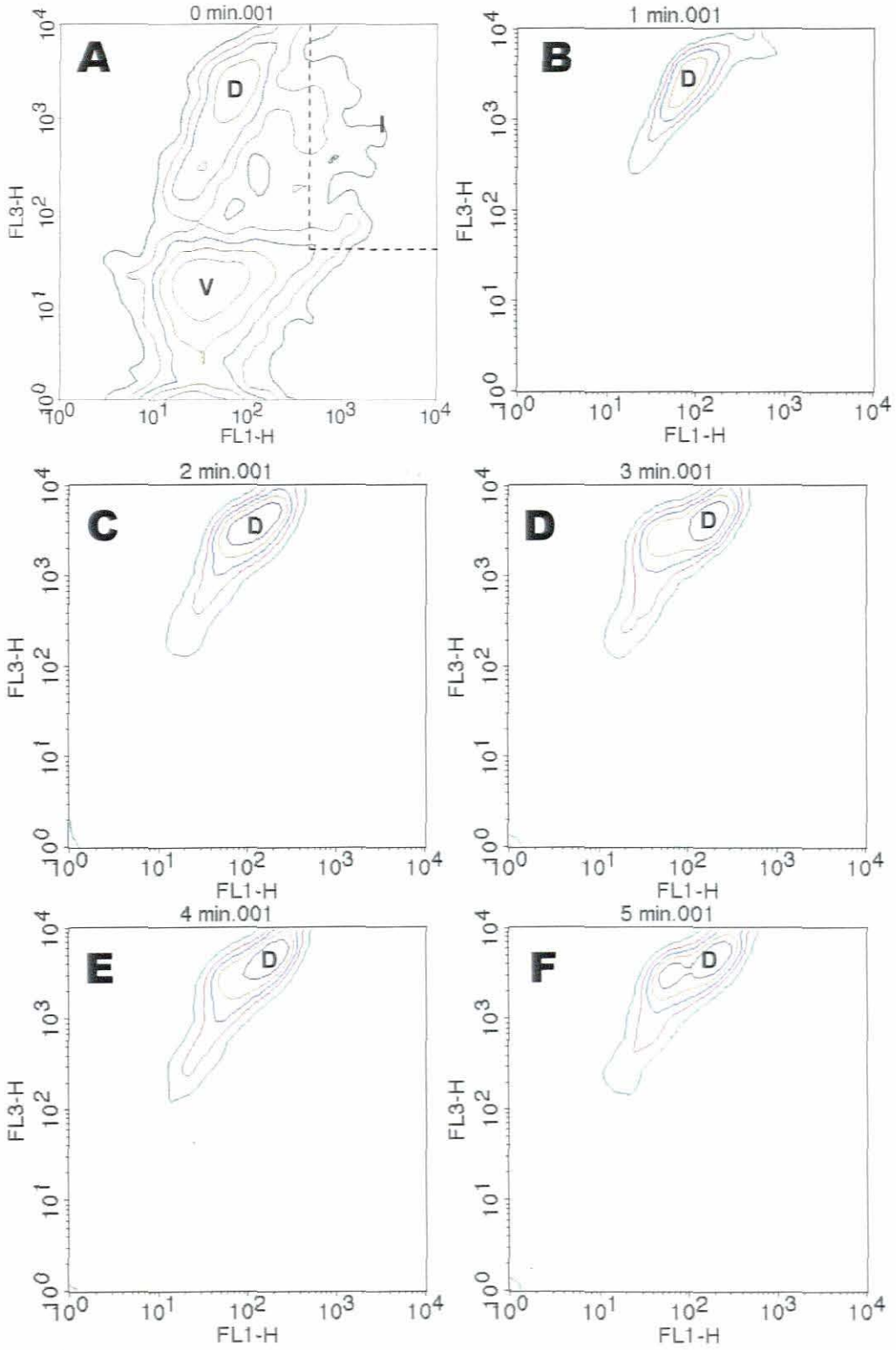

Figure 4.20: BD CellQuest contour plots showing the rapid progression of pre-sonicated late exponential (OD_{600} ~1) *S. cerevisiae* cells from viable (V), to injured (I), to death (D) when exposed to 60°C for 5 min

No populations of injured cells appear in Fig. 4.20 A – F. However, low numbers of individual cells below the threshold of the outermost contour (less than 10%) were detected and counted. These numbers are recorded in the population fractions in Section 4.3.4.2.

The pre-sonicated culture was typical of a culture sonicated for 1 min only viable and dead populations were gated. There was no definitive cell membrane injured population (Fig. 4.20). After 1 min immersion at 60°C, all *S. cerevisiae* cells were dead. Hence, by increasing the temperature by 5°C, to 60°C, the synergy between heat and ultrasound was markedly increased.

4.3.4.2 **Viable, injured and dead *Saccharomyces cerevisiae* population fractions *presonicated for 1 min before exposure to moist heat for 5 min.***

The viable, injured and dead fractions of the cultures were calculated during the 5 min of heat exposure (55 or 60°C). These data, from repeated experiments were collated and graphically depicted (Figs. 4.21 and Fig. 4.22).

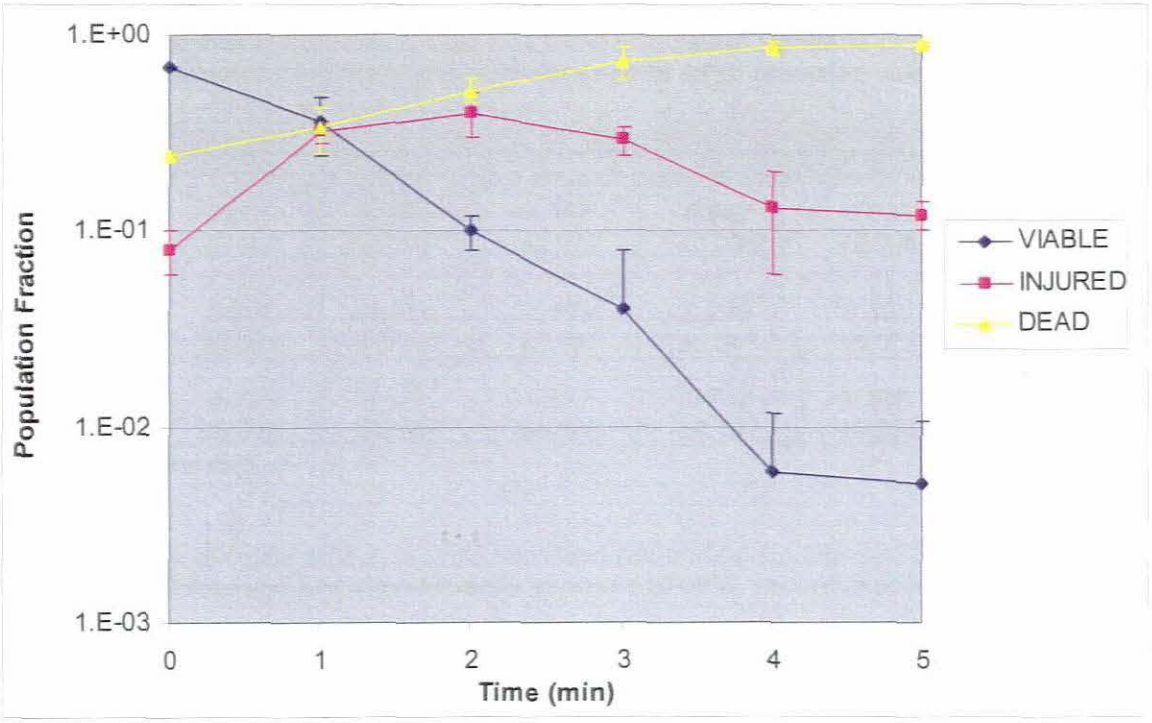

Figure 4.21: The effect of 55°C over 5 min on late exponential phase (OD_{600}~1.0) cultures of *S. cerevisiae*, pre-sonicated for 1 min. The standard deviation is indicated by the T bars (n=3)

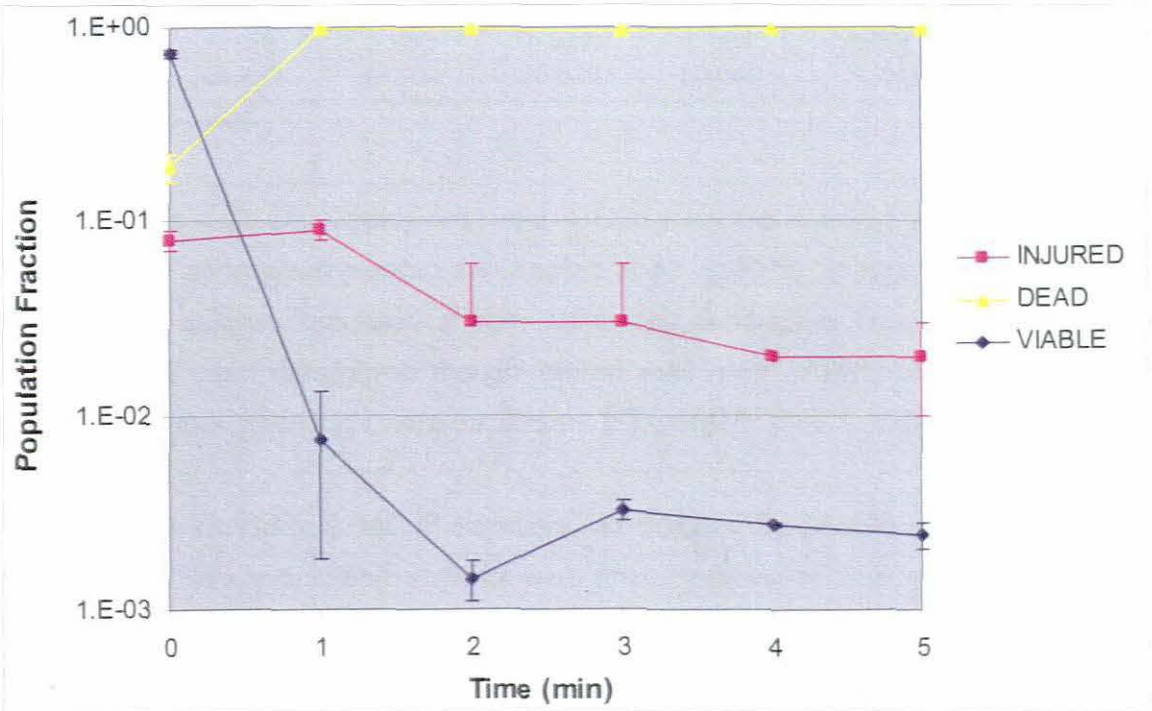

Figure 4.22: The effect of 60°C over 5 min on late exponential phase (OD_{600}~1.0) cultures of *S. cerevisiae*, pre-sonicated for 1 min. The standard deviation is indicated by the T bars (n=3)

Table 4.11: The average viable, injured and dead population fractions of *S. cerevisiae* pre-treated with ultrasound and subsequently exposed to 55°C, recorded using fluorescent flow cytometry

Population fraction	Time (min)					
	0	1	2	3	4	5
N_V	0.681 ±0.008	0.364 ±0.115	0.103 ±0.022	0.042 ±0.038	0.006 ±0.006	0.005 ±0.005
N_I	0.081 ±0.016	0.318 ±0.039	0.404 ±0.101	0.289 ±0.047	0.129 ±0.072	0.122 ±0.022
N_D	0.237 ±0.010	0.336 ±0.087	0.517 ±0.068	0.732 ±0.127	0.865 ±0.066	0.886 ±0.026

± = standard deviation

Table 4.12: The average viable, injured and dead population fractions of *S. cerevisiae* pre-treated with ultrasound and subsequently exposed to 60°C, recorded using fluorescent flow cytometry

Population fraction	Time (min)					
	0	1	2	3	4	5
N_V	0.731 ±0.037	0.008 ±0.006	0.001 ±0.000	0.003 ±0.000	0.003 ±0.000	0.002 ±0.000
N_I	0.080 ±0.009	0.093 ±0.010	0.032 ±0.026	0.033 ±0.030	0.018 ±0.005	0.019 ±0.011
N_D	0.189 ±0.029	0.900 ±0.004	0.967 ±0.026	0.964 ±0.030	0.978 ±0.004	0.979 ±0.011

± = standard deviation

Figs 4.21 and 4.22 and Tables 4.11 and 4.12 display the average population fractions of *S. cerevisiae* when pre-sonicated and heated at 55 or 60°C. At start-up, the pre-sonicated *S. cerevisiae* cultures consisted of both viable and dead cells. The number of viable cells exceeded the dead cells. Even though injured cells were present at start-up, the contour plots showed that these cells were insufficient in number to form a population.

Residual cells can form a 'tail' of survivors, as reported by Piyasena *et al.*, (2003). In this study, this tail was noted when cultures were pre-sonicated and then exposed to either 55 or 60°C for 5 min. However, a reduction in viable cells of $\log_{10}$ ~2 occurred before the "tail" formed (Figs. 4.21 and 4.22).

The time required to reduce pre-sonicated viable cells at 60°C by 1 $\log_{10}$ was more rapid than the same decrease in the 55°C-treated *S. cerevisiae* cells. In addition, at 55°C, N_V reduction was initially due to injury and then death whereas at 60°C, cells were killed rapidly. By increasing the temperature by 5°C, from 55°C to 60°C the D_{hd} value was decreased by 50% (Table 4.13).

A comparison of data obtained for the efficacy of reducing viable fractions at either 55°C or 60°C only, with those cultures pre-treated with 1 min ultrasound before undergoing similar heat treatments (hurdle) is given in (Table 4.13).

Table 4.13: Log_{10} CFU decrease and D_{hd} values of viable cells subjected to 55 or 60°C for 5 min. Samples were either pre-sonicated with 1 min ultrasound (hurdle) or subjected to heat only

Temperature	Log decrease in N_V after 5 min (log_{10})		D_{hd} value	
	Heat only	Hurdle	Heat only	Hurdle
55°C*	0.20	2.13	> 20 min	1.93 min
60°C	1.31	2.56	2.96 min	1.02 min

* culture OD_{600} = 1.058

The 1 min pre-sonication clearly injured *S. cerevisiae* cells in a manner that rendered these more susceptible to injury and death at 55 or 60°C (Table 4.13); hence sonication must have caused internal damage to *S. cerevisiae* cells making them more susceptible to heat. Other research groups have suggested the likelihood of sublethal cellular injuries. By using transmission electron microscopy (TEM), Guerrero *et al.*, (2005) showed damaged inner structures in sonicated *S. cerevisiae* subjected to 2.5 min ultrasound. Cameron (2007), using a Vibracell VCX 750 reported extensive damage to internal cellular structures, while the cell boundary appeared intact. Radel *et al.*, (2000) reported no damage to *S. cerevisiae* cell boundary when sonicated by using 2 MHz but noticed damage to vacuoles and the nuclear envelope. Cavitation occurring within the cell was hypothesised to induce the internal damage. These observations were supported by this study. Intracellular injuries caused by sonication induced a more rapid response to death caused by heating at either 55 or 60°C. The nature of these injuries is not known.

4.3.4.3 Overview of the results obtained from hurdle (55 and 60°C) experiments on *Saccharomyces cerevisiae* cultures

In summary, sequential treatment of the cells by sonication and heat effectively improved the reduction of N_V when compared to heat treatment alone. When cultures were subjected to 55°C for 5 min without pre-sonication, 57.3% remained viable after 5 min. However, when pre-sonicated for 1 min, the N_V was reduced to 0.5% after 5 min at 55°C. At 60°C the viable population was reduced to 48% after 5 min without pre-sonication. Viable cells in pre-sonicated cultures were reduced to 0.2% within 5 min at 60°C (note most of the reduction occurred in the first 2 min (Fig. 4.22).

It was noted that sonication followed by heating increased N_D rather than N_I, (Tables 4.11 and 4.12). After 5 min heating at either 55 or 60°C without pre-sonication, cultures consisted of more membrane-injured than dead cells (Tables 4.2 and 4.6).

Pre-sonication for 1 min increased the dead fraction at 55°C after 5 min from 14.6% to 88.6% and at 60°C, from 25% to 97.0%.(Table 4.14 and 4.15). The sustained period of membrane injury which occurred when cells were exposed to heat only, was almost eliminated by the sonication pretreatment.

Table 4.14: Comparison of the population fractions from the heat only and hurdle treatment (ultrasound) at 55°C

Population fraction	After 5 min	
	Heat only (55°C)*	Hurdle
N_V	0.573 ±0.005	0.005 ±0.005
N_I	0.161 ±0.189	0.122 ±0.022
N_D	0.146 ±0.014	0.886 ±0.026

*culture age = OD_{600} 1.058
± = standard deviation

Table 4.15: Comparison of the population fractions from the heat only and hurdle treatment (ultrasound and heat) at 60°C

Population fraction	After 5 min	
	Heat only (60°C)	Hurdle
N_V	0.048 ±0.003	0.002 ±0.000
N_I	0.702 ±0.061	0.019 ±0.011
N_D	0.250 ±0.049	0.979 ±0.011

± = standard deviation

4.4 Conclusion

Culture age was shown to influence response to heat. This impacted on the efficacy of microbicidal treatments; therefore it was important to test cultures of similar age

Heat treatments reduced viable cells due to membrane injury. Flow cytometric evaluation did not however detect any such membrane injury of sonicated (20 kHz) samples. However, the *SEM imagery revealed surface irregularities and physical disruption to the cell boundary of S. cerevisiae.*

The hurdle investigation confirmed that in addition to lethal membrane damage, cavitation injured cells elsewhere as resistance to heat was markedly decreased after 1 min pre-sonication. These unidentified non-lethal intracellular injuries made *S. cerevisiae* cells more susceptible to heat.

The obvious synergy between sonication and heat was demonstrated through the use of fluorescent flow cytometry. It has been reported by others that synergy occurred at 35 and 45°C but not at 55°C i.e. synergy is dependent on the heat temperature used (Guerrero *et al.*, 2001). However results reported here showed that by using bursts of ultrasound as a pre-treament, followed by heating, ultrasound impacted at both 55 and 60°C on *S. cerevisiae.* By using a sequential treatment, it was noted that the degree of impact was temperature-dependent. This observation would not have been as apparent had the sonication and heat been applied simultaneously. The time of exposure to ultrasound could be critical in this synergy, and using a flow cytometer, this could be accurately measured such that an optimum period of ultrasound is selected for each temperature used.

For designing effective hurdle technology, the advantages of using the flow cytometer were apparent, particularly with regard to the influence of culture age on heat-induced cell membrane injury.

For future experimentation, heat could be administered as a pre-treatment, followed by sonication. Other pre-treatment sonication times may also be investigated as well as more frequent sampling times within the first minute of subsequent heat treatment.

CHAPTER FIVE
CONCLUSION

The principal aims of this study were to investigate the effects of moist heat and/or sonication (20 kHz) on *S. cerevisiae* strain GC210 (*MATα lys2*) suspended in physiological saline, measured by using a fluorescent flow cytometric technique which enabled rapid identification of viable, dead and membrane-injured cells. Information gained from this study could be applied to the development of a suitable hurdle model for the killing of yeast cells contaminating various liquids in the food industry and elsewhere. Whilst aware that other intrinsic and extrinsic factors in liquids, eg pH, alcohol, suspended solids and others could act as additional hurdles, it was decided that physiological saline would provide a suitable model as the suspending medium

5.1 Reliability of the Vibracell VCX 750 in inducing and maintaining cavitation

As indicated in Chapter 1, variations in results in studies on the effects of microbes done elsewhere can be caused by variable sonication conditions during an experiment. Therefore a primary objective was to standardise cavitation conditions as much as possible. To achieve this, luminol and potassium iodide were used to provide data to assist in the optimisation of cavitation when using the Vibracell VCX 750.

Chemifluorescence produced by luminol in a liquid undergoing cavitation clearly showed zones of inertial cavitation. The amount of light generated was recorded over a 5 min for digital photographic exposure. Luminol experiments done in this study did not yield any numerical data however, for the future the method could be further developed, by using diodes to detect and quantify the light emitted. These data could relate this to the inertial cavitation generated. Nevertheless, luminol chemifluorescence studies showed that the intensity of the cavitation field differed among the three horn types tested. It also showed that the tapered microtips, despite operating at higher displacement amplitudes produced cavitation fields that were spatially irregular and weaker than the standard horn. The latter, used throughout the remainder of the study, produced an intense and reproducible zone of inertial cavitation directly below the horn tip. Luminol also showed that during cavitation microstreaming occurred which caused bubbles to move rapidly out of the cavitation zone.

Potassium iodide was successfully used to determine conditions which could be used during an ultrasound experiment to optimise/enhance cavitation. Iodine oxidation, yielding tri-iodide, showed that the sonication parameters used throughout this study (20 kHz, 124 μm,13 mm horn diameter) produced constant and reproducible inertial cavitation conditions. The work done during the current study using iodine oxidation was sensitive enough to illustrate that

many experimental design parameters influenced the inertial cavitation generated. These included horn placement, test volume, type and amount of dissolved gas, and others. Few reports published elsewhere on the influence of sonication on microbes consider variable factors which influence data, particularly for comparative purposes.

Useful data obtained with regard to optimising cavitation by using potassium iodide oxidation were;-

- The confirmation that horn type influenced both the number of cavitation bubbles generated and the intensity of bubble collapse.
- Using the standard horn, tri-iodide formation remained linear over a 10 min sonication period. This indicated that the generation of cavitation remained constant over time. The generation of cavitation was not influenced by factors such as removal of cavitation nuclei over time due to rectified diffusion or the creation of additional cavitation nuclei through bubble fragmentation. The VCX750 is designed to maintain a constant wave amplitude, and this also contributed to the "constancy" of cavitation over time.
- An inverse relationship was noted between sonication solution volume and tri-iodide generated. Doubling the sonication test solution volume decreased the tri-iodide concentration by 50%. Therefore it is suggested that volume does not influence the number of cavitation bubbles generated. Rather, because of the increased volume, the effects of cavitation are diluted. It is also hypothesised therefore that in larger volumes, microorganisms would pass through the cavitation zone less frequently and cavitation effects would take longer to appear. Therefore for any sonication equipment to be used for microbicidal observations, there is an optimal treatment volume for use.
- Tri-iodide formation was increased when the standard horn tip was positioned nearer the base of the glass treatment container. It was suggested that this was due to fragmentation of the cavitation bubbles upon impact with the container base. It was also observed that when closer to the container base, damage to the latter and the horn tip was increased. Therefore, this also needs to be determined for any other sonication equipment used under similar conditions.
- Pulse waves generated more tri-iodide than did continuous waves (CW), for the same sonication 'on' time. However, a disadvantage with pulsed waves was that to achieve the same 'on' time for all pulse ratios, the total experimental time (the sum of the 'on' and 'off' times) was extended by the 'off' times. Maximum enhancement, of ~20%, was achieved between 40 – 60% duty cycles. For a pulse wave of 50% duty cycle, the total experiment time is therefore doubled when compared with the time of a continuous wave experiment. Hence, if the same "total times" were used for both continuous wave and pulsed wave, the CW would generate higher levels of tri-iodide, as it has a 100% "on" time. The CW was therefore considered preferable for microcidal applications. Furthermore if extended

to food processing applications, pulse sound waves would unnecessarily increase processing times in the manufacturing processes.

- Dissolved gases were shown to impact on inertial cavitation. Cavitation was enhanced by saturation with argon or oxygen. Saturating beverages with argon is not feasible as argon is expensive. This would complicate food production as holding times would be required for dissolution of gases. Oxygen is impractical for the same reasons. In addition, oxygen would oxidise components of beverages, thereby decreasing the shelf life due to discolouration and tainting of flavour. Oxygen would also increase the corrosiveness of beverages towards tinplate, reducing shelf life of canned beverages. From results obtained reported here, the use of degassed solutions are recommended.

- Increasing hydrostatic pressure to 100, 200, 300, 400 and 500 kPa enhanced cavitation. A disadvantage of high pressure systems is that it is operated as a batch processes. Ultrasound however has the potential to operate as a continuous process. In addition, it was observed that wear and tear of ultrasonic equipment, particularly the horn tip and treatment vessel was exacerbated under high pressure conditions

From the results obtained, it was apparent overall that the conditions tested and selected for this study would optimise constant cavitation when using the VCX 750 Vibracell unit and standard horn. Therefore any results obtained regarding the microbistatic/cidal action of cavitation should be valid and reproducible.

For the future, it would be essential to develop an ultrasound technology that is continuous. Different frequencies could be tried. In addition, it would be of value to devise an acceptable system (ie produce GRAS products) where free radicals produced are scavenged from the solution. This would minimise associated changes in flavour in any beverage being exposed to cavitation. The fragmentation of the horn tips into the suspension is unacceptable for the production of safe beverages and this needs to be addressed for any sonochemical application in foods.

5.2 The use of fluorescent flow cytometery to detect, quantify and differentiate between viable, injured and dead *Saccharomyces cerevisiae* cells

Whilst fluorescent flow cytometry is more commonly used to assay mammalian cells, the calibration of the system used for this study provided a powerful tool for quantitative and qualitative analyses of *S. cerevisiae*. The use of thiazole orange (TO) and propidium iodide (PI) were successfully used to identify and count three populations of *S. cerevisiae* cells viz., viable, membrane-injured and dead. Wherever possible, for accurate and real time analyses

of microbes, the use of flow cytometry is recommended above the classical techniques of serial dilution and plate counting of microbes.

5.3 The influence of heat and ultrasound on *Saccharomyces cerevisiae* and the efficacy of its combined use as a hurdle application

Fluorescent flow cytometry was a novel approach and unexpectedly showed that *S. cerevisiae* cultures in differing growth phases responded differently when subjected to 55°C heat for 20 min. Not enough data were collected in this study to confirm the exact dynamics therefore further studies are required to investigate this. The trend was that younger cultures lost viability to injury and death more readily than did older cultures. It also appeared that the onset of cell death induced at 55°C was delayed in the older cultures with the injured population possibly acting as a buffer.

Fluorescent flow cytometry could be further used to investigate the influence of culture age on heat treatment, as well as other microbicidal applications. Fluorescence patterns of TO and PI indicated that the mode in which 55 and 60°C heat-injured *S. cerevisiae* were inactivated differed from the death induced by ultrasound. Heat treated cells first underwent extensive membrane injury prior to death. The time required to reduce viability depended on the temperature, where 60°C (D_{ht60} = 2.96 min) induced death in less time than did 55°C (D_{ht55} = >20 min).

By using TO and PI fluorescence, it was observed that sonicated cultures cells rapidly progressed from viable to dead (D_{us} = 3.06 min), without undergoing a phase of membrane injury. From scanning electron microscope (SEM) results, it was apparent that ultrasound as used in this study, damaged cell boundaries extensively and even caused cell fragmentation. It is therefore suggested that ultrasound-induced membrane injury is so damaging that cells die immediately. At present there are no other fluorophores available for use in yeasts for identifying the nature of these injuries using flow cytometry. A kit available for detecting changes in mammalian mitochondrial membrane potential is non-functional in yeasts (L. McMaster, pers. comm. 2008). Regarding microbicidal properties, sonication as used in this study was more effective than when *S. cerevisiae* was exposed to either 55 or 60°C. In the latter treatments, the decrease noted for viable cells was due to cell injury and not cell death. Under the conditions used in this study, it was not possible to determine whether these cells would recover or not. Certain flow cytometers (FACS Caliber, FACS Vantage, FACS Aria, BD Biosciences, San Jose, CA, USA) are able to collect selected gated cell populations directly after acquisition. For the future, such an investigation of injured cells could be of interest. For example, gated injured cells may be studied further, either by means of transmission electron microscopy (TEM) or SEM, or by re-inoculating growth media with the

injured cells and recording growth during subsequent incubation, using fluorescent flow cytometry.

In the experiments concerning the use of ultrasound and heat as hurdles, there was marked synergy between the two treatments. Using a sequential approach, it was shown that a 1 min pre-treatment with ultrasound improved the efficacy of heat (55 and 60°C) in killing *S. cerevisiae*. For pre-sonicated cells, the *D* values when treated with 55°C and 60°C heat were reduced from >20 to 1.93 min and from 2.96 to 1.02 min respectively. This clearly indicated that cavitation induced sublethal intracellular damage which increased the susceptibility of *S. cerevisiae* cells to heat. The nature of these injuries was not detected or elucidated by PI. It is likely that the duration of the ultrasound treatment could be shortened, and using fluorescence, the effects of this could be observed. Had both sonication and heat been applied simultaneously as is the nature of hurdle treatments, the extent of the damage caused by sonication would not have been distinguished from that of heat. To be able to precisely manipulate the hurdles would have considerable cost benefits for food production.

Overall, the aims and objectives of this study were achieved, and provide grounds for the extension of the experiments performed here, for example by varying temperatures, times, soundwave amplitude, frequency of sampling and others. It is now possible, using either the FACS Caliber or FACS Vantage, to detect bacteria, not possible with the FACS system used here. It would be of interest to continue these studies using bacteria in order to evaluate whether cavitation and/or heat exert similar or different effects on those cells.

REFERENCES

Ahmed, F.I.K. and Russell, C. 1975. Synergism between ultrasonic waves and hydrogen peroxide in the killing of microorganisms. *Journal of Applied Bacteriology,* 39:31-40.

Alliger, H. 1975. Ultrasonic disruption. *American Laboratory,* 10:75-85.

Apfel, R.E. 1981. Acoustic cavitation prediction. *Journal of Acoustic Society of America,* 69:1624.

Atanassova, D., Kefalas, P., Petrakis, C., Mantzavinos, D., Kalogerakis, N. and Psillakis, E. 2005. Sonochemical reduction of the antioxidant activity of olive mill wastewater. *Environment International,* 31:281-287.

Bailey, M. 2003. Personal communication.

BD Biosciences. 2002. BD CellQuest Pro Software User's Guide Part No. 349226 Rev. A. San Jose, CA 95131-1807 USA. Guide updated by L. Jackson; edited by K. Gautho; produced by P. MacFarlane.

Borthwick, K.A.J., Coakley, W.T., Mc Donell, M.B., Nowtony, H., Benes, E. and Groschl, M. 2005. Development of a novel compact sonicator for cell disruption. *Journal of Microbiological Methods,* 60:207-216.

Boyd, A. R., Gunasekera, T. S., Attfield, P.V., Simic, K., Vincent, S. F., and Veal, D.A. 2003. A flow cytometric method for the determination of yeast viability and cell number in a brewery. *FEMS Yeast Research,* 3:11-16.

Buldakov, M. A., Hassan, M. A., Zhao, Q., Feril, L. B., Kudo, N., Kondo, T., Litvyakov, N. V., Bolshakov, M. A., Rostov, V. V., Cherdyntseva, N. V. and Riesz, P. 2009. Influence of changing pulse repetition frequency on chemical and biological effects induced by low-intensity ultrasound in vitro. *Journal of Ultrasonics Sonochemistry,* 16, 392–397.

Cameron, M. 2007. Impact of Low Frequency High-Power Ultrasound on Spoilage and Potentially Pathogenic Dairy Microbes. Ph D. Thesis. Dept of Food Science, University of Stellenbosch.

Ciccolini, L., Taillandier, P., Wilhelm, A.M., Delmas, H. and Strehaiano, P. 1997. Low frequency thermo-ultrasonication of *Saccharomyces cerevisiae* suspensions: effect of temperature and of ultrasonic power. *Chemical Engineering Journal,* 65:145-149.

Cipollina, C., Val, M, Porro, D. and C. Hatzis. 2007. Towards understanding of the complex structure of growing yeast populations. *Journal of Biotechnology,* 128:393-402.

Clarke, P.R. and Hill, C.R. 1970. Physical and chemical aspects of ultrasonic disruption of cells. *Journal of Acoustic Society of America,* 50: 649 – 653.

Cunningham, T.S. and Cooper, T.G. 1991. Expression of the DAL80 gene, whose product is homologous to the GATA factors and is a negative regulator of multiple nitrogen catabolic genes in *Saccharomyces cerevisiae*, is sensitive to nitrogen catabolite repression. *Molecular and Cellular Biology,* 11: 6205-6215.

Didenko, Y.T., McNamara, W. B. and Suslick, K. S. 2000. Effect of noble gases on sonoluminescence temperature during multibubble cavitation. Physical Review Letters, 84:777-780.

Duck, F.A., Baker, A.C., Starritt, H.C. (Ed.). 1997. *Ultrasound In Medicine* ISBN 9780750305938. Institute of Physics Publishing, Bristol and Philadelphia. p214

Entezari, M.H. and Kruus, P. 1996. Effect of frequency on sonochemical reactions II. Temperature and intensity effects. *Ultrasonics Sonochemistry*, 3:19-24.

Garcia, M.L., Burgos, J., Sanz, B. and Ordonez, J.A. 1989. Effect of heat and ultrasonic waves on the survival of two strains of *Bacillus subtillus*.
Journal of Applied Bacteriology, 67:619-628.

Gogate, P.R. and Kabadi, A.M. 2009. A review of applications of cavitation in biochemical engineering / biotechnology. *Biochemical Engineering Journal*. 44:60-72.

Gould, G.W. 1988. In *Homeostatic Mechanisms in Micro-organisms*. R. Whittenbury, G.W. Gould, J.G. Banks and R.G. Board (Eds.), ISBN 0861970713 Bath University Press, Bath. p. 220.

Gould, W.A. and Gould, R.W. 1995. Sugar, salt and seasonings. In *Total Quality Assurance*. 2nd ed. ISBN 0930027205 CTI Publications Inc., Baltimore, Maryland. p. 161-187.

Graham, E., Hedges, M., Leeman, S. and Vaughan, P. 1980. Cavitational bio-effects at 1.5MHz. *Ultrasonics*, 18:224-228

Guerrero, S., Lopez-Malo, A. and Alzamora, S.M. 2001. Effect of ultrasound on the survival of *Saccharomyces cerevisiae*: influence of temperature, pH and amplitude.
Innovative Food Science and Emerging Technologies, 2:31-39

Guerrero, S., Tognon, M. and Alzamora, S. M. 2005. Response of *Saccharomyces cerevisiae* to combined action of ultrasound and low weight chitosan.
Food Control, 16:131-139

Halliday, D., Resnick, R., Walker, J. 2001. In *Fundamentals of Physics*. Sixth edition. ISBN 0-471-39222-7 John Wiley & Sons, New York, United States of America. p. 398

Hao, H., Wu, M., Chen, Y., Tang, J. and Wu, Q. 2003. Cavitation mechanism in cyanobacterial growth inhibition by ultrasound irradiation.
Colloids and Surfaces B: Biointerfaces, 33:151-156.

Hill, C.R., Clarke, P.R., Crowe, M.R. and Hammick, J.W. 1969. Biophysical effects of cavitation in a 1 MHz ultrasonic beam. *Proeedings. Conference on Ultrasonics for Industry* (London: Lliffe)pp 26-30.

Ince, N.H. and Belen, R. 2001. Aqueous phase disinfection with power ultrasound: process kinetics and effect of solid catalysts.
Environmental Science and Technology, 35:1885-1888.

Inoue, M., Okada, F., Sakurai, A. and Sakakibara, M. 2005. A new development of dyestuff degradation system using ultrasound. *Ultrasonics Sonochemistry*, 13:313-320.

Jay, J.M. 1997. *Modern Food Microbiology*. Fifth edition. ISBN 0834212307. Chapman and Hall, Maryland, United States of America.

Johnson, L.L., Peterson, R.V. and Pitt, W.G. 1998. Treatment of bacterial biofilms on polymeric biomaterials using antibiotics and ultrasound.
Journal of Biomaterials Science. Polymer edition, 9:1177-1185.

Joyce, E., Mason, T.J., Phull, S.S. and Lorimer, J.P. 2003. The development and evaluation of electrolysis in conjunction with power ultrasound for the disinfection of bacterial suspensions. *Ultrasonics Sonochemistry*, 10: 231-234.

Kinsloe, H., Ackerman E. and Reid, J.J. 1954. Exposure of microorganisms to measured sound fields. *Journal of Bacteriology*, 68:373-380.

Koda, S., Kimura, T., Kondo, T. and Mitome, H. 2003. A standard method to calibrate sonochemical efficiency of an individual reaction system.
Ultrasonics Sonochemistry, 10:149-156

Lee, B.H., Kermasha, S. and Baker, B.E. 1989. Thermal, ultrasonic and ultraviolet inactivation of *Salmonella* in thin films of aqueous media and chocolate.
Food Microbioogy, 6:143-152.

Leighton, T.G. 1994. In *The Acoustic Bubble*. First edition. ISBN 0-12-441921-6 Academic Press, London, United Kingdom

Leighton, T.G. 2007. What is ultrasound?
Progress in Biophysics and Molecular Biology, 93:3-83.

Leistner, L. 1994. Principles and applications of Hurdle Technology. In *New Methods of Food Preservation.* Gould, G.W. (Ed.), Blackie Academic and Professional. New York. pp. 1-20.

Leistner, L., Rodel, W. and Krispien, K. 1981. In *Water Activity: Influences on Food Quality*, L.B. Rockland and G.F. Stewart (Ed.), Academic Press, New York. p. 855.

Lemmon, E.W. and Jacobsen, R.T. 2004. Viscosity and thermal conductivity equations for nitrogen, oxygen, argon and air. *International Journal of Thermophysics*. 25:21-69.

Lillard, H.S. 1993. Bactericidal effect of chlorine on attached *Salmonellae* with and without sonification. *Journal Food Protection*, 56:716-717.

Lorincz, A. 2004. Ultrasonic cellular disruption of yeast in water-based suspensions.
Biosystems Engineering, 89:297-308.

Malacrino, P., Zapparoli, G., Torriani, S. and Dellaglio, F. 2001. Rapid detection of viable yeasts and bacteria in wine by flow cytometry.
Journal of Microbiological Methods, 45:127-134.

Martinez-Esparza, M., Sarazin, A., Juoy, N., Poulain, D. and Jouault, T. 2006. Comparative analysis of cell wall surface glycan expression in *Candida albicans* and *Saccharomyces cerevisiae* yeasts by flow cytometry. *Journal of Immunological Methods*, 314: 90-102.

Mason, T.J. 1999. An introduction to the uses of power ultrasound in chemistry. In:
Sonochemistry Oxford Science Publication, Oxford, United Kingdom. pp. 1-41.

McInnes, C., Engel, D. and Martin, R.W. 1990. Bacterial luminescence: a new tool for investigating the effects of acoustic energy and cavitation.
Journal of Acoustic Society of America, 88:2527-2532.

Moshaii, A., Rezaei-Nasirabad, R., Imani, K.H., Silatani, M. and Sadighi-Bonabi, R. 2008. Role of thermal conduction in single-bubble cavitation. *Physics Letters*, 372:1283-1287.

Muller, S. and Losche, A. 2003. Population profiles of a commercial yeast strain in the course of brewing. *Journal of Food Engineering*, 63:375-381.

Munkacsi, F. and Elhami, M. 1976. Effect of ultrasonic and ultraviolet irradiation on chemical and bacteriological quality of Egyptian milk. *Journal of Dairy Science,* 4:1-6.

Ordonez, J.A., Sanz, B., Hernandez, P.E. and Lopez-Lorenzo, P. 1983. A note on the effect of combined ultrasonic and heat treatments on the survival of thermoduric streptococci. *Journal of Applied Bacteriology,* 56:175-177.

Oyana, I., Takeda, T., Oda, Y., Sakata, T., Furtia, M., Okitsu, K., Maeda, Y. and Nishimura, R. 2009. Comparison between the effects of ultrasound and γ-rays on the inactivation of Saccharomyces cerevisiae: Analyses of cell membrane permeability and DNA and RNA synthesis by flow cytometry. *Ultrasonics Sonochemistry,* 16:532-536.

Pagan, R., Manas, P., Raso, J. and Condon, S. 1999. Bacterial resistance to ultrasonic waves under pressure at sublethal and lethal temperatures. *Food Microbiology,* 16:139-148.

Palacios, P., Burgos, J., Hoz, L., Sanz, B. and Ordonez, J.A. 1991. Study of substance release by uitrasonic treatment from *Bacillus stearothermophilus* endospores. *Journal of applied bacteriology,* 75:445-451

Parejo, I., Codina, C., Petrakis, C. and Kefalas, N. 2000. Evaluation of scavenging activity assessed by Co(ii)/EDTA-induced luminol chemiluminescence and DPPH free radical assay. *Journal of Pharmacological and Toxicological Methods,* 44:507-512.

Perkins, J.P. 1990. Power ultrasound. In Sonochemistry, the use of ultrasound in chemistry. Ed Mason, T.J. Royal Society of Chemistry, London, p187-210

Petin, V. G., Zhurakovskaya, G. P. and Komarova, L. N. 1998. Mathematical description of combined action of ultrasound and hyperthermia on yeast cells. *Ultrasonics,* 37:79-83.

Piyasena, P., Mohareb, E. and McKellar, R.C. 2003. Inactivation of microbes using ultrasound: a review. *International Journal of Food Microbiology,* 87:207-216.

Povey, M.J.W. and Mason, T.J. 1998. *Ultrasound in Food Processing.* First edition. ISBN 3527302050 Blackie Academic and Professional, London, United Kingdom.

Prescott, L.M., Harley, P.J. and Klein, D.A. 1996. *Microbiology.* Third edition. Boston. ISBN 0-697-29390-4 WCB. p. 145.

Qian, Z., Sagers, R.D. and Pitt, W.G. 1997. The role of insonication intensity in acoustic-enhanced killing of *Pseudomonas aeruginosa* biofilms. *Colloids and Surfaces Biointerfaces,* 9:239-245.

Radel, S., McLouglin, A.J., Gherardini, L., Doblhoff-Dier, O. and Benes, E. 2000. Viability of yeast cells in well controlled propagating and standing ultrasonic plane waves. *Ultrasonics,* 38:633-637.

Raso, J., Pagan, R., Condon, S. and Sala, J.F. 1998. Influence or the temperature and pressure on the lethality of ultrasound. *Applied and Environmental Microbiology,* 64: 465-471

Ray, B. 2003. *Fundamental Food Microbiology.* Third edition. ISBN 0849316103 CRC Press, Boca Raton, United States of America.

Rediske, A.M., Rapport, N. and Pitt, S.G. 1999. Reducing bacterial resistance to antibiotics with ultrasound. *Letters in Applied Microbiology,* 28: 81-84.

Sala, F.J., Burgos, J., Condon, S., Lopez P. and Raso, J. 1995. Manothermosonication.In: *New Methods of Food Preservation*, G.W. Gould (Ed.), Academic Press, New York. pp. 251-259.

Sams, A.R., and Feria, R. 1991. Microbial effects of ultrasonication of broiler drumstick skin. *Journal of Food Science,* 56: 247-248.

Sanz, B., Palacios, P., Lopez, P. and Ordonez, J.A. 1985. Effect of ultrasonic waves on the heat resistance of *Bacillus stearothermophilus* endospores. In: *Fundamental and Applied Aspects of Bacterial Endospores.* G.J. Dring, D.J. Ellar and G.W. Gould (Ed.), Academic Press, New York. pp. 251-259.

Scherba, G., Weigel, R.M. and O'Brien, W.D. 1991. Quantitative assessment of the germicidal efficacy of ultrasonic energy. *Appied and Enviromental Microbiology,* 57:2079-2084.

Simonin, H., Beney, L. and Gervals, P. 2007. Sequence of occurring damages in yeast plasma membrane during dehydration and rehydration.
Biochimica et Biophysica Acta, 1768:1600-1610.

Sonics and Materials. 2002. Vibra-Cell: high intensity ultrasonic liquid processors.Fifth edition. Newton, CT: Sonics and Materials. [Manual]

Sorensen, B.B. and Jakobsen, M. 1997. The combined effects of temperature, pH and NaCl on growth of *Debaromyces hansenii* analysed by flow cytometry and predictive microbiology. *International Journal of Food Microbiology,* 34:209-220.

Suslick, K.S. 1989. The chemical effects of ultrasound. *Scientific American*, 260: 80-86.

Swalwell, J. 2003. Personnel communication

Thacker, J. 1973. An approach to the mechanism of killing of cells in suspension by ultrasound. *Biochimica et Biophysica Acta*, 304:240-248.

Tsukamoto, I., Constantinoiu, E., Furuta, M., Nishimura, R. and Maeda, Y. 2004. Inactivation effect of sonication and chlorination on *Saccharomyces cerevisiae* calorimetric analysis. *Ultrasonics Sonochemistry,* 11:167-172.

Tsukamoto, I., Yim, B., Stavarache, C.E., Furuta, M., Hashiba, K. and Maeda, Y. 2003. Inactivation of *Saccharomyces cerevisiae* by ultrasonic irradiation.
Ultrasonics Sonochemistry, 11:61-65.

van Wyk, R (2004) The effect of argon, nitrogen and oxygen on the inactivation of *Escherichia coli* subjected to sonication (20 kHz). BTech Thesis. Department of Food Tehcnology, Cape Peninsula University of Technology

Vollmer, A. C., Kwakye, S., Halpern, M. and Everbach, E. C. 1998. Bacterial stress responses to 1-megahertz pulsed ultrasound in the presence of microbubbles.
Applied and Enviromental Microbiology, 64:3927-3931.

Weissler, A. 1950. Chemical effect of ultrasonic waves: oxidation of potassium iodide solution by carbon tetrachloride. *International Journal of the Amercian Accoustics Society,* 72:1769-1772.

Wrigley, D. M. and Llorca, N.G. 1992. Descrease of *Salmonella typhimurium* in skim milk and egg by heat and ultrasonic wave treatment. *Journal of Food Protection,* 55:678-680.

APPENDICES

- Appendix 2.A: - Image enhancement using Adobe Photoshop
- Appendix 2.B: - Determination of the stability of tri-iodide after sonication
- Appendix 4.A: - Additional data pertaining to 55°C heat treatment of *Saccharomyces cerevisiae*
- Appendix 4.B: - Additional data pertaining to 60°C heat treatment of *S. cerevisiae*
- Appendix 4.C: - Additional data pertaining to sonication of *Saccharomyces cerevisiae*
- Appendix 4.D: - Additional data pertaining to hurdle treatment (55 & 60°C) of *Saccharomyces cerevisiae*

APPENDIX 2.A: IMAGE ENHANCEMENT USING ADOBE PHOTOSHOP

The photographic images recorded with the Nikon E4500 were recorded in JPEG format. After downloading from the camera onto a computer, the images were opened with Adobe® Photo Deluxe™ 2.0 software, were the following adjustments were made:

- The crayon – red balance was set at –100 (increasing the crayon)
- The magenta – green was set at –100 (increasing the magenta)
- The yellow – blue was set at +100 (increasing the blue)
- The contrast was increased to 50
- The image was sharpened
- 'Dust' was removed with a setting of one pixel radius and a threshold of six levels

The images were saved and imported into Microsoft Office Word™ 2003

APPENDIX 2.B: DETERMINATION OF THE STABILITY OF TRI-IODIDE AFTER SONICATION

As discussed in Section 2.3.1.2, the tri-iodide formed during sonication is unstable reduced back to I_2 and I^- (Eq 2.3) (Weissler, 1950). The time required for sampling during sonication and subsequent testing was up to 10 min. Therefore it needed to be determined if tri-iodide in a sonicated iodine solution was stable for up to 10 min. This preliminary experiment was aimed at determining the stability of tri-iodide over 10 min after sonication.

A potassium iodide solution was made up as described in Section 2.1.1. Aliquots (100 ml) of potassium iodide solution were sonicated at 124 µm displacement amplitude in the 100 ml glass-cooling jacket, using a Vibracell standard horn (Material and Sonics). The sample was sonicated for 10 min and 50 x 1 ml samples were removed for spectrophotometric analysis. The optical density (OD_{352}) of all 50 x 1 ml aliquots was automatically recorded every 15 s for 10 min at room temperature. That equates to a total of 40 absorbance measurements per sample and therefore 2 000 absorbance measurements overall. The spectrophotometer was calibrated using 1 ml of potassium iodine solution removed from the glass cell prior to sonication. Constant absorbance detected over the 10 min period was taken to indicate the tri-iodide was stable for at least 10 min after sonication.

Results were that the absorbance (OD_{352}) of all 2 000 samples remained constant over the 10 min period after sonication. Therefore tri-iodide formed during cavitation was stable in the buffered solution for at least 10 min after sonication. This gave sufficient time for both sampling and spectrophotometric analysis after sonication. It also showed that minute fragments of the horn tip in solution, dislogged during sonication, did not influence the absorbance by reflecting light (430 nm) as it passed through the solution. Fig 2B.1 shows the corrosive effect of cavition on the horn tip.

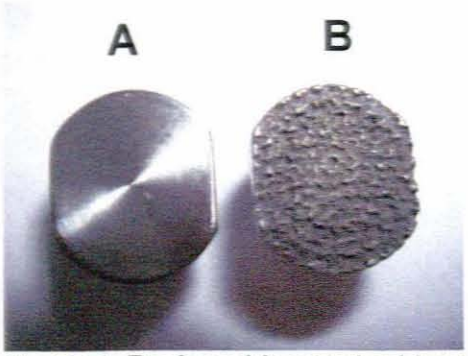

Fig 2B.1: Replaceable standard horn tips manufactured from a titanium alloy (TI-AL-4V) (Vibra-Cell) for the standard horn. (A) Is an unused tip while (B) has been exposed to of several hours ultrasound. Notice extensive pitting on (B) caused by microjets, as a result of asymmetrical collapse of inertial bubbles near the surface of the tip.

APPENDIX 4.A: ADDITIONAL DATA PERTAINING TO 55°C HEAT TREATMENT OF *SACCHAROMYCES CEREVISIAE*

Population fractions of *S. cerevisiae* corresponding to the contour plots presented in Fig. 4.1. The OD_{600} of the heat treated (55°C) *S. cerevisiae* cultures was OD_{600} 0.216

OD_{600} 0.216			
Time	Viable	Injured	Dead
0	0.965	0.030	0.005
5	0.698	0.269	0.032
10	0.554	0.399	0.047
15	0.276	0.629	0.095
20	0.126	0.547	0.327

Population fractions of *S. cerevisiae* corresponding to the contour plots presented in Fig. 4.2. The OD_{600} of the heat treated (55°C) *S. cerevisiae* cultures was OD_{600} 1.482

OD_{600} 1.482			
Time	Viable	Injured	Dead
0	0.963	0.026	0.010
5	0.782	0.105	0.113
10	0.466	0.265	0.269
15	0.305	0.335	0.360
20	0.091	0.317	0.592

APPENDIX 4.B: ADDITIONAL DATA PERTAINING TO 60°C HEAT TREATMENT OF *SACCHAROMYCES CEREVISIAE*

Population fractions of *S. cerevisiae* corresponding to the line graph presented in Fig. 4.6. The *S. cerevisiae* cultures were treated with 60°C heat for 20 min.

20 minutes heat 60°C						
Time	Viable		Injured		Dead	
0	0.903	±0.047	0.015	±0.006	0.012	±0.006
5	0.041	±0.007	0.015	±0.006	0.941	±0.084
10	0.036	±0.003	0.008	±0.005	0.858	±0.021
15	0.031	±0.000	0.005	±0.000	0.879	±0.033
20	0.021	±0.016	0.019	±0.019	0.880	±0.074

Population fractions of *S. cerevisiae* corresponding to the contour plots presented in Fig. 4.7. The *S. cerevisiae* cultures were treated with 60°C heat for 5 min

Time	Viable	Injured	Dead
0	0.971	0.025	0.003
1	0.609	0.330	0.062
2	0.243	0.650	0.132
3	0.105	0.749	0.147
4	0.057	0.748	0.195
5	0.050	0.653	0.297

APPENDIX 4.C: ADDITIONAL DATA PERTAINING TO THE SONICATION OF *SACCHAROMYCES CEREVISIAE*

Population fractions of *S. cerevisiae* recorded over 20 min, when subjected to ultrasound (n = 3)

20 min ultrasound								
Time	Viable		Injured		Dead		Total	
0	0.841	±0.107	0.123	±0.091	0.024	±0.013	1.000	±0.000
5	0.021	±0.006	0.044	±0.028	0.613	±0.095	0.682	±0.117
10	0.004	±0.004	0.020	±0.018	0.385	±0.045	0.415	±0.066
15	0.003	±0.002	0.014	±0.015	0.244	±0.011	0.266	±0.029
20	0.002	±0.001	0.013	±0.015	0.163	±0.028	0.181	±0.047

Population fractions of *S. cerevisiae* corresponding to the contour plots presented in Fig. 4.9. The *S. cerevisiae* cultures were sonicated for 5 min

Time	Viable	Injured	Dead	Total
0	0.961	0.032	0.007	1.000
1	0.568	0.148	0.354	1.071
2	0.265	0.111	0.403	0.779
3	0.111	0.072	0.620	0.803
4	0.040	0.071	0.503	0.614
5	0.022	0.066	0.486	0.574

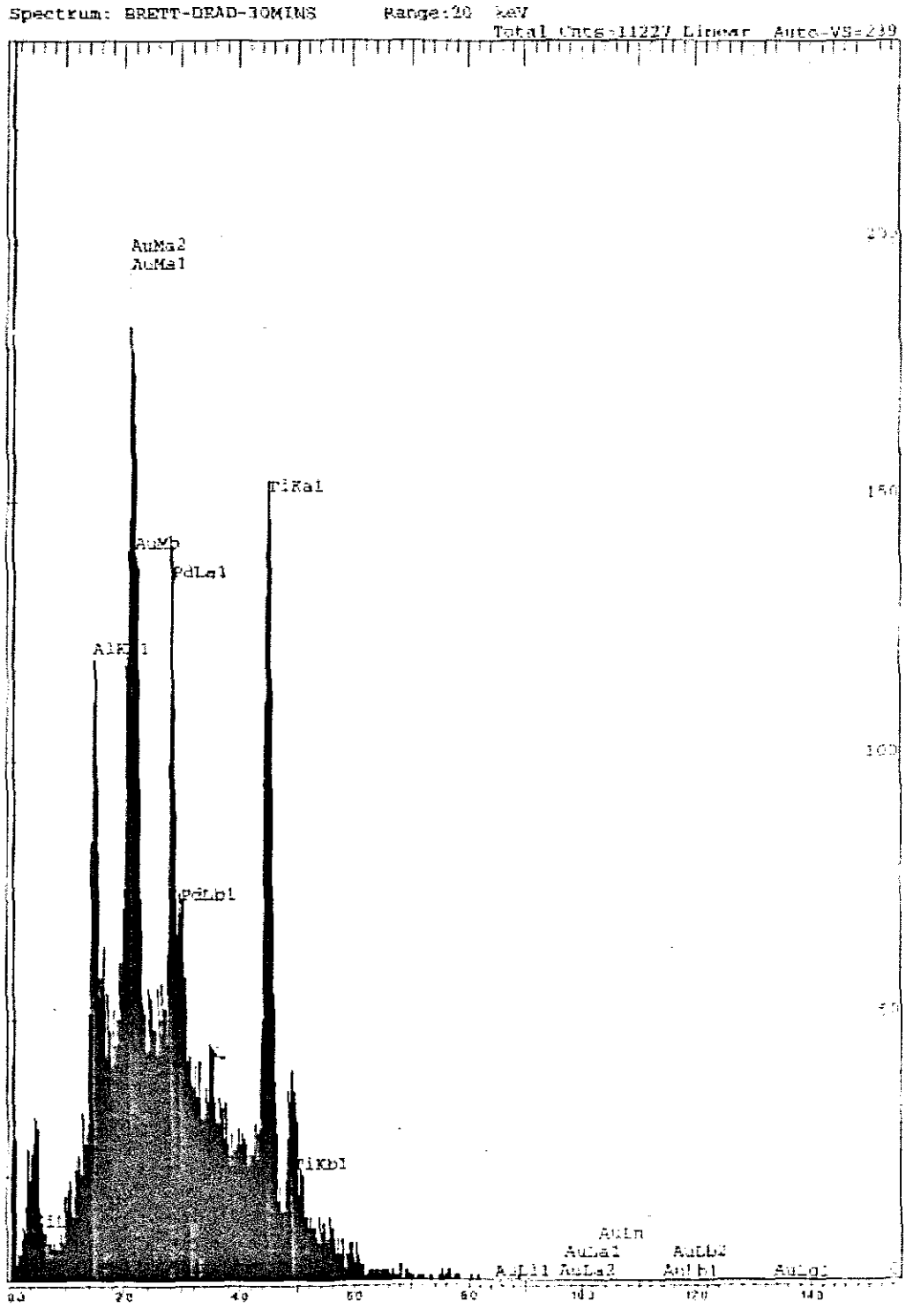

Fig 4C-1: Electron dispersion spectrophotometry of a piece of material found in sonicated solutions. The EDS analysis shows that the material was a titanium alloy, originating from the ultrasounic horn

[A N A L Y S I S R E P O R T]

GENERAL CONDITIONS

Result File	: BRETT-DEAD-30MINS
File Version	: 1
Background Method	: Fit
Decon Method	: Gaussian
Decon ChiSquared	: 2.02
Analysis Date	: 5-MAY-2005
Microscope	: SEM
Comments	:

ANALYSIS CONDITIONS

Quant. Method	: ZAF/ASAP
Acquire Time	: 60 secs
Normalization Factor	: 100.00

SAMPLE CONDITIONS

kV	: 20.0
Beam Current	: 3278.7 picoAmps
Working Distance	: 25.0 mm
Tilt Angle	: 0.0 Degrees
TakeOff Angle	: 35.0 Degrees
Solid Angle*BeamCurrent	: 20.0

Element	Line	Weight%	Error	K-Ratio	Atomic%
O	Ka	41.18	4.557	0.0668	62.04
Al	Ka	21.41	0.907	0.1255	19.13
Ti	Ka	37.42	1.188	0.3375	18.83
Total		100.01			

Fig 4C-2: Electron dispersion spectrophotometry results corresponding to the image in Fig 4C-1

APPENDIX 4.D ADDITIONAL DATA PERTAINING TO HURDLE TREATMENT (55 & 60°C) OF *SACCHAROMYCES CEREVISIAE*

Population fractions of *S. cerevisiae* corresponding to the contour plots presented in Fig. 4.20. The *S. cerevisiae* culture was subjected to a 1 min sonication pre-treatment, immediately followed by a 55°C heat treatment.

Time	Viable	Injured	Dead
0	0.673	0.093	0.235
1	0.299	0.291	0.411
2	0.127	0.333	0.540
3	0.086	0.256	0.659
4	0.010	0.078	0.912
5	0.005	0.138	0.858

Population fractions of *S. cerevisiae* corresponding to the contour plots presented in Fig. 4.21. The *S. cerevisiae* culture was subjected to a 1 min sonication pre-treatment, immediately followed by a 60°C heat treatment.

Time	Viable	Injured	Dead
0	0.705	0.086	0.209
1	0.012	0.086	0.903
2	0.002	0.014	0.985
3	0.004	0.012	0.985
4	0.003	0.015	0.981
5	0.002	0.011	0.986